Universidade de Aveiro

2021

Tânia Isabel Meleiro Lopes

Comparação de duas metodologias para o isolamento de vesículas extracelulares de células de cancro gástrico para a deteção de STn

Comparison of two extracellular vesicles isolation methodologies from gastric cancer cells for STn detection

Universidade de Aveiro

2021

Tânia Isabel Meleiro Lopes

Comparação de duas metodologias para o isolamento de vesículas extracelulares de células de cancro gástrico para a deteção de STn

Comparison of two extracellular vesicles isolation methodologies from gastric cancer cells for STn detection

Dissertação apresentada à Universidade de Aveiro para cumprimento dos requisitos necessários à obtenção do grau de Mestre em Bioquímica – especialização em Bioquímica Clínica, realizada sob a orientação científica da Doutora Daniela Freitas, Investigadora no grupo *Glycobiology in Cancer* do i3S- Instituto de Investigação e Inovação em Saúde da Universidade do Porto e coorientação do Doutor Celso Reis, líder do grupo *Glycobiology in Cancer* do i3S- Instituto de Investigação e Inovação em Saúde da Universidade do Porto e da Doutora Rita Ferreira, Professora Auxiliar do Departamento de Química da Universidade de Aveiro.

o júri

presidente	Professor Doutor Mário Manuel Quialheiro Simões Professor Auxiliar, Universidade de Aveiro
	Doutora Diana Duarte de Sousa Professora Adjunta Convidada, i3S – Instituto de Investigação e Inovação em Saúde, Universidade do Porto
	Doutora Daniela Sofia Pereira Freitas Investigadora, i3S – Instituto de Investigação e Inovação em Saúde, Universidade do Porto

agradecimentos

No decorrer deste ano, muitas pessoas contribuíram de forma direta ou indireta para o sucesso do trabalho apresentado nesta tese. Em primeiro lugar, gostaria de agradecer às pessoas que constituem o grupo *Glycobiology in Cancer*, as quais me acolheram com imensa simpatia. Desde logo, um agradecimento ao Prof. Doutor Celso Reis que, aprovando a minha entrada no seu laboratório, permitiu que eu usufruísse de uma oportunidade única no seio de um grupo bem consolidado. Em seguida, um enorme agradecimento à Doutora Daniela Freitas por me ter ensinado e orientado de forma exímia, o que tornou esta experiência extremamente enriquecedora tanto a nível profissional como pessoal. Graças à notória motivação com que encara a profissão, permitiu que crescesse em mim uma paixão pela área da glicobiologia e pelo vasto universo da investigação.

De seguida, gostaria de agradecer à Prof. Doutora Rita Ferreira pelo acompanhamento excecional ao longo de todo o meu percurso, começando desde logo pela Licenciatura até ao Mestrado. Agradeço-lhe todos os ensinamentos e motivação que me transmitiu ao longo dos últimos anos e, especialmente, pelo encorajamento para prosseguir esta área.

Por último, um agradecimento à minha família e amigos, que tornaram isto possível com todo o amor, carinho e coragem que me transmitiram.

palavras-chave Cancro gástrico, glicanos, vesiculas extracelulares, métodos de isolamento, biomarcadores

resumo

O cancro gástrico é o 5º tipo de cancro mais comum e a 3ª causa de morte relacionada com cancro, em Portugal. A pesquisa de novos biomarcadores e práticas clínicas para melhorar o diagnóstico e a estratificação dos pacientes através de técnicas menos invasivas e mais sensíveis é um tópico de investigação intensivo. A elevada expressão do *O*-glicano truncado sialil-Tn (STn) é frequentemente identificado em tecido de carcinoma gástrico e encontra-se relacionada com um pior prognóstico dos doentes. Adicionalmente, as células cancerígenas secretam níveis elevados de vesículas extracelulares (EVs) para a circulação, cuja carga reflete as alterações que ocorrem nas células de origem, representando uma fonte valiosa para a descoberta e deteção de biomarcadores.

Os objetivos deste estudo foram comparar o rendimento e pureza das EVs obtidas por dois métodos de isolamento, a ultracentrifugação diferencial (UC) e a combinação de UC com cromatografia por exclusão de tamanho (SEC) e detetar a presença de STn na membrana das EVs.

As EVs foram isoladas de duas linhas celulares geneticamente alteradas para expressarem níveis diferentes de STn e de duas linhas de células controlo de cancro gástrico por UC e UC+SEC. As EVs isoladas foram caracterizadas por *nanoparticle tracking analysis*, microscopia eletrónica de transmissão e *western blotting*, de acordo com a Sociedade Internacional de Vesículas Extracelulares. A deteção de STn na membrana das EVs foi aferida através de uma técnica de marcação com partículas de ouro. O impacto do STn na internalização de EVs foi estudado usando um sistema indireto de co-cultura.

O rendimento e pureza das EVs isoladas por UC e UC+SEC foi comparado através da análise da sua concentração, da presença de contaminantes proteicos e de marcadores de EVs como a alix, sintenina-1, Hsp70 e CD9. O protocolo UC+SEC permitiu um menor rendimento, mas uma maior pureza das EVs isoladas, facilitando a deteção de marcadores de EVs e de STn. Foi ainda possível observar que as células que expressam STn secretam mais EVs e que o STn parece ser incorporado seletivamente nas EVs. De realçar que foi possível detetar STn na membrana de EVs secretadas por células de cancro gástrico. Por fim, observamos uma capacidade diferente das células recetoras em internalizarem EVs positivas ou negativas para STn.

Em conclusão, os nossos resultados mostram que a combinação de UC com SEC levou à recuperação de EVs mais puras, facilitando a deteção de STn. Adicionalmente, o STn foi detetado em níveis mais elevados nas EVs do que nas células secretoras e encontrado na membrana das EVs, destacando o seu potencial uso como biomarcador em EVs de cancro gástrico. Na mesma linha de evidência, as células que expressam STn secretaram mais EVs, o que pode facilitar a sua deteção num contexto clínico. Por fim, a presença de STn nas EVs afetou a sua internalização em células recetoras, sugerindo um possível envolvimento durante a progressão do cancro.

keywords Gastric cancer, glycans, extracellular vesicles, isolation methods, biomarkers

abstract

Gastric cancer is the 5th most common and the 3rd deadliest cancer in Portugal. The search for biomarkers and clinical approaches to improve patients' diagnosis and stratification through less invasive and more sensitive methods is an active research topic. Overexpression of the truncated *O*-glycan sialyl-Tn (STn) is commonly identified in gastric carcinoma tissue, which has been correlated with poor prognosis of gastric cancer patients. In addition, cancer cells secrete high levels of extracellular vesicles (EVs) into circulation, which cargo reflects the changes occurring in the cell of origin, and therefore, represent a valuable source for biomarker discovery and detection.

The aims of this study were to compare the yield and purity of two different EV isolation methodologies, the ultracentrifugation (UC) and the UC combined with size exclusion chromatography (SEC) and to access the presence and detection of STn at EV membrane.

EVs were isolated from two glycoengineered cell lines that synthetize different levels of STn and two control gastric cancer cell lines negative for this glycan by UC and UC+SEC. Isolated EVs were characterized through nanoparticle tracking analysis, transmission electron microscopy and western blotting, according to the International Society of Extracellular Vesicles. The detection of STn at EV membranes was assessed using an immunogold labeling technique. Furthermore, the impact of STn in EV uptake was studied using an indirect co-culture system.

UC- and UC+SEC-EV isolates were compared regarding yield and purity through the analysis of EV concentration, presence of protein contaminants and EV markers such as alix, syntenin-1, Hsp70 and CD9. Results showed that UC+SEC isolated EVs with a lower yield but higher purity, facilitating the detection of both EV markers and STn. It was also possible to observe that cells expressing STn showed to secrete more EVs and that the STn seemed to be selectively packaged in EVs. Remarkably, we were able to detect STn at the membrane of EVs secreted by gastric cancer cells. Finally, we observed a different uptake capacity of the EVs positive and negative for STn by the recipient cells.

In conclusion, our results showed that the combination of UC with SEC led to purer EVs, which facilitated the STn detection. Additionally, STn was highly expressed in EVs compared to the secreting cells and it was present at the EV membrane, highlighting its potential use as EV biomarker in gastric cancer. In the same line of evidence, cells that express STn secreted more EVs, which may facilitate its detection in the clinical context. Finally, the presence of STn in EVs affected its internalization by recipient cells, suggesting a role during cancer progression.

Contents

Table of Figures

Abbreviations

AF4 – Asymetric flow field-flow fractionation

Asn – Asparagine

BSA – Bovine serum albumin

BabA – Antigen binding adhesin

CA-125 – Cancer antigen 125

CA 19-9 – Carbohydrate antigen 19-9

CA 72-4 – Carbohydrate antigen 72-4

CAFs – Cancer-associated fibroblasts

CDKs – Cyclin dependent kinases

CS – Chondroitin sulphate

DAPI - 4′,6-Diamidine-2′-phenylindole dihydrochloride

Dol-P – Dolichol pyrophosphate

DS - Dermatan sulphate

ECL – Enhanced chemiluminescence

ECM – Cell-extracellular matrix

EGFRvIII – Epidermal growth factor receptor variant III

EMT – Epithelial to mesenchymal transition

ER – Endoplasmic reticulum

ESCRT – Endosomal sorting complex required for transport

FBS – Fetal bovine serum

GAGs – Glycosaminoglycans

GalNAc – N-acetylgalactosamine

Glc – Glucose

GlcA – Glucuronic acid

GlcN – Glusosamine

GlcNAc – N-acetylglucosamine

GnT-V – β – 1,6-GlcNAc transferase V

GPI – Glycosylphosphatidylinositol

HA – Hyaluronan

HS – Heparan sulphate

HSPs – Heparan sulfate proteoglycans

ILVs – Intraluminal vesicles

IM – Intestinal metaplasia

KS – Keratan sulphate

mAb – Monoclonal antibody

Man – Mannose

MHC – Histocompatibility complex

MMPs – Matrix metalloproteinases

MVBs – Multivesicular bodies

NTA – Nanoparticle tracking analysis

ODG – Optiprep Density gradient

O-GlcNAc – *O*-linked β-N-acetylglucosamine

PD-L1 – Programmed death-ligand 1

ppGalNAc-Ts – Polypeptide N-acetylgalactosaminyltransferases

Pro – Proline

PTMs – Post-translational modifications

SabA – Sialic acid binding adhesin

SC – SimpleCell

SDS-PAGE – Sulphate-polyacrylamide gel eletrophoresis

SEC – Size exclusion chromatography

Ser – Serine

SLe^a – Sialyl-Lewis^a

SLe^x – Sialyl-Lewis^x

STn – Sialyl-Tn

TBS – Tris-buffered saline

TEM – Transmission electron microscopy

TF – Tissue factor

Thr – Threonine

UC – Ultracentrifugation

WT – WildType

1. Introduction

1.1. Cancer

Cancer is one of the major public health problems worldwide and is becoming a leading cause of death over the last years. According to the International Agency to Research on Cancer, in 2020 more than 19 million of new cases were diagnosed and about 10 million cancer-related deaths all around the world, highlighting that cancer burden is emerging[1]. The most common types of cancer worldwide include lung, breast, colon, and gastric cancer. Cancer is caused by an uncontrolled division of abnormal cells in a tissue of the body that can lead to multiple alterations compromising the normal function of the organism. Cancers are classified according to the tissue where they originate, that can be in the epithelial tissue that is found in the internal and external lining of the body (carcinoma); in the connective tissue that is found in the bones, tendons, cartilage, muscle and fat (sarcoma); in the blood that originate from bone marrow (leukemia) or in the lymph system (lymphoma)[2]. Generally, when normal cells have a DNA damage, they activate DNA-damage response mechanisms to repair the error, allowing the resumption of normal cell functioning. When the error cannot be repaired, the cells undergo senescence or apoptosis, blocking the process of replication[3]. However, sometimes the previous mechanisms fail, mutations occur, which might compromise the integrity and viability of the genome. In fact, with aging, the risk of mutations increases due to successive replications of cells. During the replication process, the mutated genes are inherited by daughter cells and the defects in the capacity to properly respond to DNA repair are transmitted, enabling cells to survive and reproduce[4]. Importantly, this genome aberrations can lead to multiple diseases, namely cancer where genomic instability is a fundamental feature for cancer development[5]. Through the progressive carcinogenic process, cells acquire some characteristics that are needed to guarantee their survival and replication under hostile conditions. These are also called hallmarks of cancer and include replicative immortality, genome instability, evasion of growth suppressor signals, resistance to cell death, sustained proliferation, alter metabolism, avoiding immune destruction, tumor-promoting inflammation, angiogenesis and activation of invasion and metastasis[6]. The accumulation of irreversible mutations in normal cells due to a deficiency in DNA repair generates a genome instability that increases the probability of cancer development. To promote the progression and dissemination of the tumor, cancer cells

need to pass several checkpoint steps. First, cancer cells need to avoid the G1/S checkpoint in the replication process that usually decides which cells can undergo proliferation or remain quiescent[7]. This restriction point is usually regulated by cyclin-dependent kinases (CDKs), like CDK2, CDK4 and CDK6 and D-type cyclins that exhibit oncogenic properties, therefore contributing to cancer progression. Their expression is controlled by CDK inhibitors and tumor suppressor genes like, retinoblastoma protein and p53. p53 is a transcription factor capable of inducing cell cycle arrest and apoptosis, preventing tumor progression[21]. However, if cancer cells can progress through the cell cycle, it will find another barrier at G2/M transition. This checkpoint stage is regulated by activation and deactivation of complexes composing of cyclins and CDC- family proteins, like CDC2/ cyclin B1 complex. Here, p53 also plays an important role in lowering the intracellular levels of CDC2/ cyclin B1 complex, inhibiting mitotic initiation[10]. Moreover, in cancer cells, elevated levels of cyclin B1 are known to contribute to chromosomal instability, favoring tumorigenesis. Even after completing the cell cycle, cancer cells can suffer apoptosis in response to abnormal proliferation, triggered by p53-dependent mechanisms that inhibit tumor growth[9]. In cancer cells, p53 protein is often under expressed or mutated, leading to tumor development and progression[20].

Due to this instability in the genome, the transformed cells acquire the ability to alter the normal tissue structure and function. Thus, they can dysregulate the expression of growth-promoting signals, control their proliferation rate and originate a preneoplastic cell. Contrary to normal cells that can activate cell death in response to a DNA damage or mutation, cancer cells are able to resist apoptosis by up-regulating pro-survival signals and, thus, sustaining proliferation[12]. Another barrier that cancer cells need to overtake to survive is the immune system. Naturally, it protects us from external antigens, recognizing foreign tissue and activating an efficient inflammatory response[13]. However, sometimes cancer cells can go unnoticed and promote an aberrant immune response by selecting aggressive clones, inducing immunosuppression, and contributing to tumor progression and metastasis. Tumor cells produce cytokines and chemokines that attract several elements of the leucocyte family, including neutrophils, macrophages, eosinophils, mast cells and lymphocytes, triggering chronic inflammation that increase the risk for cancer development[14]. As tumor cells avoid immune destruction, they continue to grow and proliferate in the body. To compensate the nutritional needs of tumor cells and the hypoxic environment, cells trigger an angiogenic switch that promote the formation of new blood vessels to supply the tumor that can grow to macroscopic levels[15]. Yet, the tumor vasculature shows poor organization, irregular blood flow and leak blood vessels that

facilitate the invasion of tumor cells into the circulatory or lymphatic systems. For that, cancer cells are obliged to suppress cell-cell adhesion, acquiring a high mobility and migration capacities, reflecting a mesenchymal phenotype. The detachment of cells from the primary tumor, facilitates their invasion and metastisation into the surrounding tissues or organs. The cell-cell adherent junction is a specialized region of the plasma membrane connected with cytoskeleton actin filaments, where cadherins act as Ca^{2+}-dependent adhesion molecules. E-cadherin and P-cadherin are integral membrane glycoproteins linked to the actin cytoskeleton through catenin proteins, such as α-catenin and β-catenin, playing a key role in the maintenance of the intercellular junctions in epithelial cells[16]. E-cadherin is strictly expressed in normal epithelial cells, whereas P-cadherin expression shows unique tissue distribution, detected in myoepithelial cells with high proliferative potential. Mutations in these adhesion molecules can lead to their dysregulation and consequent loss of adhesive function, promoting epithelial-to-mesenchymal transition (EMT)[17]. During EMT, the expression of cell-cell and cell-matrix adhesion molecules and their aberrant regulation is crucial for metastasis formation. In fact, expression of P-cadherin has been reported as an indicator of poor prognostic in several cancer types, such as breast and ovarian cancers, relating with tumor aggressiveness and an invasive phenotype[18,19]. Similar to cell-cell adhesion, cell-extracellular matrix (ECM) adhesion is also altered in cancer cells. Integrins mediate the interaction between cells and the extracellular matrix, through linkage with the actin cytoskeleton. Aberrant expression of these adhesion molecules also stimulate the activation of intracellular signaling pathways that participate in cytoskeletal and ECM assembly, cell migration, proliferation, differentiation and death[20]. Thus, aberrant integrin expression is related with cancer recurrence[21]. Once cells detach from the primary tumor site, they can enter the bloodstream and reach distant organs. The majority of cells that enter in blood vessels are killed, diminishing the metastatic potential[22]. The cells that survive the mechanical destruction caused by blood circulation and surveillance of immune cells, leave the blood system, and can begin to grow in the secondary tissue, creating a metastasis. This process occurs only when certain tumor cells reach the proper microenvironment in the secondary organ, according to the “seed and soil hypothesis” proposed by Stephen Paget[23]. This hypothesis determines that some tumor cells selectively metastasize to specific tissues. For example, breast cancers often metastasize to liver and rarely to kidneys. Thus, metastatic outgrow requires a proper niche for cancer cells survival, development and proliferation[24–26]. Metastasized tumors create another grade of aggressiveness, contributing to poor prognosis and survival of cancer patients.

Furthermore, metastasis is not dependent of the tumor size but requires a more aggressive therapy, compromising the patient's quality of life[27].

To concretize the malignant process, cancer cells communicate with a complex and highly dynamic tissue, the tumor microenvironment (TME) that ensure the ideal conditions for cancer development. The TME include nonmalignant cells, blood vessels, fibroblasts, immune cells, bone marrow-derived inflammatory cells, and the ECM[28]. During tumorigenesis, tumor cells interact with the tumor microenvironment by communication will endothelial cells, cancer-associated fibroblasts, mesenchymal stem cells, and immune cells such as lymphocytes and tumor-associated macrophages. These multiple interactions between cancer cells and the stroma determine cancer growth and metastasis[29]. Thus, TME contains the ideal niche for cell-cell and cell-ECM interactions that set the crosstalk between cancer cells and the surrounding environment, shaping cancer development and progression. The ECM is the major structural component of the TME and consists of water, proteins, and glycoconjugates[30]. The fibrous ECM proteins include collagen, elastins, laminins, and fibronectins that together form a network of fibers surrounded by a hydrogel containing proteoglycans. Collagen is the major fibrous protein within the ECM and provide tensile strength, regulate cell adhesion, support chemotaxis and migration, and direct tissue development[31]. Collagen can associate with elastins, recoiling tissues that suffer repeated stretch[32]. Fibronectins, the major adhesive ECM glycoprotein, mediate cell attachment and function, playing a crucial role in cellular growth and migration[33]. Also, laminins and fibronectins modulate cancer cell invasiveness and increase the metastatic potential[34]. In cancer, ECM metabolism is dysregulated, and the tumor cells become stiffer due to ECM deposition and remodeling, showing loss of tissue organization and increased cell tension. These alterations can lead to tissue fibrosis that promote tumor progression, inducing angiogenesis and invasion[35]. In addition to the fibrous proteins, the repertoire of proteoglycans participates in the maintenance of structural and functional integrity of the ECM. Heparan sulphate proteoglycans (HSPs) can bind to a variety of molecules like collagens, growth factors and other ECM proteins, to improve adhesion strength[36]. Also, versican is found on the ECM of almost all tissues and organs. This chondroitin sulphate (CS) proteoglycan serve as molecular bridge between cells and the ECM, regulating cell proliferation[37]. Relating to the glycan signature of the ECM, the hyaluronic acid is the major glycan component of the interstitial gel that embeds the fibrous proteins. In tumors, HA is produced by both tumor stroma and tumor cells, and its binding to cellular receptor activates intercellular signaling pathways that promote tumor survival, motility and invasion[38]. Moreover, glycans dictate proteolysis

patterns and regulate ligand-receptor interactions, migration, cell-cell, and cell-matrix adhesion[39]. Concerning this, glycans have been studied as potential biomarkers for cancer diagnosis and progression, with several FDA-approved cancer glycobiomarkers used in clinical practice[40,41]. In this study, we will focus on gastric cancer aberrant glycosylation.

1.2. Gastric cancer

Based on the GLOBOCAN 2020 data, gastric cancer is the 5th most common cancer worldwide, with more than one million cases diagnosed. Also, gastric cancer is the 4th cause of cancer-related deaths with about 768,000 deaths in 2020, corresponding to 7.7% of cancer-related mortality all around the world. In 2020, the number of new gastric cancer diagnosed cases in Portugal exceeded 2900, with more than 2300 deaths, corresponding to 4.9% and 7.7% of incidence and mortality, respectively, considering all types of oncogenic diseases[42]. Incidence and mortality of gastric cancer is especially dependent of each region, diet, and *Helicobacter pylori* infection[43]. Gastric cancers are mainly adenocarcinomas, a neoplasia of epithelial tissue, that arise from the mucosa of the stomach[44]. Gastric cancer adenocarcinomas can be distinguish in two different types: intestinal type, when moderate to well differentiated cancer cells formed glands, and diffuse type when cells were found to be more dispersed either as single cells or as small clusters of cells, according to Lauren's classification[45].

The intestinal type is the most common form of gastric cancer and can be caused by genetic factors which promote alterations in growth factors, cytokines and adhesion molecules that determine the progress of cancer[46]. *Helicobacter pylori* infection is the most common cause of gastritis and peptide ulcer and when the infection is prolonged, it can also increase the risk of gastric cancer development. It is well established that the intestinal type of carcinogenesis contemplates a multistep pathway were *Helicobacter pylori* triggers a chronic inflammatory process that can result in the development of gastric cancer. The progressive changes in the gastric mucosa start with chronic gastritis, followed by intestinal metaplasia, dysplasia, and gastric cancer (Figure 1). Gastritis is characterized by increased infiltration of the lamina propria, with loss of normal glandular tissue[47]. The intestinal phenotype of the glands is observed in intestinal metaplasia (IM), a more advanced stage of atrophy. The IM can be distinguished in two types: the small intestine or complete type and colonic or incomplete type. The complete type is characterized by the presence of goblet cells that express intestinal mucins, instead of

gastric mucins, changing the pattern of mucus secretion. On the other hand, incomplete type of IM expresses both gastric and intestinal mucins, resembling a large bowel phenotype. In fact, the incomplete type is considered to represent a higher risk for gastric cancer development[48]. Dysplasia presents a neoplastic phenotype, in terms of cell morphology and structure. At this stage, epithelial cells show large, hyperchromatic, and crowded nuclei, and are irregular in shape. These alterations precede the acquired capacity of cells to invade and degrade the surrounding tissue, developing gastric carcinoma.

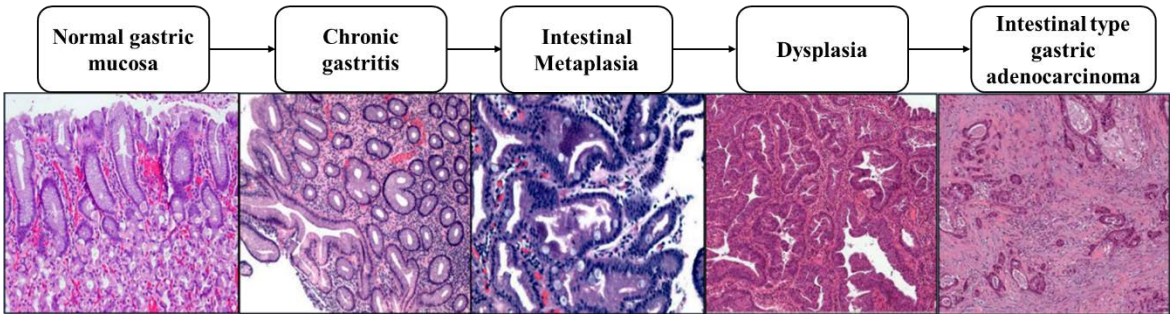

Figure 1. Sequential events of gastric cancer carcinogenesis according to the Correa cascade model. Adapted from I. Riquelme *et al.* (2015)[49].

In diffuse gastric cancer, cancer cells lie within a rich fibrous stroma that extends into the submucosal layers and infiltrate into adjacent tissue in a highly invasive manner, worsening patient's prognosis[50,51]. Contrary to the intestinal-type gastric cancer, the environmental factors have a weaker influence on the diffuse-type gastric cancer. Instead, somatic and germline mutations like *CDH1* and *RHOA* mutations have a stronger contribution for the occurrence of diffuse-type gastric cancer[52]. Also, increased inflammation of the gastric mucosa by *Helicobacter pylori* induces diffuse gastric cancer without passing through the premalignant lesions[53].

Since stomach is an internal organ, it is difficult to detect alterations that can help the diagnosis of precancerous lesions. Moreover, symptoms like difficult swallowing, bloated stomach after eating, heartburn, nausea, and stomach pain can be confused with other pathologies. Vomiting and unintentional weight loss are often the symptoms that cause suspicious and lead patients to consult a clinician. As mentioned above, *H. pylori* contributes to activate the gastric carcinogenic pathway, together with dietary habits and genetic factors. It is known that maintaining healthy habits like avoiding alcohol and tobacco, eating fresh fruits and vegetables and controlling the weight help to prevent gastric cancer[54,55]. Despite the improvements in diagnosis and treatment of gastric cancer, the prognosis remains poor due to the low rate of diagnosis during the early stages.

Consequently, when gastric carcinoma is detected, usually corresponds to an advanced stage, limiting the patient's treatment options and survival[56]. Currently, endoscopy is used to detect gastric cancer, distinguishing between superficial and advanced gastric cancer[57]. Thus, it is extremely important to define new strategies to diagnose this disease in an easily and less-invasive way, as early as possible.

Tumor-associated carbohydrate antigens have been extensively studied since most of proteins expressed by cells are glycosylated[58]. In fact, alterations in the expression and in the glycosylated patterns of serum and membrane proteins constitute potential biomarkers for health and disease. Thus, glycans and glycoproteins are used in clinic practice for screening and management of gastric cancer. Such markers include carbohydrate antigen 19-9 (CA19-9), carbohydrate antigen 72-4 (CA 72-4) and cancer antigen-125 (CA-125). CA19-9 is a modified Lewis^a blood group antigen that shows elevated levels in gastric carcinoma compared with normal tissues. However, high levels can also be found in non-cancerous pathologies, compromising its value as a diagnostic tool. Normally, expression of CA19-9 is restricted to the gastric epithelial tissues, but when cancer cells detach from the ECM and access to the circulation, these markers can be detected in the blood. Moreover, high levels of CA19-9 are associated with poor prognosis[59]. However, the measurement of this marker is not an effective method of screening and cannot be applied in early gastric cancer diagnosis. In contrary, a high molecular weight protein denominated as tumor-associated glycoprotein-72 (TAG-72), renamed CA 72-4, detects STn expressed in mucins and presents higher sensitivity and sensibility to monitor gastric cancer[60]. Increased levels of CA 72-4 are related with a more advanced tumor stage, lymph node involvement, metastasis and consequently, poor survival rate and higher risk of death[60–62]. Additionally, the tumor antigen CA-125 is a high molecular glycoprotein, MUC16, related with cancer progression[63]. It has been reported that elevated levels of CA-125 can be predictive of higher metastatic potential of tumor cells and poor prognosis of gastric cancer patients[64]. Despite the elevated levels of CA-125 observed in advanced gastric carcinomas, the expression of this marker is not remarkable in localized cancer tissues, which compromise the efficiency in the detection of early malignant lesions[65].

Due to the limitations on specificity and sensitivity on the current tumor markers, it is essential to identify additional biomarkers for the early detection of gastric cancer. Those improvements have been done in recent years, in order to provide the best clinical outcome for gastric cancer patients. Since the majority of serum proteins are glycosylated, the study of glycoproteomic signature becomes a target for further investigations to

discover novel potential biomarkers for early diagnosis and prognosis of some pathological conditions, including gastric cancer[66].

2. Glycosylation

Proteins undergo post-translational modifications (PTMs) to form mature products that can be used in processes like cell signaling and ligand binding[67], therefore contributing to increase the proteome complexity. Among the different PTMs, glycosylation is one of the most common enzymatic modifications that occur in translated proteins and lipids and is known to play an important role in regulatory and functional processes in the cells, such as cell adhesion, endocytosis, protein folding, intracellular trafficking, and receptor activation[68]. Glycosylation mostly occurs in membrane proteins, secreted proteins, and proteins in the luminal side of organelles like endoplasmic reticulum (ER), Golgi complex and lysosomes. This process is characterized by the covalent attachment of a carbohydrate to proteins, lipids, or another molecule, producing a variety of biopolymers. Glycan diversification is accomplished by the linkage of one of the nine nucleotide sugar donors to a variety of protein and lipid acceptors that then become glycosylated by the multiple saccharide epitopes. Glycosylation occurs in the ER and Golgi apparatus and is catalyzed by glycosyltransferases and glycosidases, depending on factors like substrate concentration, enzyme activity, and enzyme location in the organelles[69]. The addition of a glycan varies according to different species and cell types and can change the size, cargo, and solubility of the glycoconjugates[70]. The main types of glycoproteins include *N*-glycans, *O*-glycans, and proteoglycans. *N*-glycosylation refers to an oligosaccharide chain linked to the nitrogen atom of asparagine (Asn) in the sequence Asn-X-Ser/Thr, where X corresponds to any amino acid except proline (Pro). *N*-glycosylation requires the formation of an oligosaccharide precursor dolichol pyrophosphate (Dol-P)[71] that goes to the ER lumen where mannose (Man) and glucose (Glc) units are added. The carbohydrate-protein conjugate is processed in the ER that usually include glucose removal and addition, which contributes to protein folding and degradation[72]. As shown in Figure 2, the glycan core consists of two *N*-acetylglucosamine (GlcNAc) residues and three Man residues, to which GlcNAc, galactose, sialic acid and fucose residues can be added. This addition occurs in the Golgi apparatus, producing oligomannose, hybrid and complex *N*-glycoproteins as end products. The composition of the mature products is affected by the expression levels of glycosyltransferases, the accessibility of the

glycoprotein glycosylation sites and the time that it remains in the ER and Golgi apparatus[70].

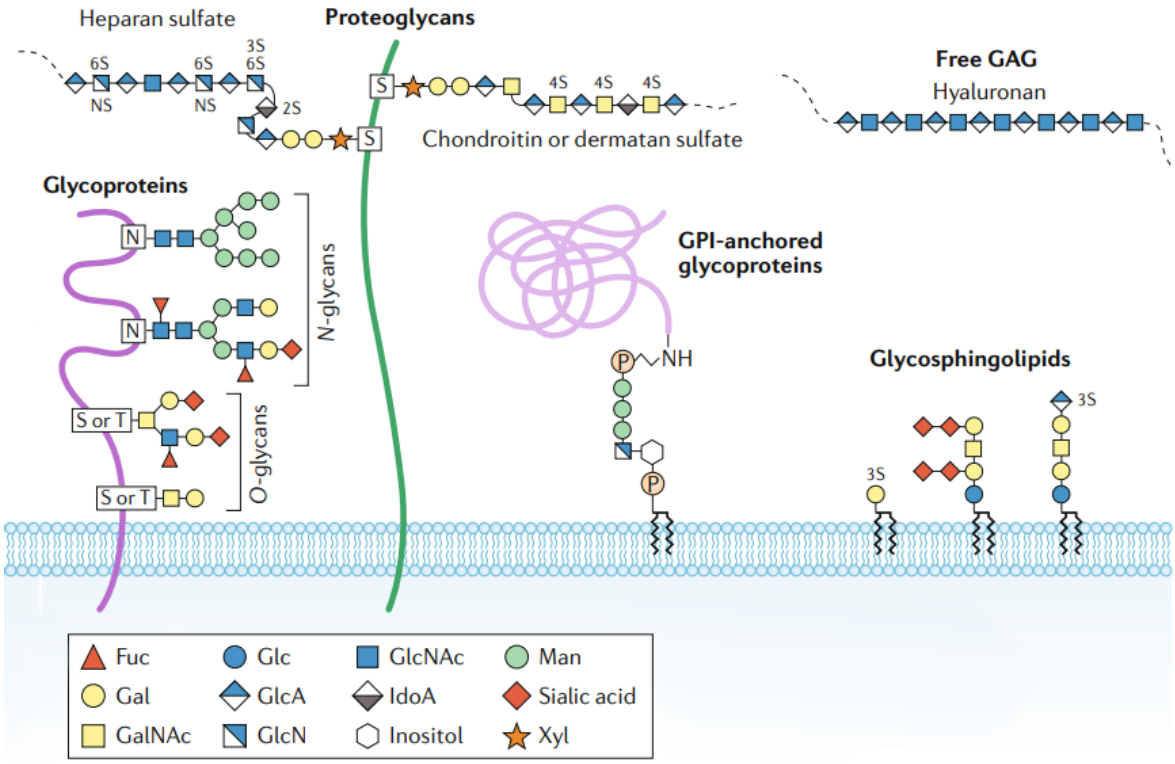

Figure 2. Schematic representation of the different families of glycoconjugates commonly synthesized by human cells. *N*- and *O*-glycans are the main types of glycoproteins. *N*-glycans contain a common core region of GlcNAc and Man residues that can be further diversified with the addition of different terminal structures such as sialic acid, galactose and fucose residues. *O*-glycans initiated with GalNAc represent the majority of the *O*-linked glycoproteins, also known as mucin-type *O*-glycans. Glycosaminoglycans (GAGs) are linear co-polymers of repeated disaccharides units that can remain free in the extracellular matrix or attached to proteoglycans through a serine (Ser) motif. Glycosylphosphatidylinositol (GPI) – anchored proteins and glycosphingolipids are another type of glycoproteins and can be found in the outer leaflet of the plasma membrane. Adapted from Reily *et al.* (2019)[73].

The biosynthetic process of *O*-glycosylation involves the addition of a glycan to the oxygen atom of a functional hydroxyl group of serine (Ser) or threonine (Thr) residues, catalyzed by *N*-acetylgalactosamine (GalNAc) transferases in the Golgi apparatus[74]. *O*-

glycans can be classified according to the first sugar attached to the protein and the additional sugar structures added to the initial glycan. The addition of GalNAc is the most common type of *O*-glycosylation found in eukaryotic cells. The produced glycoconjugates are often called mucin-type *O*-glycans[75]. Mucins can be classified into secretory and membrane-associated forms. Secretory mucins form a physical barrier that provides protection for epithelial cells that line the respiratory and gastrointestinal tracts. Membrane-associated mucins have a single membrane-spanning domain and a cytoplasmic tail in addition to the extracellular domain composed by the tandem repeated units with high content in Pro, Ser and Thr. These repeated units create multiple sites for *O*-glycosylation, forming clustered structures that play an essential connection between epithelial cells and the external mucosa surfaces of the body with protective and adhesive functions[76]. *O*-glycans are also distinguished by the type of glycans linked to the initial GalNAc, producing eight core structures that can be further extended. Contrarily to *N*-glycosylation, *O*-glycosylation does not require an oligosaccharide precursor, making the biosynthetic process of *O*-glycans simplest[77]. In this case, GalNAc is transferred from UDP-GalNAc donor into the Ser or Thr residues of a polypeptide chain of a fully folded protein. Other types of *O*-glycans include *O*-mannose, *O*-fucose, *O*-galactose and nucleocytoplasmic *O*-linked β-*N*-acetylglucosamine (*O*-GlcNAc) that occur in specific proteins or protein domains[78]. Since *O*-glycans regulate different processes such cell metabolism and immune response, alterations in these structures are crucial in many pathological conditions, including cancer[79].

Glycosaminoglycans (GAGs) are characterized by the presence of long unbranched sugar repeat chains that can occur free in the extracellular matrix or attached membrane proteins via *O*-linked glycan motifs (Figure 2). Some examples of GAGs include heparan sulfate (HS), chondroitin sulfate (CS), dermatan sulfate (DS), keratan sulfate (KS) and hyaluronan (HA). The first three have the same core structure consisting of xylose and two galactose units, followed by one glucuronic acid (GlcA). KS consists of repeated disaccharides of galactose and GalNAc, while HA involves repeated disaccharides of GlcA and GlcNAc[80]. GAGs can interact with a large variety of macromolecules depending on their negative charge, conferred by sulfate and uronic acid groups, and structural conformation, thus playing key roles in some biological functions[81]. The core protein synthetized in the ER carry the information to post-translational modification that attach GAGs covalently to the protein and produce proteoglycans with different structures and functions[82]. Proteoglycans can be subsequently classified accordantly to the predominant anionic GAG, as syndecan, versican, and lumican which contain HS, CS and KS,

respectively. During the past decades, proteoglycans were identified in connective tissues, cell membranes and intracellular compartments, where they can exert their functions depending on the characteristics of the GAG type and the core protein[80]. Advances in glycobiology have shown several biological processes controlled by proteoglycans such cell-cell and cell-matrix interactions, transport of proteins and activation of growth factors, chemokines, and cytokines[83]. Since proteoglycans are the major component of the human extracellular matrix, modifications in their biosynthesis and degradation will impact the development of several diseases, including congenital disorders and cancer[84].

Glycosphingolipids are another type of glycoconjugates where a glycan is linked to a lipid ceramide. Glycosphingolipids are the major component of the outer cell plasma membrane and are synthetized through the addition of sugars first to the ceramide residue and then to the growing glycan moiety. Depending on the additional residues, glycosphingolipids can be neutral, sialylated or sulfated[85]. As shown in Figure 2, GPI proteins are attached to the membrane through phosphatidylinositol. The core of the GPI-anchored protein is composed of phosphoethanolamine linked to three units of Man and glucosamine (GlcN). Some GPI proteins are known to play a key role in cell-cell and cell-matrix interactions and may act as differentiation markers and membrane receptors. GPI-anchored glycoproteins are essential in multiple biological functions, including cell adhesion, metabolism, and proliferation and some of them are responsible for tumorigenesis and progression[86].

2.1. Gastric cancer aberrant glycosylation

Aberrant glycosylation occurs almost in all types of human cancer cells and leads to the expression of tumor-associated carbohydrate antigens[69,87]. The most commonly occurring glycosylation alterations in cancer include sialylation, fucosylation and modifications in the glycan chain length, producing shorter *O*-glycans and more branched *N*-glycans[88]. There are some factors responsible for altered expression of glycans in cancer cells, including the under- or overexpression of glycosyltransferases/glycosidases[89,90], disfunction of chaperone activity[91], changes in the tertiary conformation of the peptide core, variability of acceptor substrates, availability and abundance of sugar nucleotide donors and cofactors[92], and the expression and location of specific glycosyltransferases in the Golgi apparatus[93]. Among all, changes in the

expression of glycosyltransferases and glycosidases involved in the synthesis and catabolism of glycans seems to be the principal mechanism responsible for aberrant glycosylation in cancer.

Increased expression of complex β1,6-branched *N*-glycans often occurs in cancer cells, induced by the expression of the β1,6-GlcNAc transferase V (GnT-V)[94]. *N*-glycans can be further modified and elongated with repeated Galβ1,4GlcNAcβ1,3 units in the Asn residues and topped with sialic and fucosyl epitopes (Figure 3). In gastric cancer cells, overexpression of GnT-V glycosyltransferase induces loss of E-cadherin function, which compromises cell adhesion and assembly[95]. Interestingly, E-cadherin expression in gastric mucosa cells is dependent on the presence of β1,6-branched *N*-glycans, being its functional impairment correlated with increased invasive and metastatic potential[96]. Among the formation of β1,6-GlcNAc-branched *N*-glycans, the GnT-V glycosyltransferase also enhance the production of integrin-mediated cell migration in gastric cancer cell lines. This protumorigenic activity of the GnT-V can be inhibited by the GnT-III glycosyltransferase, which negatively regulate cell migration[97].

Abnormal expression of UDP-GalNAc polypeptide N-acetylgalactosaminyltransferases (ppGalNAc-Ts), the family of enzymes that catalyzes the primary step of mucin *O*-glycans formation, shows to be involved in the regulation of truncated structures and exposure of the peptide backbone. Furthermore, studies concerning the expression patterns of different types of ppGalNAc-Ts show that these molecules participate in some carcinogenic events, including venous invasion, tumor differentiation and metastasis in gastric cancer[98]. Also, sialyltransferase expression in gastrointestinal cancer cells became relevant in the past decades since they add sialic acid to the terminal carbohydrate, stopping chain growth and producing sialyl T (ST) and sialyl Tn (STn) antigens that are related with patients' poor clinical outcome[99].

Increased expression of sialylated terminal structures and accumulation of simple-mucin-type glycans were found during gastric carcinogenic cascade. Incomplete synthesis and neo-synthesis processes are the principal mechanisms underlying the tumor-associated alterations of cell surface carbohydrates structures[100]. The incomplete synthesis process occurs mainly on early stages of tumor and results from the impairment of the normal synthesis of complex glycans, leading to the accumulation of truncated structures like STn antigen, observed in gastric carcinomas[101]. On the other hand, the neo-synthetic pathways occur in more advanced stages and is due to the induction of genes related with the expression of sialyl-Lewis^{a} (SLe^{a}) and sialyl-Lewis^{x} (SLe^{x}). Together with Le^{a} and Le^{b}, SLe^{a} are classified into type 1 Lewis blood group, whereas

SLe^x, Le^x and Le^y are known as type 2 Lewis antigens[102]. In gastric carcinogenesis, the recognition of receptor ligands is crucial to bacterial interaction and dissemination of *Helicobacter pylori*[103]. Thus, as demonstrated in some studies, the blood group antigen binding adhesin (BabA) recognizes ABO(H)/$Lewis^b$ blood group antigens expressed in glycoproteins of the gastrointestinal tract while the sialic acid binding adhesin (SabA) mediates *H. pylori* attachment through binding to SLe^a and SLe^x carried by glycosphingolipids and glycoproteins. Additionally, expression of BabA adhesin provides a higher risk of developing gastric lesions that can evolve to gastric cancer[104,105].

Another family of enzymes involved in the formation of tumor-associated antigens are fucosyltransferases. Among all, FUT1, FUT2 and FUT3 code for the enzymes responsible for the synthesis of type 1 and 2 Lewis antigens in epithelial cells. Thus, FUT 1 and FUT2 participate in the biosynthesis of $SLe^{a/b}$ and $SLe^{x/y}$ percursors and FUT3 is responsible for the addition of fucose residues into these structures to produce SLe^a and SLe^x antigens. Also, increased expression of SLe^x occurs in response to the overexpression of ST3GalT, a sialyltransferase induced by *H. pylori* infection[106]. Increased levels of sialylated epitopes are due to the upregulation of these enzymes, altering the glycoproteome phenotype of infected patients. Furthermore, the expression of sialylated molecules such as STn, SLe^a and SLe^x has been observed in gastric cancer cells and correlates with invasiveness and metastasis, providing a poor prognosis for cancer patients[39,107].

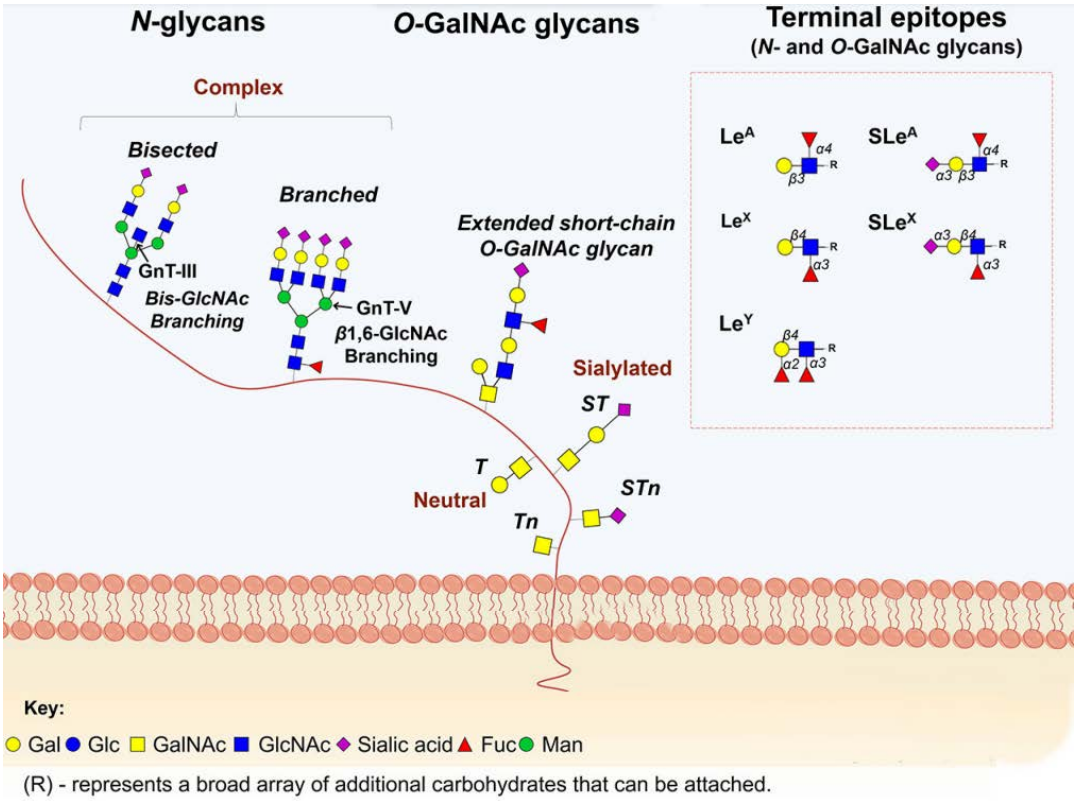

Figure 3. Main classes of glycans in cancer. *N*-glycans experience further structural maturation to generate complex bisected and branched structures. The simplest *O*-GalNAc glycans T and Tn antigens can be further elongated into different core structures that serve as scaffolds for more complex *O*-GalNAc glycans like ST and STn antigens. Both *O*- and *N*-glycan chains are generally branched and/or elongated and may present sialic acids, Lewis's blood group related antigens and/or their sialylated counterparts as terminal structures. Adapted from A. Peixoto *et al.* (2019)[108].

Like all mucosal tissues, the mucous layer of the human gastric antrum is predominantly composed by mucins and represents the ideal niche for *H. pylori* adhesion[103]. Thus, aberrant expression of glycans disrupt the protective function of mucins and enhances *H. pylori* infection, leading to gastritis and gastric cancer[109]. Mucin carbohydrate chains are the major carriers for Lewis's blood group antigens, being the expression of mucins and sialylated structures co-regulated in normal gastric mucosa. Moreover, Le^a, Le^b and SLe^a co-localize with superficial cells expressing MUC5 mucin and Le^x, whereas Le^y co-localize with MUC6 in deeper glands[48,110]. Also, the expression of mucin-type *O*-glycans suffers alterations when epithelial cells became malignant and may allow the monitor of pathological conditions observed during gastric carcinogenesis. The

human gastric epithelium is characterized by the expression of high levels of MUC1, MUC5 and MUC6, whereas gastric carcinomas show decreased levels of these mucins and higher levels of MUC2, MUC3 and MUC4, normally found in intestinal cells[111]. MUC1 is a transmembrane highly glycosylated protein, produced by glandular epithelial cells and has been recently identified as an *H. pylori* binding target[103]. Additionally, the expression of under-glycosylated forms of mucins and high levels of MUC1 are related with a poor prognosis of gastric cancer patients[112]. Overexpression of MUC1 interferes with cell-cell and cell-matrix adhesion since it is considered as an anti-adhesion molecule[113]. Diminished adhesion in tumor cells may have consequences in cancer progression, invasion, and metastasis. Compared expression of different types of mucins demonstrated the expression of MUC1 and MUC5AC in foveolar cells and MUC6 in deeper gastric glands[114], showing that the characteristic cell- and tissue-specific distribution may be related with the specific function of each mucin[111]. The study of MUC2 expression showed elevated levels in gastric cancer carcinomas[114], being this intestinal-type mucin the major carrier of STn antigen in intestinal metaplasia and gastric cancer[48]. Like MUC2, MUC3 is often expressed in the intestinal epithelium. However, studies demonstrated expression of MUC3 in gastrointestinal cells, suggesting the loss of normal mucin regulation[79,111].

Abnormal expression of glycans is related with several stages of the gastric cancer cascade, including cell adhesion, differentiation, invasion, and metastasis[115]. Thus, the gastric cancer aberrant glycosylation constitutes an important research field for clinicians and investigators to improve our understanding of the physiological and pathological mechanisms regulated by glycans. Concerning this, glycans have proven to play crucial roles in cellular behavior and carcinogenesis, being a useful biomarker for screening intestinal metaplasia and gastric cancer[116]. Strategies that exploit this aberrant performance can enhance and improve the clinical diagnosis and prognosis of gastrointestinal cancer patients.

2.2. Truncated *O*-glycans in gastric cancer

The premature termination of *O*-glycans elongation constitute a mechanism by which immature glycoforms are produced. Truncated *O*-glycans occur on the majority of epithelial cancers and in pre-malignant lesions, considered as potential biomarkers for cancer detection[117]. Truncated *O*-glycans include T (Galβ1-3-GalNAcα1-O-Ser/Thr), Tn (GalNAcα1-O-Ser/Thr), ST (NeuAcα2,6-Galβ1-3-GalNAcα1-O-Ser/Thr) and STn

(NeuAcα2,6-GalNAcα1-O-Ser/Thr) antigens[118]. Their up-regulated expression is associated with tumor aggressiveness and has a major impact in the prognosis of gastric cancer patients[115,119]. Profiling the expression of these tumor-associated carbohydrate antigens show a high prevalence of Tn and STn, whereas T antigen was less common in gastric carcinomas[119].

T antigen, also known as core 1 structure, is an intermediate structure during mucins maturation since it can be further modified and elongated. T antigen is not detected in healthy tissues neither in gastric pre-malignant lesions. However, it is expressed in gastric cancer cells, associated with immune response invasion[102]. T antigen is found in the Golgi area of the foveolar cells and mucous glands, being its expression related with wall and lymphatic invasiveness of gastric tumors[103].

In normal cells, Tn antigen suffers elongation to produce T antigen by the addition of a galactose residue regulated by the C1GalT1 glycosyltransferase together with the *COSMC* chaperone. However, in the case of mutations or loss of heterozigoty of the *COSMC* gene, can result in the homologous expression of Tn and STn[99]. Tn antigen is detected in the supranuclear region of the cells of the surface epithelium and in the mucous glands of the antral mucosa[121]. Tn antigen is expressed in the early stages of tumor development and its expression is related with clinical progression, poor prognosis and survival[119].

The biosynthesis of STn is regulated by ST6GalNAcI, a sialyltransferase expressed in several epithelial cancers, including gastric cancer. ST6GalNAcI also plays an important role in gastric cell behavior, being correlated with tumor development, progression, migration, and invasion[84]. STn is often co-expressed with Tn antigen and therefore mechanisms that regulate Tn expression are implicated also in STn expression, as alterations in *COSMC*, alterations in Golgi apparatus and glycosyltransferases dynamics[106]. STn expression is observed in the cytoplasm of the neck cells and adjacent foveolar epithelium, and more rarely, in mucous glands. Additionally, STn is considered the most abundant carbohydrate structure in goblet cells[119]. Studies with monoclonal antibodies specific for STn reveal that detection of this antigen is rare in normal tissues, whereas is overexpressed in diverse cancer tissues[115]. Furthermore, there is evidence that higher levels of STn expression in gastric carcinoma appear in advanced tumors stages, leading to poor prognosis compared with tumors that express low levels of STn, reflecting a higher tumor burden. Thus, differences in the degree of expression of STn with respect to age, tumor stage, invasion and metastasis constitute proof of the predictive value of this carcinogenic antigen in prognosis of gastric cancer[126]. Pre-lesions of gastric

cancer, like dysplasia and intestinal metaplasia also express STn, thus contributing to early detection of gastric cancer[121,127]. The presence of STn in early-stage patients corroborates its powerful usefulness as tumor maker, allowing to distinguish between patients that need a closer follow-up and a rapid activation of treatment measurements. Although not every gastric tumor cells express STn and its expression depends on each patient, several studies demonstrate that the level of expression is strongly correlated with survival outcome[115,128]. Additionally, is has been proven that STn induce major phenotypic alterations in gastric cancer cell lines with *COSMC* knock-out. The manipulated gastric cancer cell lines show increased expression of the STn antigen responsible for the acquired mesenchymal-like morphology and enhancement of cellular motility. Also, the expression of STn antigen interferes with cell-cell and cell-matrix adhesion, promoting an invasive phenotype of gastric cancer cells. This can be due to the upregulation of the *SRPX2* and *RUNX1* genes and *O*-glycosylation of some adhesion molecules, namely laminins and integrins[129]. Overall, genomic alterations and overexpression of STn can induce invasiveness and metastasis, the major causes associated with cancer death. Besides the regulation of STn on metastasis, this antigen can, as well, play a role in cellular recognition by the immune system, protecting metastatic cells from degradation in the blood stream[99]. Diverse studies concerning the relationship between STn expression and its prognostic value reported correlation with gastric wall penetration, lymphatic invasion, metastasis and stage of gastric carcinoma[119, 123,130]. Concerning the crucial role of STn in the different cancer hallmarks, this antigen should be further investigated as it shows potential to be used in the clinical practice as prognostic biomarker in gastric cancer patients. Importantly, our group pioneered the detection of STn in extracellular vesicles secreted by gastric cancer cells, which constituted an significant proof of the potential usefulness of STn as gastric cancer biomarker[131].

3. Extracellular vesicles biogenesis and uptake

Extracellular vesicles (EVs) were first observed as procoagulant platelet-derived particle in plasma in 1946[132] and referred as “platelet dust” in several other studies[133]. In the past decade, the scientific and clinical interest in EVs have emerged and it became necessary to standardize EVs nomenclature and protocols. To facilitate the classification of these nanoparticles, the International Society of Extracellular Vesicles suggested the term EVs to describe particles naturally released by almost all types of cells, delimited by

a lipid bilayer and lacking the capacity of replication[134]. EVs are released by different types of cells, including platelets, leukocytes, erythrocytes, and epithelial cells, and are detected in several body fluids. Moreover, EVs can be categorized into exosomes, microvesicles and apoptotic bodies depending on the physiologic characteristics of vesicles, such as size, cargo, density, and composition[135].

Exosomes are cell-derived vesicles with 40-150 nm of diameter and are present in almost all types of human body fluids, including blood, serum, plasma, urine, and cerebrospinal fluid. Exosomes are used to describe small EVs secreted by eukaryotic cells when membranes of multivesicular bodies (MVB) fuse with the plasma membrane, during endosome maturation[136]. The biosynthesis of exosomes involves the formation of intraluminal vesicles (ILVs) within MVB, essential intermediates in endolysosomal transport formed by the invagination and scission of buds from the endosomal limiting membrane into the lumen[137] (Figure 4). Current studies on exosomes biogenesis show that endosomal sorting complex required for transport (ESCRT) proteins are involved in endosomal membrane invagination to generate ILVs in the lumen of the organelles[138]. Proteins such ESCRT component Tsg101 and the complex alix-syntenin-syndecan govern the selection of endocytic cargo and physical membrane-remodeling and abscission required for exosome formation. Thus, stimulation of these complexes induces endosomal synthesis and release. Exosome formation can also occur independent of the ESCRT machinery by the conversion of sphingomyelin to ceramide, inducing a curve shaped morphology of the endosomal membrane[139]. Independently on the biosynthetic pathway, the release of exosomes is mediated by Rab family GTPases, namely Rab11, Rab27, and Rab35[140–142]. Rab11 and Rab35 regulate the recycling of membrane components from the endosomal compartment to the plasma membrane, enhancing cytokinesis and cell migration. Rab27 act on the transport of endosomal compartments to the plasma membrane, playing an important role in exosome secretion. Moreover, downregulation of these proteins diminishes the secretion and release of exosomes to the extracellular space. On the other hand, microvesicles are nanoparticles with 50-2000nm of diameter, released from the plasma membrane under both physiologic and pathological conditions[126]. Microvesicles are formed by outward protrusion or budding of the plasma membrane and their release is regulated by stimulation of cell surface receptors in a Ca^{2+}-dependent manner. Interestingly, a recent study provided evidence for the recruitment of ESCRT component Tsg101 to the plasma membrane during microvesicle biogenesis[145]. Finally, apoptotic bodies measure 100-5000nm and originate from dying cells as they disintegrate[146]. Besides the differences between the subpopulations of EVs, the isolation

of these nanoparticles shows some limitations. For instance, the size ranges of exosomes and microvesicles may overlap, making it difficult to separate and characterize these particles. For this reason, the term EVs it will be used as a general term referring to nanoparticles released by cells to the extracellular environment.

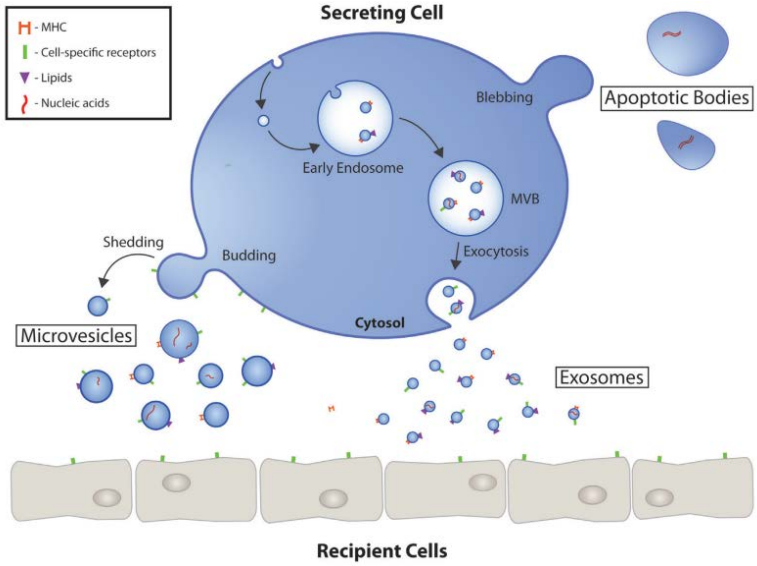

Figure 4. Schematic representation of EV biogenesis and secretion by eukaryotic cells. Exosomes are formed as intraluminal vesicles within multivesicular bodies during endosome maturation. Microvesicles arise from the outward budding and fission of the plasma membrane. The largest EVs, apoptotic bodies, are formed during programmed cell death. Adapted from D. Gustafson *et al.* (2017)[147].

After the release into the surrounding area, EVs can be broken down exhibiting their cargo or enter the circulation to fuse with target cells. EVs exert their cargo to target cells through direct contact with cell membrane, endocytosis of vesicles or fusion of vesicles with cell membrane, contributing to horizontal reprogramming of the host cell[148,149]. EVs transport proteins, lipids, glycans and nucleic acids including both RNA and DNA derived from the originating cell[150–152]. In fact, the proteins found in EVs come almost exclusively from plasma membrane, cytosol, or endocytic compartments, confirming their biosynthetic pathway. Additionally, the protein composition of EVs and their post-translational modifications determine their functionality in several ways, including their biodistribution, binding of EVs to target cells or to the ECM[153]. Specific membrane proteins such as major histocompatibility complex (MHC), tetraspanins, ESCRT (Alix and Tsg101) and heat shock proteins (Hsp60, Hsp70 and Hsp90) participate in the interaction of vesicles with

target cells, triggering integrins and calcium signaling pathways. The most studied proteins are tetraspanins such as CD9, CD63 and CD81, which mediate cellular penetration, invasion, and fusion, acting as EV markers[154]. Also, the lipid content of EVs plays a key role in signaling and sorting. EVs share common lipid structures with the cell of origin, however some lipids can be specifically associated with different types of EVs[152]. Furthermore, EVs are enriched in cholesterol, sphingomyelin and glycosphingolipids, when compared with the cells that originate them, suggesting that its membranes contain lipid raft-like domains[155]. Like the other molecules, lipids are not included in EVs through a randomly process, but accurately selected since they are crucial to EVs rigidity, protection, and resistance. Additionally, EVs can carry messenger and microRNAs, inducing intercellular signaling through the acquisition of genetic material by fusion or endocytosis[156]. Thus, mRNA transfer to target cells have been shown to enhance proliferation and apoptosis resistance under stress conditions. Data shows significant differences in the gene profile analysis of exosomal mRNA compared to donor cells. Also, miRNAs were found to be highly secreted to EVs, confirming that some miRNA may be uniquely packed into the vesicles. DNA has also been found[151] as well as long and short non-coding RNA and tRNA fragments, in a small number of cases[154].

The significance of EVs relies on the capacity of intercellular communication through horizontal transfer of cargo between different cells within an organism and the influence over recipient cell's function, occurring mostly by phagocytosis, endocytosis and micropinocytosis reviewed elsewhere[157]. Despite the evidence, EV uptake has not been completely studied and still needs further investigation to unravel the key mechanisms involved in this process. The vast repertoire of glycans present in EVs interfere with cellular uptake, protein sorting to EVs and interaction with target cells[135]. In fact, EV uptake shows to be dependent on heparin-sulphate proteoglycans (HSPs) that act as true internalizing receptors of EVs in recipient cells[160]. This can be translated for the potential use of drug delivery therapies on cancer cells using HSP-binding properties of cancer-derived EVs. Also, the uptake selectivity might be more dependent on the recipient cell type rather than on EVs, as EVs are mostly tracked by generic fluorescent lipophilic membrane dyes such as PKH26[161], PKH67[162], DiD[163], DiI[164] and CellMask[165]. To access the role of surface glycans in EV uptake, two hepatic murine cell lines were treated with PNGase F that cleaves *N*-glycans and neuraminidase that removes sialic acid residues from glycans[164]. Both treatments show an increased efficiency in EV uptake, with different glycosylation profiles leading to different uptake affinities. Also, the enrichment of specific glycans in cancer-derived EVs have shown to modulate EV uptake by an ovarian cancer

cell line[166]. In this study, the removal of sialic acid residues increased, however non-significantly, EV uptake. This effect was observed both *in vitro*[158] and *in vivo*[167] studies, showing that sialylation play an important role in interactions with recipient cells. However, further investigations are required to stablish a bridge between EV glycomics and functional experiments.

3.1. Current strategies for EV isolation

Due to the limitations on size overlap and similarities in morphology and composition, most EV isolation methods do not unequivocally purify specific types of vesicles, but separate complex mixtures. To date, EVs have been isolated from several biological fluids, including blood, saliva, breast milk and urine. The most studied methods for EV isolation based on density and size include ultracentrifugation[168,169] (UC) and size exclusion chromatography[170] (SEC). Microfiltration, microfluidic isolation, density gradient separation and immunoaffinity capture methods are also used aiming to separate and characterize pure subpopulations of EVs[168,171–173]. Differential UC uses centrifugal force to isolate and enrich an EV population according to their buoyant density by applying increasing centrifugal speeds and/or time[174]. During each centrifugation, the particles that are heavier than the supernatant will sediment. The multiple centrifugation steps with increasing centrifugation speeds lead to the separation of cells, cell debris and EV pellets[169]. UC is the most commonly method used for EV isolation due to its applicability in isolating EVs from large volumes of cell culture medium and biological fluids and do not impact EV downstream analysis. However, the EV populations can be contaminated with protein complexes that sediment at the same time of EVs due to similarities in density, limiting its use in the clinical setting[175]. This problem can be solved by different methodologies that separate EVs considering its size. SEC, also known as gel-filtration chromatography, separates EVs from proteins by trapping the molecules to the stationary phase[176,177]. The EV content elutes first than proteins, thus showing to be an adequate method for EV isolation, obtaining purified EV populations that retain integrity and functionality[178]. These characteristics make the SEC an adequate method to be easily applied in the clinical setting for diagnosis purposes, despite its high cost and the need for a previous EV concentration for certain downstream applications[170, 176,179,180]. To this date, there is no gold standard method for EV isolation, as different protocols present different advantages and disadvantages. Our group have already demonstrated that different EV

isolation methodologies lead to different EV protein and glycan profiles, reflecting distinct EV purities[131]. Comparing four different EV isolation protocols, EVs isolated by the combination methodologies of UC with Optiprep density gradient (ODG) and UC with SEC showed higher purity confirmed by western blotting analysis of protein and glycan content. With their results, it is assumed than an extra step of EV purification, such as ODG or SEC, must be necessary for EV biomarker research. Others, also demonstrated that ODG isolated less but purer EV populations compared with UC, total exosome isolation and exoQuick protocols[181]. Another technique used to isolate nanoparticles is asymmetric flow field-flow fractionation (AF4) technology that consider density and hydrodynamic properties to separate a heterogeneous population of EVs by two perpendicular flows. AF4 allows to distinguish different subpopulations of EVs, namely small and large exosomes and exomeres, based on biophysical and molecular content[182]. In addition, the use of immunoaffinity methods has shown a marked increase, suggesting new applications to achieve better yield and purity of EVs. Affinity methods use magnetic beads coated with monoclonal antibodies against a specific EV surface marker[168]. Proteins like CD9, CD63 and CD81 serve as EV markers and were already used to isolate EVs based on the immunoaffinity properties. However, antibody coated beads against these markers may select a subpopulation of EVs since not all vesicles express the same proteins[183]. Therefore, the subsequent analysis will not reflect the whole population of EVs within a sample. In fact, a study with different EV enrichment methods show distinct subpopulations of urinary EVs since they have specific affinity to EV markers[184].

Many efforts have been done in order to standardize isolation protocols since different isolation methods have demonstrated different capacities to isolate EVs and influences the depletion of lipoproteins, protein contaminants and the overall yield of EVs[181]. Nevertheless, it cannot be claimed that there is a unique method to isolate EVs or the one that guarantees complete purity. The combination of multiple-step protocols has been applied to isolate EVs with higher purity to efficiently discover EV biomarkers, validate EV-related functions in biological processes and translate EV specificities to clinical practices[185,186].

3.2. Cancer-derived extracellular vesicles

Cancer-derived EVs play an important role in all cancer hallmarks, altering the physiology of both surrounding and distant non-malignant cells and allowing dissemination

and growth of cancer cells. Whereas the size of EVs is similar between healthy and cancer patients, cancer-derived EVs are secreted in higher levels, showing altered cargo in a stage dependent manner[187]. A pilot clinical study demonstrated that circulating EVs were reduced after operative treatment compared with preoperative plasma samples, suggesting that tumors are partially responsible for the secretion and release of EVs[188]. However, high levels of EVs can also be the result of tumor response under stress conditions. Thus, tumor-derived EVs are used by the primary tumor to promote angiogenesis, invasion, and metastasis, altering tumor microenvironment, and supporting progression of cancer cells[189]. As tumor grows, EVs derived from cancer cells can suppress immune cells, avoiding immune detection and become pro-tumorigenic and metastatic. Cancer-derived EVs can promote these processes by different mechanisms, including the induction of vascular development[190], the release of active matrix-degrading enzymes[191], and production of tissue factor[192].

Tumor-derived EVs play an important role in the differentiation of fibroblasts into cancer-associated fibroblasts (CAFs) as well as in the induction of mesenchymal stem cells to become tumor supportive cells. This occurs by transfer of growth factors and cytokines that promote tumor proliferation such as transforming growth factor-β and several miRNAs[193]. Interestingly, EVs derived from breast cancer cells carrying miRNAs induce motility and stemness[194]. Also, tumor-derived EVs secrete oncogenic proteins such as epidermal growth factor receptor variant III (EGFRvIII) that activates the mitogen-activated protein kinase and Akt signaling pathways responsible for cancer growth[195]. The transfer of EGFRvIII to cells that lack this oncoprotein give them an advantage to contribute to the horizontal transmission of pro-tumorigenic proteins, increasing tumor cells growth[195]. Particularly in gastric cancer, exosomes seem to potentiate tumor growth and proliferation through the activation of these mechanisms[196]. Moreover, the angiogenic and metastatic potential of cancer cells result from loss of cell-cell and cell-ECM contact. EVs are strongly associated with ECM remodeling and degradation by the secretion of matrix metalloproteinases (MMPs) such as MMP-1, namely from gastrointestinal cancer cells[197]. MMP3, MMP9 and MMP13 were also reported to be responsible for the spread of tumor cells and invasion in squamous carcinoma cells[198]. Additionally, coagulation and angiogenesis can be regulated by EVs transporting tissue factor (TF) or other procoagulant factors playing a putative role in tumor cancer survival. High levels of EVs containing TF protein have been reported in the plasma of breast cancer patients, favoring thrombosis[199]. Also, TF correlates with immune invasion and metastasis in many human malignancies[200]. To evade the immune system, tumor-derived EVs can regulate T cells

expansion, impair the antigen presentation, or interfere with host's immune response. Studies reported that tumor-derived EVs have the capacity to inhibit the growth of cytolytic effector cells such $CD8^+$ T cells and NK cells, responsible for anti-tumor activity[201]. The stimulatory effects of tumor-derived EVs on $CD4^+$ T cells and the inhibitory impact on $CD8^+$ T cells confirms the role of tumor-derived EVs on the escape from the host immune system. Invasion and metastasis can also be modulated by EVs through the molecules involved in EMT or by preparing a pre-metastatic niche, reprogramming non-malignant cells at distant sites[202]. Moreover, tumor-derived EVs were further reported to play a significant role in the metastatic behavior of human melanoma cells through the receptor tyrosine kinase Met[189]. The Met oncoprotein is co-expressed with hepatocyte growth factor in several malignancies including breast and pancreatic cancer[203,204]. Interestingly, Met activation induces cell dissociation and motility, facilitating invasion of epithelial cells through extracellular matrices[205]. Furthermore, metastatic melanomas release EVs that carry programmed death-ligand 1 (PD-L1) on their surface, responsible for the suppression of cytotoxic activity of $CD8^+$ T cells, facilitating tumor growth and proliferation at the metastatic site. The binding of PD-L1 to its receptor and consequent inhibition of T lymphocytes protects tumor from immune surveillance[206].

Since glycans play a constitutive role at EV surface, they have gained importance in the last decades to understand their influence in EV biogenesis. EVs secreted by cancer cells show an aberrant glycosylation pattern which allows the fully analysis of the impact of glycans in cancer and the identification of stem-cell-like phenotypes. Importantly, the presence of high mannose epitopes, complex *N*-glycans, sialic acid residues and fucosylated epitopes, with the simultaneous absence of blood group antigens A/B were detected in EVs from several cell lines, confirming the role of glycans in protein sorting. Another study detected EVs secreted by ovarian cancer cells enriched in specific high mannose and sialylated structures, namely LGALS3BP, an abundant sialoglycoprotein[166]. ST6GalNAc1, the enzyme responsible for STn production, can be transferred to recipient cells through secreted EVs and lead to significant changes in cellular behavior. ST6GalNAc1 can sialylate cell-surface proteins such as β1-integrins, confirming the role in potentiating malignant transformation, and regulating metastasis[207]. Furthermore, STn was reported to be present in secreted EVs from human gastric cancer cell line[131], which is associated with cancer cell aggressiveness and patient's poor prognosis[115].

The ability of EVs to secrete a vast repertoire of glycans provide an open area of research to understand their role in tumorigenesis. The study of EV glycosylation has emerged, however their function in EV biogenesis and protein sorting remains poorly

understood. In this field, many efforts have been done to determine the glycan signature of different populations of EVs. Importantly, glycans can be extensively used as biomarkers in cancer detection and monitoring, in addition with the capacity to distinguish between malignant and non-malignant lesions. The emerged research in EV glycosylation may possibly open new perspectives in cancer diagnosis, prognosis, and therapeutics.

3.3. Extracellular vesicles as cancer biomarkers

The vesicles and their cargo have been considered as potential biomarkers since they are capable of transport and transfer specific cargo secreted by cancer cells to recipient cells[195]. In fact, its phospholipid bilayer provides a greater stability to EV cargo, resulting in higher resistance to degradation and higher capacity to travel long distances, compared to free proteins, lipids, and nucleic acids in the cytoplasm[208]. In addition, EVs can circulate in several body fluids and can be used in minimally invasive tools to monitor disease stage. Studies showed elevated levels of circulating EVs depending on disease state in several cancer types including renal and lung cancers[173,194]. Thus, circulating EVs can be used as biomarkers since their composition reflects the changings taking place in their corresponding cell of origin and, in the case of cancer, the tumor cargo, extending perspectives for biomarker measurements[211,212].

Among the components of EVs, proteins and miRNAs have been the most studied molecules with regard of their potential as tumor biomarkers for cancer diagnosis and monitoring. EGFRvIII was identified as EV tumor-specific marker in glioblastoma cancer patients[195]. In melanoma patients, increased levels of CD63 expressed in EVs correlates with an increase in tumor size[213]. Elevated levels of CD63 were also found in patients with oral squamous cell carcinoma, as well as caveolin-1[188]. The relationship between levels of these markers before and after surgery show that EVs secretion correlates with prognosis and overall survival of patients[188]. Recently studies reveal the presence of CD97 on the membrane surface of EVs in gastric cancer patients, related with local growth, invasiveness and metastasis[214]. Also, exosomes secreted by HER2-overexpressing breast carcinoma cells block the therapeutic activity of anti-HER2 antibody, demonstrating the impact of tumor EVs in therapeutics[215]. HER2 presents a high expression pattern in gastric cancer-derived exosomes compared with controls[216]. In addition to proteins, miRNAs within circulating EVs have gained attention regarding their highly promising diagnostic and prognostic potential for many cancer types. Ovarian malignancies can be

distinguished from benign lesions based on the expression of exosomal miRNAs[217]. Other exosomal miRNAs were found to be associated with specific cancers, including urine-derived exosomal miR-107 and miR-574-3p in prostate cancer[218], plasma-derived exosomal miR-195 in breast cancer[219], and serum-derived exosomal miR-21 in glioblastoma[220]. All these exosomal miRNAs are highly expressed in tumor compared with normal tissues, reflecting the tumor burden. A study from gastric cancer biopsies found that downregulation of miRNA-101 in exosomes supports tumor cell proliferation[221]. Although the role of EV glycosylation is still being explored, the investigation on EV glycome is emerging to understand the impact of glycans on diagnosis, prognosis and therapeutics.

3.3.1. EV glycans as cancer biomarkers

Along with proteins and RNAs, glycans are highly detected in EVs and thus, are considered as powerful biomarkers. Increased levels of CA19-9, refleting high levels of SLe^a, correlates with poor prognosis of cancer patients[60]. The combination of serum CA19-9, exosomal CD82 and exosomal glypican-1 was employed to diagnose and monitor the clinical state of the pancreatic cancer patients[222]. CA125 assay detects circulating mucin glycoprotein MUC16 which aberrant STn glycoforms of MUC16 have been found to be elevated in invasive epithelial ovarian cancer patients[223]. Also, increased expression of CA125 was found in exosomes, showing improved diagnosis sensivity[224]. The presence of EpCAM glycoprotein in exosomes is elevated during ovarian cancer progression and considerably higher when compared to benign lesions or healthy donors[225]. The same study reveals EVs containing *N*- and *O*-glycosylated GPI-anchor CD24 protein that plays a role in diagnostics and shows to be related with poor prognosis of several cancer types. The membrane glycoprotein CD133 has been used as a marker to identify cancer stem cells of solid tumors, including pancreatic cancer, since its expression is exclusively found in tumor cells[226]. The investigators suggest that exosomal levels of CD133 are an independent risk factor that contributes to tumor progression and poor overall survival[227]. The glycosylation profile of CD133, which includes the presence of sialic acids, can also be used to stratify pancreatic cancer patients. Also, sialic acids present at EVs surface show to affect EV recognition and adhesion to target cells, modulating receptor signaling and cell phenotype[228,229]. Increased levels of the

sialoglycoprotein LGALS3BP were detected in EVs from ovarian carcinoma cells, with implications in target cell recognition and EV uptake[209]. Ovarian carcinoma EVs were analyzed by lectin blotting, which detected the presence of T antigen, emphasizing the importance of EV glycosylation as a cancer biomarker[210]. Similar to T antigen, STn expression is increased in cancer and has already been correlated with poor overall survival of gastric cancer patients[115]. Applying different isolation approaches, STn was extensively detected in EVs secreted by a glycoengineered gastric cancer cell line MKN45[131]. Also, proteomic data revealed that STn secreted EVs carried several cancer-related proteins. However, up to this date, glycoproteins bearing *O*-glycans with STn antigen were not detected in EVs from cancer cell patients. In fact, the major studies on EV glycome are focused on *N*-glycosylation because of the increased difficulty in deciphering *O*-glycosylation[232]. In this field, STn has achieved great interest due to several reasons. First, STn is not expressed in normal gastric tissue[119]. Second, it is expressed in intestinal metaplasia and dysplasia, suggesting a correlation with malignant transformation in the stomach[115]. Third, STn levels are increased in gastric cancer patients and finally, its expression has been reported to be associated with poor prognosis[126]. This characteristics give to STn the proper recognition as a potential biomarker for gastric cancer, as it can help to select patients for a closer follow-up and to implement a more rapid and effective treatment[115]. The importance of STn is revealed by the association between its expression and the poor survival and resistance to chemotherapy of cancer patients[233]. To this purpose, a synthetic STn-keyhole limpet haemocyanin (KLH) vaccine (Theratope) was designed to induce STn-specific IgG in mice[234]. A phase II clinical trial in breast cancer patients demonstrated that effective STn-specific humoral responses can be induced with Theratope, which correlated with the increased survival of patients[235]. However, in the next phase III clinical trial, the investigators described no benefit for treated patients when compared to controls[236]. An improved diagnosis and stratification of cancer patients based on the expression of STn in EVs might be required for more effective to design new therapeutic intervention strategies.

4. Objectives

Gastric cancer is the 5th most common type of cancer and the 4th cause of cancer-related deaths worldwide. In Portugal, gastric cancer is the 3rd deadliest carcinogenic disease, mainly due to late diagnosis and consequent limited treatment options[1]. Since most of proteins expressed by cells are glycosylated[58], our study will focus on the expression of the truncated *O*-glycan STn that was found in gastric cancer and is related with increased invasiveness, aggressiveness, metastatic potential and poor prognosis of gastric cancer patients[115, 129,237]. Also, as extracellular vesicles (EVs) are highly secreted by cancer cells and encapsulate multiple components of the originating cell type, they serve as vehicles to transport and transfer cargo to local and distant sites, constituting a valuable source for biomarker discovery and detection. Our group have already demonstrated the presence of STn in EVs derived from a poorly differentiated gastric cancer cell line, isolated by different protocols[131].

The main aim of this study is to compare the yield and purity of two different EVs isolation methodologies from gastric cancer cells synthetizing different levels of STn to access its detection. EVs will be isolated by ultracentrifugation (UC) and by the combination of UC with size exclusion chromatography (SEC). Also, we aim to detect STn at EV membranes and study the impact of the presence of this cancer-associated *O*-glycan in EV uptake by recipient cells.

In this study, we will use the same genetically engineered cell line model derived from a poorly differentiated gastric adenocarcinoma cell line MKN45 to study the expression of STn. MKN45 SimpleCell (SC) cells have a fully characterized homogeneous *O*-glycoproteome with elevated levels of STn and were obtained by targeting the *C1GALTC1* (*COSMC*) gene by zinc-finger nuclease[66]. MKN45 ST6 cells display a vast repertoire of heterogeneous *O*-glycans with high levels of STn expression[101], which better mimic STn expression *in vivo.* For these reasons, we choose these cell lines to study the impact of different EVs isolation approaches in the expression of STn.

To accomplish these goals, we define more specified objectives, as follows:

<u>Compare the yield and purity of UC and UC+SEC protocols for EV isolation:</u>

For EV isolation, we purpose to use two glycoengineered gastric cancer cell lines (MKN45 ST6 and SC) and two control cell lines (MKN45 Mock and WT) that grow in conditions deprived from FBS, since it contains high levels of glycosylated proteins that may interfere with the downstream analysis of EV glycosylation[238]. Our group have also defined optimized UC and SEC protocols for EV isolation that will be reproduced in this

study[131]. Therefore, UC- and UC+SEC-isolates will be characterized according to the guidelines established by the International Society of Extracellular Vesicles, namely nanoparticle tracking analysis (NTA), transmission electron microscopy (TEM) and western blotting[135,239]. EV markers such as alix, Hsp70, syntenin-1 and CD9 will be tested for all EV isolates and compared regarding EV yield and purity. Also, UC and UC+SEC will be pursued to compare STn detection on EV samples. With this specific aim, we envisage to obtain pure EV populations for EV markers and STn detection.

Detect STn at EV membrane:

To detect STn at EV membrane, we will perform an immunolabelling technique with coupled gold particles. EV isolates will not undergo any membrane permeabilization to avoid the antibodies to penetrate EV membrane. The fact that STn might be present at EV membrane, may suggest a role of this cancer-associated antigen in cellular communication. Also, this achievement holds the potential for new EV isolation methodologies development directed against STn.

Impact of STn in EV uptake by recipient cells:

In this study, we will use an indirect co-culture system to study the capacity of different recipient cells to internalize STn-negative and STn-positive EVs. For that, cells will be labeled with a lipophilic dye and visualized at ZOE fluorescent cell imager microscope. The internalization of secreted dye-labeled EVs by unlabeled recipient cells will be analyzed after 24 and 48 hours. With the fluorescent cell image microscope, it will be possible to compare the relative number of cells that became fluorescent and analyze the differences regarding the STn presence at EVs. The definition of the timepoint when most EVs are internalized by recipient cells and the impact of STn in EV uptake may be useful to apply in future functional experiments.

5. Materials and Methods

5.1. Cell lines and culture conditions

To investigate the expression of STn we used genetically engineered cell line models derived from a poorly differentiated gastric adenocarcinoma cell line MKN45 obtained from the Japonese Collection of Research Bioresources. The parental human gastric carcinoma cell line MKN45 correspond to WildType cells (WT). The MKN45 SimpleCells (SC) were obtained by targeting the *C1GALTC1* (*COSMC*) gene by zinc-finger nuclease as previously described[66]. Also, the MKN45 WT cells were stably transfected with the full-length *ST6GalNAc1* gene (ST6) or with an empty vector pcDNA3.1 (Mock) as previously described[240,241]. All cells were cultured in monolayer in RPMI 1640 GlutaMAX, HEPES medium supplemented with 10% fetal bovine serum (FBS). MKN45 Mock and MKN45 ST6 cells were supplemented with 0.6% G418 antibiotic (all from Invitrogen, Carlsbad, CA, USA). Cultured cells were maintained at 37ºC in an atmosphere of 5% CO_2 and tested for mycoplasma contamination.

5.2. Viability and proliferation assays

Considering that FBS contains high levels of glycosylated proteins, it was necessary to remove this component from the cell culture medium before proceeding with the isolation and analysis of EVs. The effect of FBS removal was then tested by viability and proliferation assays. MKN45 cells (Mock, ST6, WT and SC) were seeded at 50,000 cells/mL in six wells of two 24-well plates (one plate with FBS and another to remove FBS). After 24h, cells of three wells per cell line were collected, and live and death cells were counted in a Neubauer chamber using trypan blue (Gibco, Waltham, MA, USA). At this moment, all cells of one plate were washed twice with PBS and 1 mL of medium depleted of FBS was added at each well. After 72h, cells in medium with and without FBS were counted. Two independent experiments with two technical replicates per condition were performed. Results are shown as average ± SEM. One-way ANOVA was used for statistical analysis.

5.3. Antibody purification from hybridoma cells

Hybridoma cells were used for B72.3 monoclonal antibody (mAb) purification. Cells were cultured as adherent and suspension cells in RPMI 1640 GlutaMAX, HEPES medium supplemented with 10% FBS, 1% penicillin/streptavidin and 1% pyruvate. Cells were maintained until the media was changed to medium depleted of FBS and all hybridoma supernatant were collected for B72.3 antibody purification. For B72.3 purification, a HiTrap Protein G HP column (Sigma Aldrich, St. Louis, MO, USA) was used with 0.1M glycine-HCl to elute 12 fractions of 200µL, neutralized with 1M Tris-HCl, pH 8.8 to avoid antibody deterioration caused by acidic pH at the time of elution. The fractions collected were then read at 280nm in the Nanodrop 1000 software to calculate the protein concentration in mg/mL. For a more accurate measure, fractions were read at 750nm using the Gen5.11 software (Synergy Mx). In this case, standards from the Protein Assay kit (Bio-rad, Waltham, MA, USA) were used to establish a calibration curve were 5µL of standards and samples were placed in a 96-well plate with a flat bottom. Then, 25µL of the BCA kit (1:50 dilution – reagent S: reagent A) and 200µL of reagent B were added. The 96-well plate were incubated at 37ºC for 15 minutes before read. Standard triplicates were used to establish the calibration curve. Pure B72.3 antibody was used for immunolabelling protocols and hybridoma supernatant for western blotting and immunofluorescence experiments.

5.4. Immunofluorescence

The effect of FBS removal and the presence of the *O*-glycan STn were tested in all cell lines by immunofluorescence. Cells were grown in two Ibidi slides (Gräfelfing, Germany) with a removable 12-well silicone chamber for 24h (one slide with FBS and another to remove FBS). Then, cell culture medium of one 12-well slide were collected and 200µL of medium depleted of FBS was added to each well. After 72h, cells were fixed with 4% paraformaldehyde (Alfa Aesar, Haverhill, MA, USA) at RT for 15min, washed three times with 0.01% PBS-Tween20 for 5min, to rehydrate the cell membrane, and permeabilized for 5min with 0.02% Triton™ X-100 (Sigma- Aldrich, Saint Louis, MO, USA). Cells were washed three more times for 5min with 0.01% PBS-Tween20 and incubated in normal goat serum diluted 1:5 in 10% of BSA for 1h at room temperature followed by overnight incubation with the STn antibody (B72.3) diluted 1:5 in 5% BSA at 4ºC. In the next day, all steps were performed in the dark. Cells were PBS washed five more times and incubated with the secondary anti-mouse antibody conjugated with Alexa

Fluor 488 (Life Technologies, Carlsbad, CA, USA) diluted 1:500 in 5% BSA for 45 minutes. Lastly, DAPI (4′,6-Diamidine-2′-phenylindole dihydrochloride) (Sigma-Aldrich, Saint Louis, MO, USA) was used for nuclear staining at RT for 10min followed by three 0.01% PBS-Tween20 washes. Then, slides were mounted with a coverslip using a mounting medium (Vector Laboratories, Burlingame, CA, USA), sealing the edges with nail varnish. The images were acquired with a Zeiss Axio Imager Z1 Apotome microscope (Zeiss, Oberkochen, Germany). For immunofluorescence assays, two independent experiments with three technical replicates per condition were performed.

5.5. Extracellular vesicle isolation by differential ultracentrifugation

Cells from all MKN45 cell models were seeded in dishes with 150mm and grown until confluency 80-90%. Before extracellular vesicle collection, FBS was removed from the cell culture medium and MKN45 cells grow without serum supplementation for 72 hours. Then, EVs were collected in a total of 120mL of cell culture medium depleted of FBS and isolated by differential ultracentrifugation (UC). The protocol starts with a centrifugation at 800g for 5min, followed by a centrifugation at 2,000g for 10min. The supernatant was vacuum filtered using a 0.22µm constant pore filtration system (Corning, NY, USA). Then, media was centrifuged for 20h (Optima XE 100, SW32 Ti rotor, Beckman Coulter) in thin wall ultra-clear centrifuge tubes at 100,000g and 4ºC. A washing step with saline solution 0.9% of NaCl (Wells, Porto, PT) was performed for 3h at 100,000g and 4ºC. EV pellets were resuspended in saline solution and characterized by nanoparticle tracking analysis (NTA), transmission electron microscopy (TEM), protein quantification and western blotting. The number of cells at EV collection day was counted in trypan blue using a Neubauer chamber, for cell viability and quality control.

5.6. Extracellular vesicle isolation by size exclusion chromatography

To evaluate the purity and efficacy of UC-isolated samples, we decided to implement size exclusion chromatography (SEC) as an extra step of EV purification in all MKN45-derived EVs. Furthermore, it was possible to compare the analysis of EVs isolated by two different methodologies. Extracellular vesicles were obtained by SEC, performed according to the manufacturer's instructions of the qEV column (Izon, Christchurch, New Zealand). The pellet obtained after UC was resuspended in 0.9% NaCl to make a total of 500µL and overlaid on top of the qEV column. A total of 15 fractions of

500µL were collected as previously reported[131]. Fractions from 7 to 12 were collected and pulled together to be concentrated by ultrafiltration with 10kDa Amicon Ultra-15 centrifugal filter units (EMD Millipore). EV pellets were characterized by NTA, TEM, protein quantification and western blotting.

5.7. Protein Quantification

For protein quantification, EVs were resuspended and lysed in RIPA lysis buffer together with 1mM of sodium orthovanadate (Na_3VO_4), 1mM of phenylmethylsulphonyl fluoride (PMSF) and complete protease inhibitor cocktail (Roche, Basel, Switzerland) on ice for 20min, with vortex at each 5min. Samples were then centrifuged at 16,000g for 20min at 4ºC. Standards from the Pierce BCA Protein Assay kit (Thermo Scientific, Waltham, MA, USA) were used to establish a calibration curve were 10µL of standards and samples were placed in a 96-well plate with a flat bottom. Then, 200µL of the BCA kit was added (1:50 dilution – reagent B: reagent A). The 96-well plate were incubated at 37ºC for 30min and read using the Gen5.11 software (Synergy Mx) at absorbance 562nm. With the calibration curve obtained (absorbance 562nm vs protein concentration µg/mL) and the protein concentration in the initial sample, it was possible to calculate the line equation of the standards. For the cell lines MKN45 Mock and MKN45 ST6, EVs were isolated by UC in four independent experiments and only one subjected to UC+SEC. For the cell lines, MKN45 WT and MKN45 SC, EVs were isolated by UC in three independent experiments and by UC+SEC in four independent experiments. Results are shown as average ± SEM. Unpaired t-test was used for statistical analysis.

5.8. Nanoparticle tracking analysis

Nanoparticle tracking analysis was performed to evaluate the size and concentration of EVs using a NanoSight NS300 system (Malvern Technologies, Malvern, UK) configured with a Blue 488 laser to illuminate the particles. The system also contains a high sensitivity scientific sCMOS camera that captures EV's Brownian motions through the static solution by recording their average velocity and the corresponding light scattering of each particle. For NTA analysis of the EVs, saline solution was used as diluent that was injected with a syringe pump with constant flow injection and three videos of 60 seconds were captured with 749 frames and camera level at 15–16. The videos were recorded and analyzed with NTA software version 2.3 to determine the size and

concentration of the particles in the sample as well as their size distribution through the Strokes-Einstein equation, which relates the diffusivity constant to the radius of the particle to be studied. For this analysis, two technical replicates were prepared for each NTA measurement. Results are shown as average ± SEM. Unpaired t-test was used for statistical analysis.

5.9. Negative staining transmission electron microscopy

EV size, morphology, and integrity were visualized by transmission electron microscopy using negative staining. For this, 5µL of fresh EV sample solution was mounted on formvar/carbon film-coated mesh nickel grids (Electron Microscopy Sciences, Hatfield, PA, USA) where EVs were adsorbed for 10min. The excess liquid was removed with filter paper, and 5µL of 1% uranyl acetate was added onto the grids for 10 seconds, allowing the contrast between the vesicles and the background and facilitating their visualization carried out on a JEOL JEM 1400 TEM at 120 kV (Tokyo, Japan). The images were digitally recorded using a CCD digital camera (Orious 1100W Tokyo, Japan). For UC-isolates, three independent experiments, for both MKN45 WT- and SC-derived EVs and four independent experiments for both MKN45 Mock- and ST6-derived EVs, were performed. For SEC-isolates, two independent experiments, for both MKN45 WT- and SC-derived EVs and one experiment for both MKN45 Mock- and ST6-derived EVs were performed.

5.10. Immunogold labelling of extracellular vesicles

The surface *O*-glycan STn was visualized by immunogold labelling applied to transmission electron microscopy. First, 5µL of fresh EV sample was directly applied on formvar/carbon film-coated mesh nickel grids (Electron Microscopy Sciences, Hatfield, PA, USA) where it was adsorbed for 20 minutes. The excess liquid was removed with filter paper, and 2% paraformaldehyde was added for 20 minutes. The grids were washed with 50mM of glycine in TBS (Tris-buffered saline) four times for 5 minutes. A blocking step was performed with 2% of bovine serum albumin (BSA) in TBS for 30 minutes. Then, 15µL of the purified primary antibody B72.3 diluted 1:10 and 1:20 in 5% BSA was added to the grids for 1 hour at room temperature. The grids were washed with 0.5% BSA six times for 3 minutes. The grids were then incubated with 15 µL of secondary gold-conjugated anti-mouse antibody for 20 minutes and washed with TBS and purified water

six times for 3 minutes. Lastly, 5µL of 1% uranyl acetate was added onto the grids, enhancing the contrast between the labelled EVs and the background, facilitating their visualization by JEOL JEM 1400 TEM at 120kV (Tokyo, Japan). Images were digitally recorded using a CCD digital camera (Orious 1100W Tokyo, Japan). Two independent experiments for both MKN45 WT- and SC-derived EVs isolated by UC+SEC were performed. A grid without sample and primary antibody was used as negative control of the experiment to ensure that the secondary antibody do not bind to the grid.

5.11. Analysis of protein and glycan expression by western blotting

The western blotting technique was performed to detect the presence of specific EV markers according to the guidelines established by the International Society of Extracellular Vesicles[135], including transmembrane protein such as the tetraspanin CD9, the cytosolic proteins HSP70, syntenin-1, actin, alix and the mitochondrial protein cytochrome c as well as to detect the presence of the truncated *O*-glycan STn. The information related to the primary and secondary antibodies used in this technique (clone, source, dilution, and host species/class) is presented in Tables 1 and 2. EV samples were lysed in RIPA lysis buffer supplemented with 1mM of Na_3VO_4, 1mM of PMSF and complete protease inhibitor cocktail (Roche, Basel, Switzerland). Protein lysates were then separated based on their molecular weight by 12% sodium dodecyl sulphate-polyacrylamide gel electrophoresis (SDS-PAGE) followed by transference to a nitrocellulose membrane (GE Healthcare, UK). These membranes were then blocked for at least 1h with 5% BSA or 5% nonfat dry milk prepared with 0.1% PBS-Tween20, depending on the type of primary antibody to be used (Table 1). Membranes were incubated overnight at 4ºC with the following antibodies: anti-Alix, anti-syntenin-1, anti-cytochrome C, anti-CD9 and anti-STn (Table 1). The next day, the membranes were washed with 0.1% PBS-Tween20 three times for 20 minutes and incubated for 45 minutes at room temperature with the respective secondary antibodies (Table 2): anti-mouse (in 5% milk for syntenin-1 and cytochrome C), anti-mouse (in 5% BSA for alix), anti-rabbit (in 5% BSA for CD9) and IgG1 (in 5% BSA for STn). The chemiluminescence signal was obtained using enhanced chemiluminescence (ECL) detection reagent (GE Healthcare Life Sciences). The membranes were then washed with 0.1% PBS-Tween20 for at least 1 hour and left in 0.1% PBS-Tween20 overnight at 4ºC. Then, the membranes were reincubated with the antibodies anti-HSP70 and anti-actin overnight at 4ºC. As previously described, the membranes were washed and incubated for 45 minutes at room

temperature with secondary antibodies: anti-rabbit (in 5% BSA for HSP70 and actin). Once again, it was possible to visualize each marker due to the ECL detection reagent. Five independent experiments were performed for MKN45 WT and MKN45 SC cell lines and six independent experiments were performed for MKN45 Mock and MKN45 ST6 cell lines.

Table 1. List of primary antibodies used in western blot for the detection of specific EV markers and STn.

Primary antibody	Clone	Dilution	Diluent	Host species/class	Source
STn	B72.3	1:5	5% BSA	Mouse monoclonal	Produced in the laboratory[242]
Syntenin-1	S-31	1:200	5% milk	Mouse monoclonal	Santa Cruz Biotechnology
Cytochrome C	7H8	1:200	5% milk	Mouse monoclonal	Santa Cruz Biotechnology
HSP70	Hsp70A-1	1:1000	5% BSA	Rabbit polyclonal	System Biosciences
CD9	CD9A-1	1:1000	5% BSA	Rabbit polyclonal	System Biosciences
Actin	13E5	1:1000	5% BSA	Rabbit monoclonal	Cell signalling Technology
Alix	3A9	1:1000	5% BSA	Mouse monoclonal	Cell signalling Technology

Table 2. List of secondary antibodies used in western blot for the detection of specific EV markers and STn.

Secondary antibody	Dilution	Host species/class	Source
anti-mouse IgG1	1:25000	Goat polyclonal	Jackson ImmunoResearch
anti-rabbit	1:10000	Goat polyclonal	System Biosciences
anti-mouse	1:5000	Goat polyclonal	Jackson ImmunoResearch

5.12. EV uptake assay

For the EV uptake assay, MKN45 WT and MKN45 SC cells were used as donor and recipient cells in a co-culture system with 0.4µm inserts. Both cell lines were analyzed regarding the uptake of EVs secreted by their own cell line or from the other cell model. Thus, four conditions with two time points were established: MKN45 WT cells with MKN45 WT- or MKN45 SC-derived EVs and MKN45 SC cells with MKN45 WT- or MKN45 SC-

derived EVs, all tested after 24 hours and 48 hours of co-culture. First, 50,000 cells of MKN45 WT and MKN45 SC cells were seeded in a 24-well plate in 500µL of RPMI supplemented with 10% of FBS and designated as recipient cells. At the same time, 500,000 cells of both cell lines were seeded in each insert in RPMI + 10%FBS direct labeled with 15µL of 1mM Vybran DiI Cell-Labelling Solution (Invitrogen). Those were designated as donor cells. After 20h of growth, cell culture medium of recipient and donor cells was removed, the cells were washed twice with PBS and grown with RPMI depleted of FBS. At this moment, the inserts containing the donor cells were transferred to the 24-well plate containing the recipient cells to establish the indirect co-culture system. After 24 hours and 48 hours of EV production by donor cells and uptake by recipient ones, the inserts were removed, and recipient cells were visualized at ZOE fluorescence cell imager microscope to analyze the internalization of DiI-labeled EVs. Additionally, unlabeled cells from both cell lines were seeded in 24-well plates and grown in RPMI supplemented with FBS to serve as negative controls. The same procedure was executed for positive controls but adding 1µL of DiI dye to the suspension of 200,000 cells. Both negative and positive controls were visualized at ZOE fluorescent cell imager microscope.

6. Results

In this study, we used a parental gastric cancer cell line MKN45 characterized by a heterogeneous glycosylation profile of elongated *O*-glycans (MKN45 WT). This cell line was genetically modified by targeting the *C1GalTC1* (also known as *COSMC*) gene by zinc-finger nuclease as previously reported[66,243]. MKN45 SimpleCell (MKN45 SC) produced by *COSMC* knockout show a homogeneous glycosylation profile, with inhibition of *O*-glycan elongation and enhanced biosynthesis of Tn and STn antigens (Figure 5A). Also, the parental cell line was stably transfected with the full length human *ST6GalNac1* gene, who is responsible for an alternative glycosylation pathway adding an α-2,6-sialic acid residue to GalNAcα-O-Ser/Thr structures[101]. This MKN45 ST6 cells display a heterogeneous glycan profile with elongated and truncated *O*-glycans such as STn (Figure 5A), whereas MKN45 Mock cells express core 2 *O*-glycans, and therefore negative for Tn and STn, due to the transfection with the corresponding empty vector pcDNA3.1, as previously described[240]. The presence of STn can be recognized by monoclonal antibodies such as B72.3, which is reactive with an epitope carried either by high molecular weight ($M_r \geq 10^6$) mucins or non mucin glycoproteins[244–246]. For B72.3 purification, it was established a calibration curve with absorbance at 750 nm in the y axis and concentration in mg/mL in the x axis, which allowed us to calculate the concentration of purified antibody collected in fractions 1 to 12 (Figure 5B). Fractions 6 and 7 were the most concentrated samples, with 1.8mg/mL and 0.6mg/mL, respectively. Purified B72.3 was further used for STn detection.

Cell morphology, viability, and proliferation rate, as well as STn detection by immunofluorescence was accessed in the four cell lines in the presence and absence of FBS. Since FBS contains high levels of glycosylated proteins that can interfere with further EV glycosylation analysis, we first evaluate the effect of FBS removal of the cell culture medium[238]. Differences in cell morphology were noted in brightfield images (Figure 5C) with FBS removal leading to the acquisition of a more elongated phenotype. This effect occured in all cell models, mostly pronounced in MKN45 ST6 and MKN45 SC when compared to MKN45 Mock and WT. As expected, STn expression was not affected by FBS removal, with MKN45 Mock and MKN45 WT cells showing a complete absence of STn expression and MKN45 ST6 and MKN45 SC cells showing different levels of expression due to their process of STn biosynthesis (Figure 5A). In MKN45 ST6 cells, the ST6GalNac1 sialyltransferase is the enzyme responsible to add a sialic acid to the N-acetylgalactosamine structure (Tn) in order to synthetize STn, anticipating the *O*-glycan truncation[240]. However, in this cell line, the synthesis of elongated *O*-glycans is not fully

disrupted and the Tn structure can be further elongated to form other core glycans. Thus, MKN45 ST6 cells express both elongated and truncated *O*-glycans, with most cells showing upregulated levels of STn[240]. On the other hand, MKN45 SC cells exhibit a homogeneous glycosylation profile with the synthesis of truncated *O*-glycans Tn and STn[66]. Core 1 synthase C1GalT1 is the enzyme responsible for Tn elongation and is dependent on *COSMC* chaperone. Thus, *COSMC* knockout leads to Tn accumulation, which serves as ST6GalNAc1 substrate, leading to STn synthesis in the totality of MKN45 SC cells, as shown in our experiments (Figure 5C).

Additionally, cell proliferation rate was tested in the presence (10% FBS) and absence (0% FBS) of FBS after 72h of growth (Figure 5D). All four cell models showed a significant decrease in proliferation when grow in medium with 0% FBS (Figure 5D), as expected since serum contains necessary nutrients for cell growth[247]. Our results showed that MKN45 Mock cells were able to divide approximately half the times when cultured in medium with 0% FBS (1.37±0.16) when compared to 10% FBS (2.85±0.15). The proliferation rate of MKN45 ST6 cells also decreased when cultured with 0% FBS (1.72±0.42) compared to when cultured with 10% FBS (3.09±0.55). The same tendency was observed in MKN45 WT and MKN45 SC cell proliferation rate. The proliferation rate of MKN45 WT cells when cultured in medium with 10% FBS (2.91±0.20) decreased when cells were cultured in medium with 0% FBS (1.30±0.07). Finally, MKN45 SC cells showed a lower proliferation rate when cultured with 0% FBS (1.59±0.24) compared to medium supplemented with 10% FBS (3.13±0.27) (Figure 5D). Although significant differences were obtained in cell proliferation rate, cell viability was not affected by FBS removal from cell culture medium (Figure 5E). Similar cell viability was obtained for MKN45 Mock cells when cultured with 10% FBS (94.88%±0.33%) or 0% FBS (93.08%±2.00%). The viability of MKN45 ST6 cells cultured in medium with 10% FBS (95.14%±1.15%) or 0% FBS (94.66%±0.77%) was very alike. MKN45 WT cells achieved similar cell viability when cultured with 10% FBS (95.21%±0.90%) or 0% FBS (92.22%±1.28%). Lastly, MKN45 SC cells presented close cell viability percentages when cultured in medium with 10% FBS (93.39%±0.73%) or with 0% FBS (92.58%±0.59%) (Figure 5E). Considering the results for cell characterization, extracellular vesicles isolation procedures were taken without FBS and with cell viability over 90%.

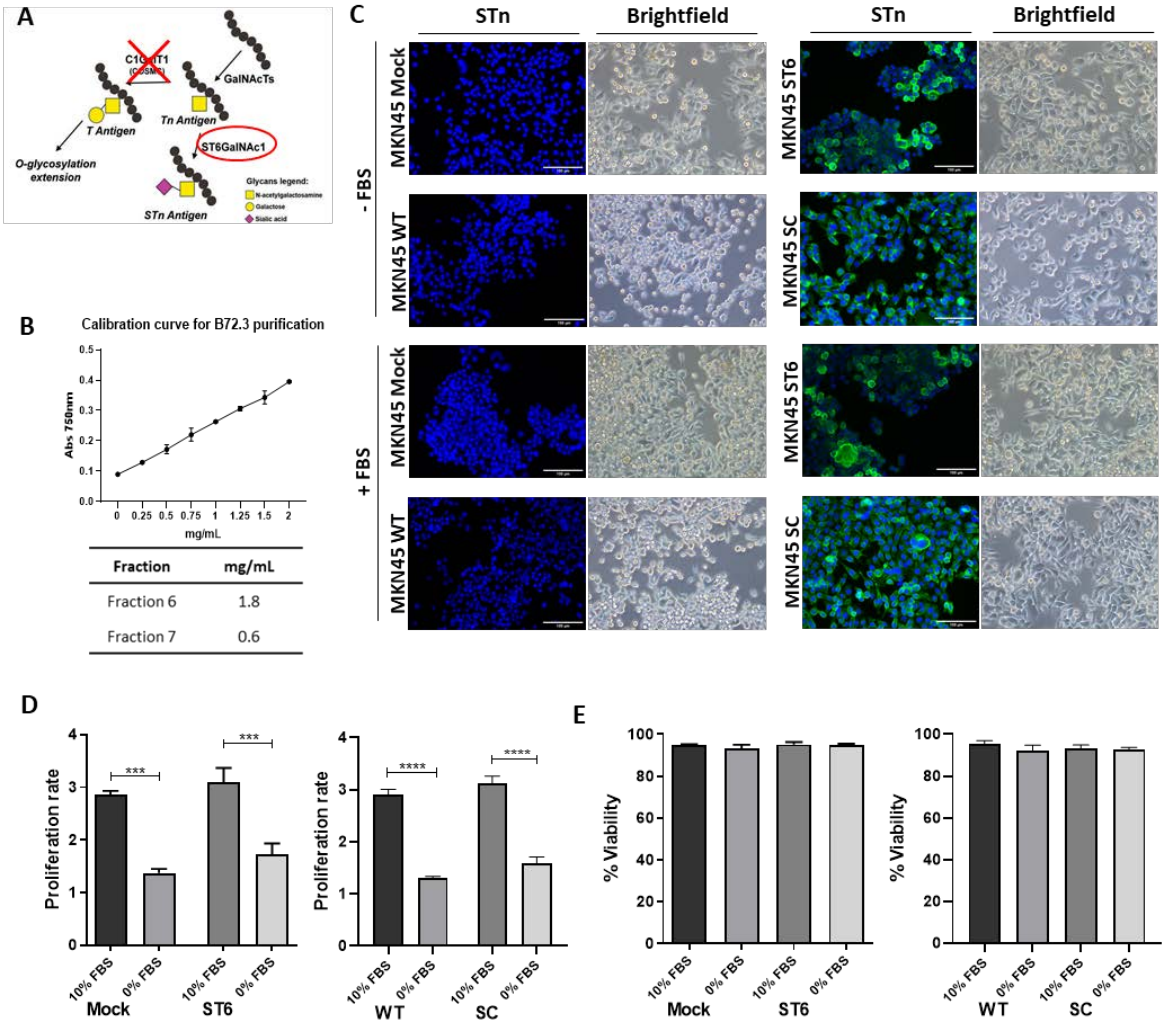

Figure 5. Characterization of four MKN45 cell lines regarding FBS removal and its effects on cell morphology, proliferation, and viability. A) Schematic representation of STn biosynthesis. Increased expression of ST6GalNAc1 enzyme or absence of COSMC chaperone increase STn synthesis. In the latest, the production of elongated *O*-glycan structures is further prevented. Image adapted from Freitas et al. (2019)[131]. B) Calibration curve obtained for B72.3 antibody purification with standards concentration (mg/mL) in the x axis and absorbance at 750nm in the y axis. Pure B72.3 was obtained in fractions 6 and 7 with 1.8mg/mL and 0.6mg/mL respectively. Purified B72.3 from hybridoma cells was used to evaluate the presence of STn. C) Cells were grown in the absence (0% FBS) or presence (10% FBS) of FBS in culture medium were fixed and stained with DAPI (blue) for nuclear staining and tested for the presence of STn (green). Images were taken with fluorescence microscope in 200x amplification (scale bar represents 100µm). Differences

in cell morphology were observed in brightfield images taken with an inverted microscope with 50x amplification. D) Comparison of cell proliferation rates when cultured with 10% or 0% of FBS for 72h. Two independent experiments with two technical replicates per condition were performed. Results are shown as average ± SEM. One-way ANOVA was used for statistical analysis: p-value < 0.05 was considered significant. E) Comparison of cell viability when cultured with 10% or 0% of FBS for 72h. Two independent experiments with two technical replicates per condition were performed. Results are shown as average ± SEM. One-way ANOVA was used for statistical analysis: p-value > 0.05 was considered not significant.

Extracellular vesicles were isolated from all four cell lines by UC, with or without SEC as an additional step of EV purification (Figure 6A). UC is the most used method to isolate EVs and it uses increasing centrifugal speeds and/or times to obtain an EV enriched sample[174]. First, the cell culture medium was centrifuged at 800g for 5 minutes to pellet dead cells, followed by 2,000g for 10 minutes to separate cell debris. Then, the remaining supernatant was filtered with a 0.2 µm system and centrifuged at 100,000g for 20 hours. Lastly, EV pellet was washed with 0.9% NaCl for 3 hours at 100,000g (Figure 6A). The remaining EV pellet was used for further analysis of UC-isolated samples or submitted to an additional step of SEC purification to obtain UC+SEC-isolated samples. SEC is based on the differential elution profiles of particles or molecules of different sizes running through a porous polymer that constitutes the stationary phase called gel filtration matrix and carried through the mobile phase of the SEC column[176]. Small particles, such as proteins, are trapped into the column and elute later than EVs. Fractions 7-12 were pulled together to be concentrated with centrifugal filter units as these fractions contain high amounts of EVs as demonstrated before by our group[131]. EVs isolated either by UC or UC+SEC (Figure 6A) were then used for further analysis, regarding parameters such as yield, purity, morphology, size, and EV markers, using NTA, TEM and western blotting as recommended by the International Society of Extracellular Vesicles[135,239].

According to the guidelines established by the International Society of Extracellular Vesicles, EVs isolated samples must be characterized by, at least, three different techniques[239]. For that reason, we performed NTA (Figure 6), TEM (Figure 7) and western blotting (Figure 8). EV concentration and size distribution were measured by NTA based on particle Brownian motion, as described before[248]. The results suggested differences in EV yield and purity when using two different methodologies. MKN45 Mock- and MKN45

ST6-derived EVs were successfully isolated four times by UC (Figure 6B and C) and once by UC+SEC (Figure 6G and H). MKN45 WT- and MKN45 SC-derived EVs were isolated three times by UC (Figure 6L and M) and four times by UC+SEC (Figure 6Q and R). The cells of origin were counted at the day of EV isolation to calculate the number of EVs isolated per cell after both UC and UC+SEC protocols. By NTA analysis, it was possible to observe that MKN45 ST6 cells secrete more EVs per cell (3163.0±324.2) than MKN45 Mock cells (2219.0±301.0) when EVs were isolated by UC (Figure 6D). When SEC was performed and fractions 7-12 were combined, the particles per cell ratio between MKN45 ST6 (134) and MKN45 Mock (152), were similarly counted (Figure 6I). However, MKN45 Mock- and MKN45 ST6-derived EVs were isolated only one time by UC+SEC, so we cannot establish a tendency at the risk of being faced with a random event. MKN45 SC cells secrete more EVs per cell (2542.0±640.9) than MKN45 WT cells (1412.0±587.0) when EVs were isolated by UC (Figure 6N) and even more evident after UC+SEC (Figure 6S). When a SEC purification step was performed, significantly more MKN45 SC-derived EVs are detected (713.8±140.4) when compared to MKN45 WT-derived EVs (231.7±63.9). This enhanced significance can be explained by the more accurate purification of EVs when isolated by UC+SEC, highlighting the differences between EVs secreted by MKN45 WT and MKN45 SC cells.

Together with NTA, protein quantification of EV samples by BCA assay allowed us to calculate the ratio of protein per EV to estimate the presence of EV-enclosed proteins. Using UC, each MKN45 Mock-derived EV carried more protein content ($3.6x10^{-10}$±$6.7x10^{-11}$µg) compared to MKN45 ST6-derived EV ($2.4x10^{-10}$±$3.8x10^{-11}$µg) (Figure 6E). This effect can be due to a greater protein cargo carried by MKN45 Mock-derived EVs or to a major protein contamination in those EVs. A similar result was observed in MKN45 WT-derived EVs that carried more protein ($2.7x10^{-10}$±$4.7x10^{-11}$µg) than MKN45 SC-derived EVs ($2.0x10^{-10}$±$2.7x10^{-11}$µg) using UC (Figure 6O). However, when SEC was performed, the trend reversed with MKN45 ST6-derived EVs ($3.7x10^{-10}$µg) and MKN45 SC-derived EVs ($3.0x10^{-10}$±$3.0x10^{-11}$µg) showing higher protein content, compared to MKN45 Mock-derived EVs ($2.5x10^{-10}$µg) and MKN45 WT-derived EVs ($1.8x10^{-10}$±$3.7x10^{-11}$µg), respectively (Figure 6J and T). This result may exclude the hypothesis that MKN45 Mock- and MKN45 WT-derived EVs contained a higher protein cargo. Both EV/cell and protein/EV results suggest that samples isolated by UC have a higher yield but less purity, since contaminants, such as soluble proteins, were co-isolated with EVs. On the other hand, UC+SEC allowed to isolate less but purer EV samples.

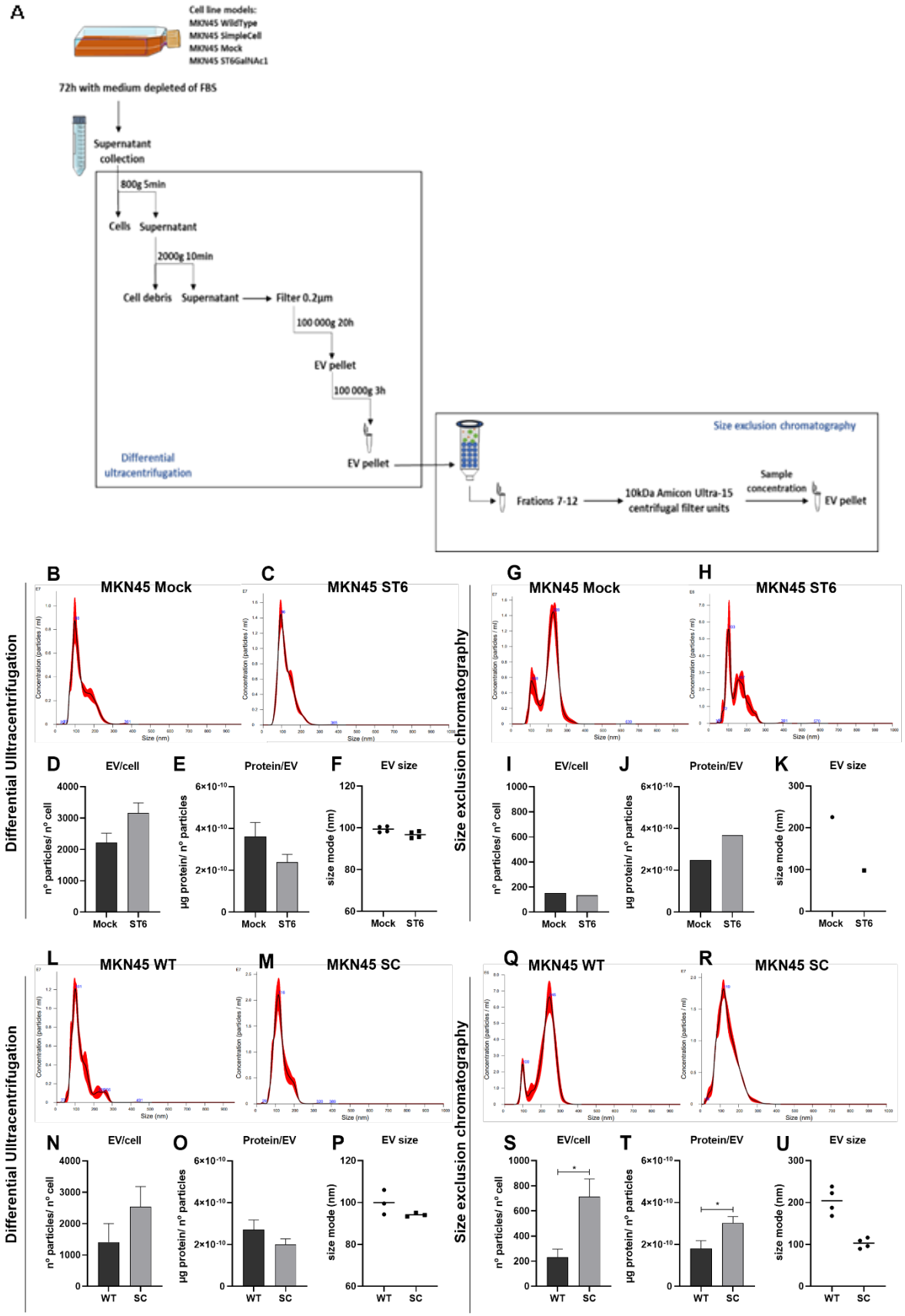

Figure 6. Characterization of EVs isolated from four different MKN45 cell lines by two different methods: UC and UC+SEC. A) Schematic representation of the two

methodologies used to isolate EVs. EVs were isolated by UC with or without SEC as an extra step of purification. B), C), G), H), L), M), Q) and R) Representative histograms of NTA, demonstrating the concentration of EVs displayed in the y axis as $10^6/10^7$particles/mL distributed by EV size in the x axis measured in nm. For NTA analysis, four independent experiments were performed for MKN45 Mock and MKN45 ST6 isolated by UC and only one experiment by UC+SEC. D) Number of UC-isolated EVs secreted per MKN45 Mock and ST6 cells. E) Protein per MKN45 Mock and MKN45 ST6 UC-isolated EV. F) Size mode of MKN45 Mock and ST6 UC-isolated EVs. I) Number of UC+SEC-isolated EVs secreted per MKN45 Mock and ST6 cells. J) Protein per MKN45 Mock and ST6 UC+SEC-isolated EV. K) Size mode of MKN45 Mock and ST6 UC+SEC-isolated EVs. N) Number of UC-isolated EVs secreted per MKN45 WT and SC cells. O) Protein per MKN45 WT and SC UC-isolated EV. P) Size mode of MKN45 WT and SC UC-isolated EVs. S) Number of UC+SEC-isolated EVs secreted per MKN45 WT and SC cells. T) Protein per MKN45 WT and SC UC+SEC-isolated EV. U) Size mode of MKN45 WT and SC UC+SEC-isolated EVs. Results are shown as average ± SEM. Statistical analysis was achieved using unpaired t-test: p-value < 0.05 was considered significant.

Regarding the size of the particles, a laser beam is directed into solution, and the Stokes-Einstein equation is used to measure the mean velocity of the particles, which can then be used to calculate their size[249]. After UC, the EV population obtained from MKN45 Mock cells showed a similar size (99.3±0.7nm) to MKN45 ST6-derived EVs (96.7±0.8nm) (Figure 6F). Also, MKN45 WT cells secrete EVs with similar diameter (99.9±3.4nm) when compared to MKN45 SC-derived EVs (94.1±0.5nm) (Figure 6P). After SEC, the size mode between MKN45 Mock- and MKN45 ST6-derived EVs and between MKN45 WT- and MKN45 SC-derived EVs were more differentiated. Using the combination of UC+SEC, NTA detected larger MKN45 Mock-derived EVs (225.4nm) and size-similar MKN45 ST6-derived EVs (97.8nm) (Figure 6K). Similarly, an abundant population of larger MKN45 WT-derived EVs (204.1±16.0nm) were detected when compared to MKN45 SC-derived EVs (102.7±6.0nm) (Figure 6U). The decreased diameter mostly noticed in MKN45 Mock- and MKN45 WT-derived EVs when isolated by UC could be due to the coexistence of soluble proteins that shifted the size peak to the left in the x axis. Adding an extra step of EV purification, it was possible to observe that MKN45 Mock- and MKN45 WT-derived EVs are larger in diameter when compared to MKN45 ST6- and MKN45 SC-derived EVs, respectively. Together with the size peak at approximately 200nm, it also persists a

subpopulation of EVs with 100nm of diameter, showing that MKN45 Mock and MKN45 WT cells secrete a heterogeneous EV population, when compared to MKN45 ST6- and MKN45 SC-derived EVs. No significant changes were observed regarding the size of the EVs isolated from both MKN45 ST6 and MKN45 SC cells after the SEC purification step, suggesting that in these samples less non-EV content is co-isolated with EVs during the UC isolation protocol. Again, differences in the EV size accomplished by the two different methodologies, continues to suggest that the combination UC+SEC leads to purer isolated EVs. Nevertheless, since NTA does not distinguish EVs from non-EV content, these results are not sufficient to estimate EV yield and purity. Despite the evidence, further analysis was taken to estimate EV purity and EV markers performing TEM and western blotting, respectively.

TEM was used to evaluate the presence of EVs, their morphology, size, and integrity, as well as the presence of protein aggregates co-isolated with EVs. Overall, EVs were successfully isolated using the two methodologies and preserved their integrity with a typical cup-shaped morphology when visualized by TEM. Corroborating the information obtained by NTA measurements, TEM images showed that both MKN45 Mock and MKN45 WT cells secrete larger EVs compared to MKN45 ST6- and MKN45 SC-derived EVs, most evident when applying UC+SEC protocol (Figure 7E-H). Altogether, TEM results provided visual validation that different MKN45 cell models secrete EVs with variable size depending on the EV isolation method, as previously demonstrated by our group[131]. As TEM allows to distinguish EVs from non-EV particles, it was possible to relatively compare the quality of UC- and UC+SEC-isolates regarding the presence of soluble proteins or protein aggregates that co-isolate with EVs. High image and background quality was achieved when MKN45-derived EVs were isolated by UC+SEC (Figure 7E-H), showing the concomitant removal of soluble proteins (green arrows) and an enrichment of EVs (red arrows), compared to UC-isolated samples (Figure 7A-D). This reduction in protein contamination when applying SEC protocol is mostly noticed in MKN45 Mock and MKN45 WT-derived EV samples. Together, these results sustain the notion that the combination of UC+SEC protocols led to more pure EV samples.

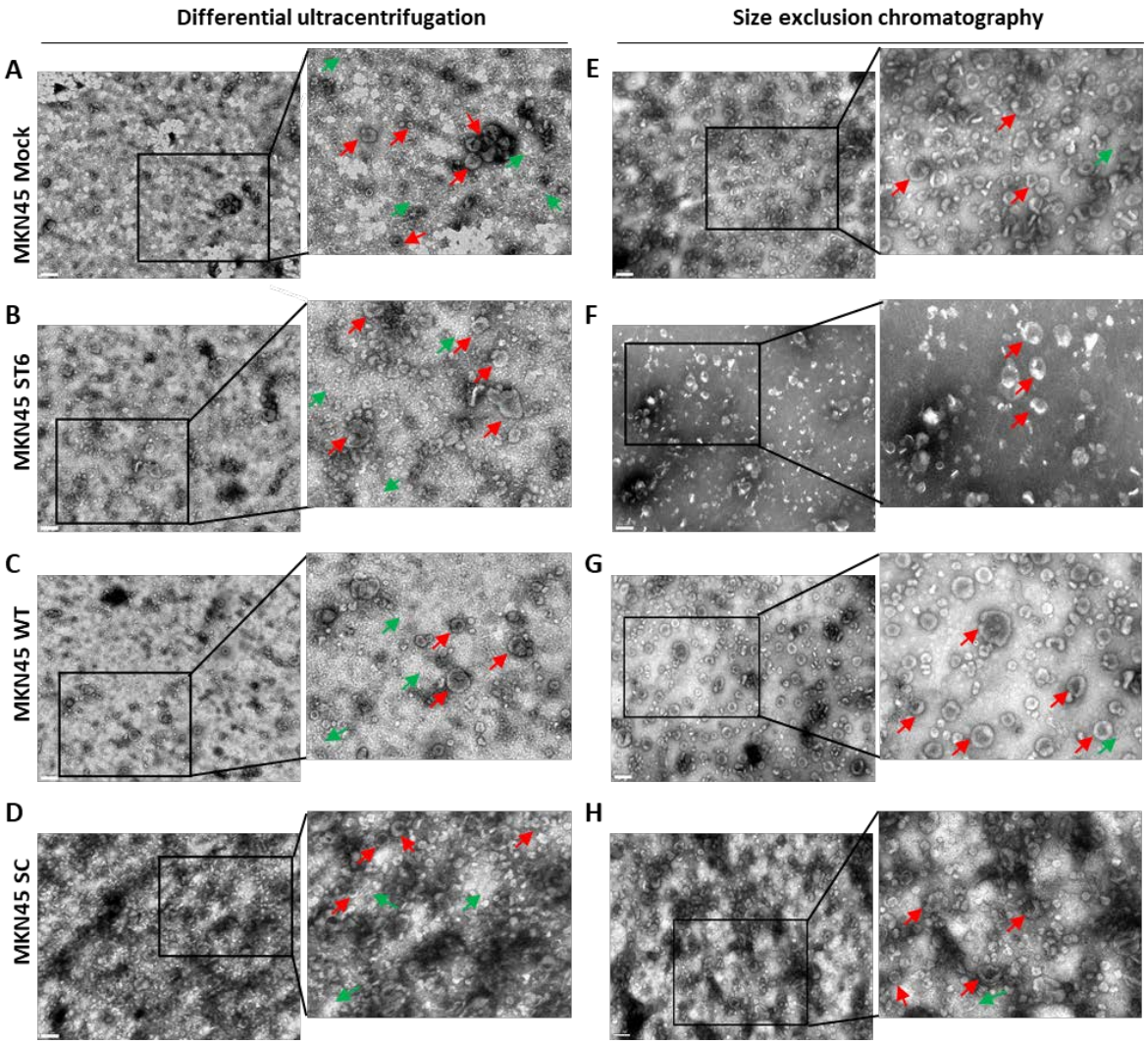

Figure 7. Representative images of TEM showing the different EV populations obtained depending on the cell line and EV isolation method applied. This technique was used to access EV size, integrity, purity and morphology analysis. A) TEM imaging was performed in UC-isolated EVs derived from MKN45 Mock cells, B) from MKN45 ST6 cells, C) from MKN45 WT cells and D) from MKN45 SC cells. E) TEM imaging of UC+SEC-isolated EVs secreted by MKN45 Mock cells, F) MKN45 ST6 cells, G) MKN45 WT cells and H) MKN45 SC cells. UC+SEC protocol allowed the recovery of purer EVs (red arrows), with less protein contamination (green arrows) compared to UC-isolates. Images were acquired with lower magnification (left panel) with scale bar representing 200nm and zoomed twice (right panel).

The efficacy of the two isolation strategies and the enrichment of the typical EV markers was monitored by western blotting (Figure 8). Both MKN45 Mock, MKN45 ST6, MKN45 WT and MKN45 SC cells and secreted EVs isolated by UC or UC+SEC were analyzed regarding EV markers and STn profile. Considering the complexity and the variety of methodologies applied to EV studies, the International Society of Extracellular Vesicles defined some criteria for accurate definition of the presence of EVs in isolated samples, namely the presence of, at least, three different positive EV markers, including transmembrane or lipid-bound proteins and cytosolic proteins, and one negative marker[239]. We access the presence of positive EV markers such as Alix, Hsp70, synthenin-1 and CD9 and a negative EV marker such as cytochrome c (Figure 8).

Notably, all EV isolates were positive for the mentioned positive EV markers particularly when isolated by the combination of UC+SEC, while different expression profiles were obtained when EVs were isolated by UC (Figure 8). Alix (100kDa) and syntenin-1 (32kDa) support their biogenesis and govern the selection of endocytic cargo and membrane trafficking[138]. Therefore, it was expected to observe its presence and enrichment in EV lysates compared to the secreting cells, which confirmed their biosynthetic pathway. Alix did not appear in MKN45 cell lysates, probably because of the quantity of protein loaded was not sufficient to detect a signal or due to the noted loss of efficacy of the antibody used. MKN45-derived EVs isolated by UC+SEC (Figure 8C and D) showed an enrichment of Alix compared to EVs isolated by UC (Figure 8A and B), which proved the higher purity obtained when adding SEC. The same results occurred with sintenin-1, a cytosolic protein with ligand binding capacity, which showed a stronger signal in EV lysates compared to the secreting cells and an enrichment when EVs were isolated by UC+SEC (Figure 8C and D), compared to UC isolates (Figure 8A and B). Like Alix, Hsp70 (70kDa) is another cytoplasmatic protein that has been reported to be involved in EV biogenesis[138]. However, contrary to what was observed for Alix and syntenin-1, Hsp70 showed stronger evidence in secreting cells over isolated EVs, whereas isolated by UC with or without SEC, which suggested that is lesser packaged into EVs at the time of their formation. Also, Hsp70 signal in EVs isolated by UC+SEC (Figure 8C and D) is slightly stronger than when EVs were isolated by UC (Figure 8A and B). As referred, CD9 (20kDa) is also described as expected to be present in EV isolates as argues their engagement in EV formation. Our results showed that CD9 is present in all EV isolates, independent of the EV isolation approach. Also, is noteworthy that there was an enrichment in EVs isolated by UC+SEC (Figure 8C and D) compared to EVs isolated by UC (Figure 8A and B), proving once more the purity of the UC+SEC samples. Contrary

to EVs, CD9 did not appear in the cells of origin, which does not mean that it is absent from cells but may be present in quantities not able to be detected by the conditions we used for western blotting. Western blot analysis revealed that cells were positive for actin (42kDa), one of the major protein components of cell cytoskeleton, which explains the intense signal observed. We also detected actin in MKN45-derived EVs isolated by UC+SEC (Figure 8C and D), which signal was enhanced compared to EVs isolated by UC (Figure 8A and B). Lastly, the presence of cytochrome c (15kDa), an intracellular protein associated with mitochondria and expected to be absent in EV samples was tested. Our results are concordant with previous reports that detected cytochrome c in all cell lysates, whereas absent in all EV samples, confirming that EV isolates were not contaminated with cellular content. Noteworthy, EV markers were highly intense in EVs isolated by UC+SEC, confirming the higher level of purity achieved by the combination of these protocols.

Together with the protein profile, the expression of the cancer-associated *O*-glycan STn was tested in all cell lysates and EV isolates using the monoclonal antibody B72.3 produced in the laboratory (Figure 8E-H). As expected, MKN45 WT and MKN45 Mock cells and secreted EVs were negative for STn. On the other hand, STn was detected in MKN45 SC cell line (Figure 8F and H). Our results showed that EVs isolated from MKN45 SC carry the STn antigen (Figure 8F and H). Indeed, a more intense STn signal was detected in MKN45 SC-derived EVs when compared to MKN45 SC cells, suggesting that STn is preferentially packaged and highly enriched in the isolated EVs. Moreover, MKN45 SC-derived EVs isolated by UC+SEC (Figure 8H) presented a more intense band profile between 50-250kDa, compared to EVs isolated by UC (Figure 8F). The presence of STn was also tested for MKN45 ST6 cell lysates and EV isolates (Figure 8E and G). Western blotting analysis showed that glycoproteins carrying STn have an enhanced signal in MKN45 ST6-derived EVs compared to MKN45 ST6 cells. Unexpectedly, MKN45 ST6-derived EVs isolated by UC+SEC (Figure 8G) did not show an enhanced signal intensity of the band profile between 50-250kDa, compared to those isolated by UC (Figure 8E). This event might be due to a technical error during the sample loading into the gel. More western blotting experiments must be performed to confirm this lack of enrichment. Altogether, our results showed that the two different EV isolation methodologies allow the detection of STn in EV samples, which was facilitated by UC+SEC protocol, due to the purer EV samples obtained by this combination.

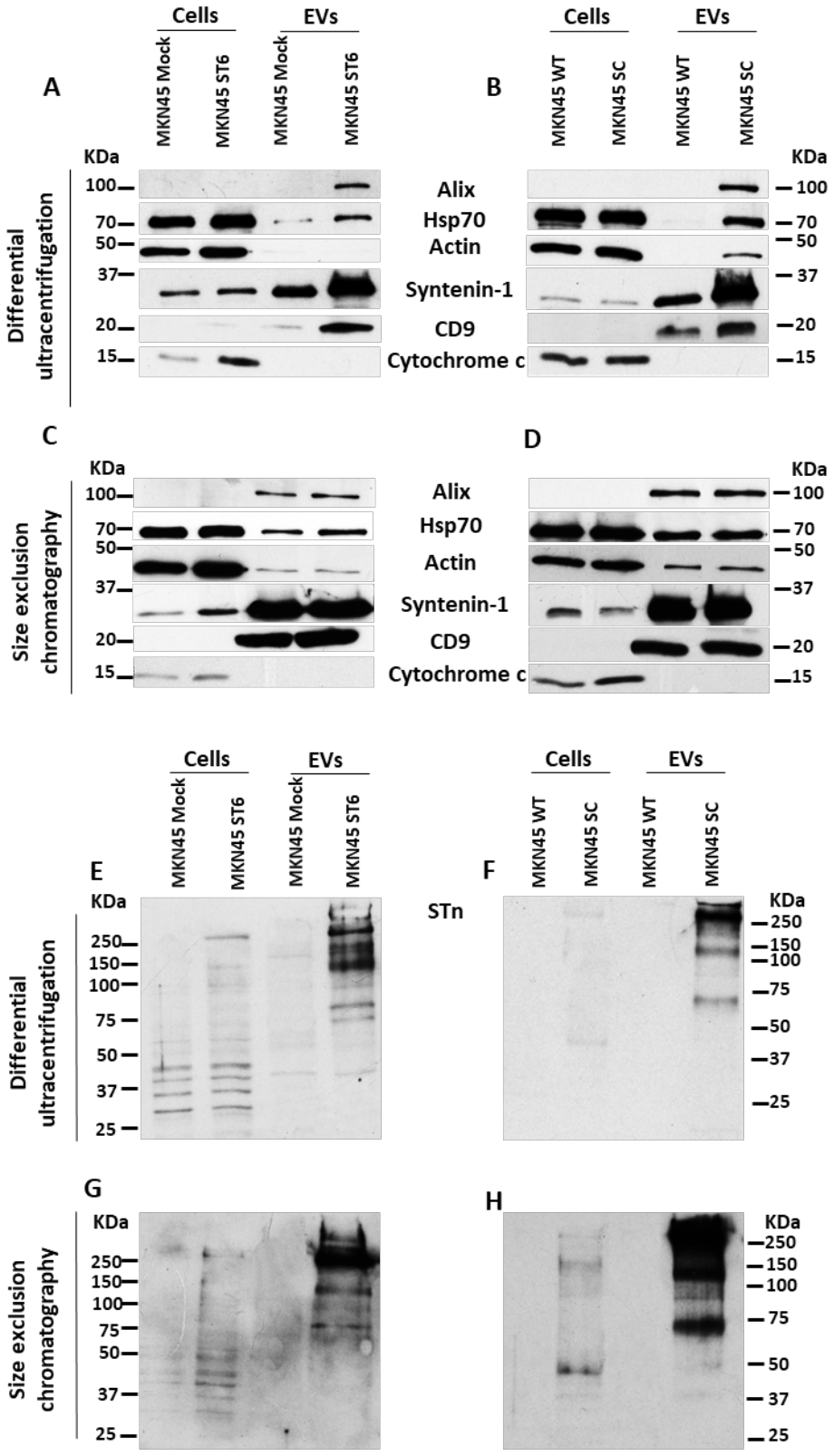

Figure 8. Protein profile and STn detection of four MKN45 cell lines and corresponding EVs isolated by UC and UC+SEC protocols. Western blotting was performed to detect a

panel of EV markers such as alix, syntenin-1, Hsp70, and CD9. Similarly, actin and cytochrome c as cytoskeleton and mitochondria markers, respectively, were performed in all cell and EV lysates. Analysis of EV markers for A) MKN45 Mock- and ST6-derived EVs isolated by UC; B) MKN45 WT- and SC-derived EVs isolated by UC; C) MKN45 Mock- and ST6-derived EVs isolated by UC+SEC and D) MKN45 WT- and SC-derived EVs isolated by UC+SEC. STn detection in E) MKN45 Mock- and ST6-derived EVs isolated by UC; F) MKN45 Mock- and ST6-derived EVs isolated by UC+SEC; G) MKN45 WT- and SC-derived EVs isolated by UC and H) MKN45 WT- and SC-derived EVs isolated by UC+SEC.

Immunolabelling of MKN45-derived EVs was used to detect STn at EV membrane. First, the protocol was performed in EVs isolated by UC and after freezing and thaw cycles, however it was difficult to distinguish EVs and some of them were found degraded due to freezing process. Also, considering that TEM is a highly sensitive technique, the greater amount of protein contamination verified in UC-isolates compromised the quality of images. In addition, we only use MKN45 WT- and MKN45 SC-derived EVs for immunolabeling. Therefore, some protocol optimizations were performed to obtain clearer images and more intense labelling. Considering the previous results of TEM and western blotting analysis, we opted to use only EV samples isolated by UC+SEC that showed a higher degree of purity. Also, we used UC+SEC-isolated samples that have not undergone any freeze-thaw cycle. Another critical point that needed to be adjusted was the dilution of the purified monoclonal antibody B72.3 produced in the laboratory and used to incubate EVs on the grids. At first, we used B72.3 at a dilution of 1:20, which allowed the detection of STn at EV membrane. However, the percentage of unlabeled EVs were much superior to the labeled ones, which suggest us to increase the concentration of the antibody making a dilution of 1:10, as represented in the images (Figure 9).

To the best of our knowledge, we were the first to detect the cancer-associated *O*-glycan STn in the membrane of MKN45 SC-derived EVs through an immunogold labelling technique (Figure 9B). The staining (black dots) occurred at EV membrane since no membrane permeabilization was performed to avoid the antibodies to penetrate EV membrane. MKN45 WT- and MKN45 SC-derived EVs isolated by UC+SEC were directly applied to carbon grids and incubated with a specific antibody for STn detection, the mAb B72.3. Adding the incubation with an antibody directed against STn and coupled to gold particles it was possible to detect the presence of STn (red arrows) in the membrane of MKN45 SC-derived EVs (Figure 9B). As expected, MKN45 WT-derived EVs showed no

signal for STn (Figure 9A), as well as the control for the secondary antibody prepared without EV sample and B72.3 antibody incubation (Figure 9C). Despite the need of more protocol optimizations, it was possible to detect STn at EV membrane of gastric cancer MKN45 SC-derived EVs. This result highlights the potential value of STn as a gastric cancer biomarker in EVs.

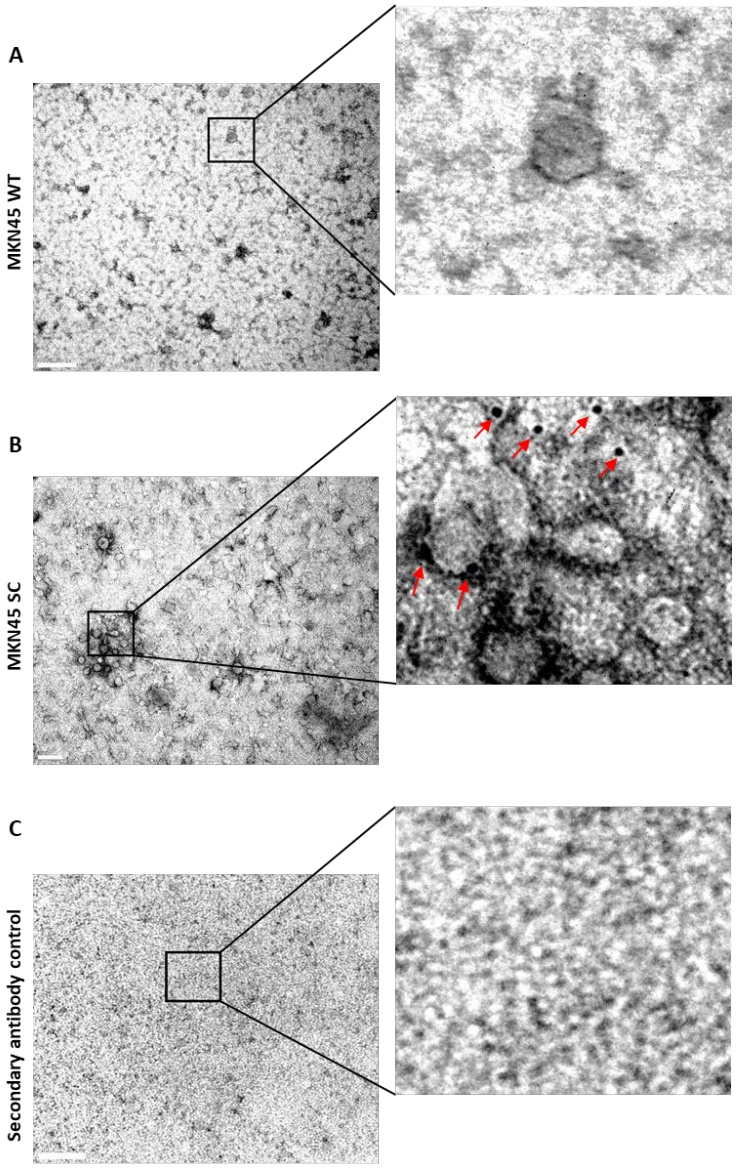

Figure 9. An immunolabeling technique was performed using an antibody directed against STn and conjugated with gold particles. A) MKN45 WT-derived EVs isolated by UC+SEC showed no signal. B) STn detection at the membrane of MKN45 SC-derived EVs isolated by UC+SEC (red arrows). C) The control for the secondary antibody, which was prepared without EV sample and primary antibody, showed no signal. Scale bar represents 200nm (left panel), and images were zoomed eight times (right panel).

To study the role of the *O*-glycan STn in EV uptake we co-cultured unlabeled MKN45 WT and SC cells (recipient cells) with labeled MKN45 WT and SC cells (donor cells) using an indirect co-culture system that allowed the passage of EVs and soluble factors but not cells from donor to recipient cells (Figure 10A). MKN45 WT and MKN45 SC cells were both used as recipient and donor cells and cultured in the wells of a 24-well plates or in 0.4µm inserts of a different plate, respectively. The suspensions of donor cells were labeled with 15µL of DiI, a lipophilic dye that diffuses laterally and intercalate within the cell membrane, staining the entire cell[250]. After 20h, recipient MKN45 WT cells were co-cultured with MKN45 WT or MKN45 SC DiI-labeled cells as donor cells and recipient MKN45 SC cells were co-cultured with MKN45 WT and MKN45 SC DiI-labeled cells as donor cells. At this time, EVs produced by DiI-labeled cells were able to pass through the insert and be internalized by recipient cells. Negative controls of MKN45 cells were performed seeding the corresponding cells in 24-well plates and grown in cell culture medium (Figure 10B). No signal was observed when cells were visualized in a fluorescent cell imager microscope, as expected (Figure 10B). MKN45 cells were directly labeled with DiI for positive controls, which demonstrated the efficiency of the stained procedure (Figure 10C).

As EVs are of endosomal or outward budding membrane origin, DiI-labeled cells release EVs that carry DiI in their membranes, allowing the visualization of stained EVs at the fluorescent cell imager microscope. Our results demonstrate that both cell lines have the capacity to internalize EVs secreted either by MKN45 WT cells or MKN45 SC cells and there was an evident increase in the relative quantity of stained EVs internalized by cells after 48 hours (Figure 10F and G) when compared to 24 hours (Figure 10D and E). MKN45 SC cells were able to uptake MKN45 WT- and MKN45 SC-derived EVs at a similar proportion after 24 hours when compared to the total number of cells visualized in brightfield images (Figure 10E). On the other hand, MKN45 WT cells only internalized MKN45 WT-derived EVs at 24 hours (Figure 10D). In fact, there seems to be a tendency for cells to uptake preferentially EVs secreted by themselves, mostly noticed when cells were co-cultured for 48 hours (Figure 10F and G). Intriguingly, it was only possible to detect DiI-labeled MKN45 SC-derived EVs internalized by MKN45 WT cells after 48 hours, suggesting a lesser capacity of these cells to uptake EVs from another origin (Figure 10F). As only one experiment was performed, further experiments are required to confirm the obtained results. However, significant changes were observed when comparing the uptake of different DiI-labeled EVs co-cultured with MKN45 WT and

MKN45 SC cells for 24h and 48h, which incite us to investigate in the future the effect of STn in the internalization of EVs.

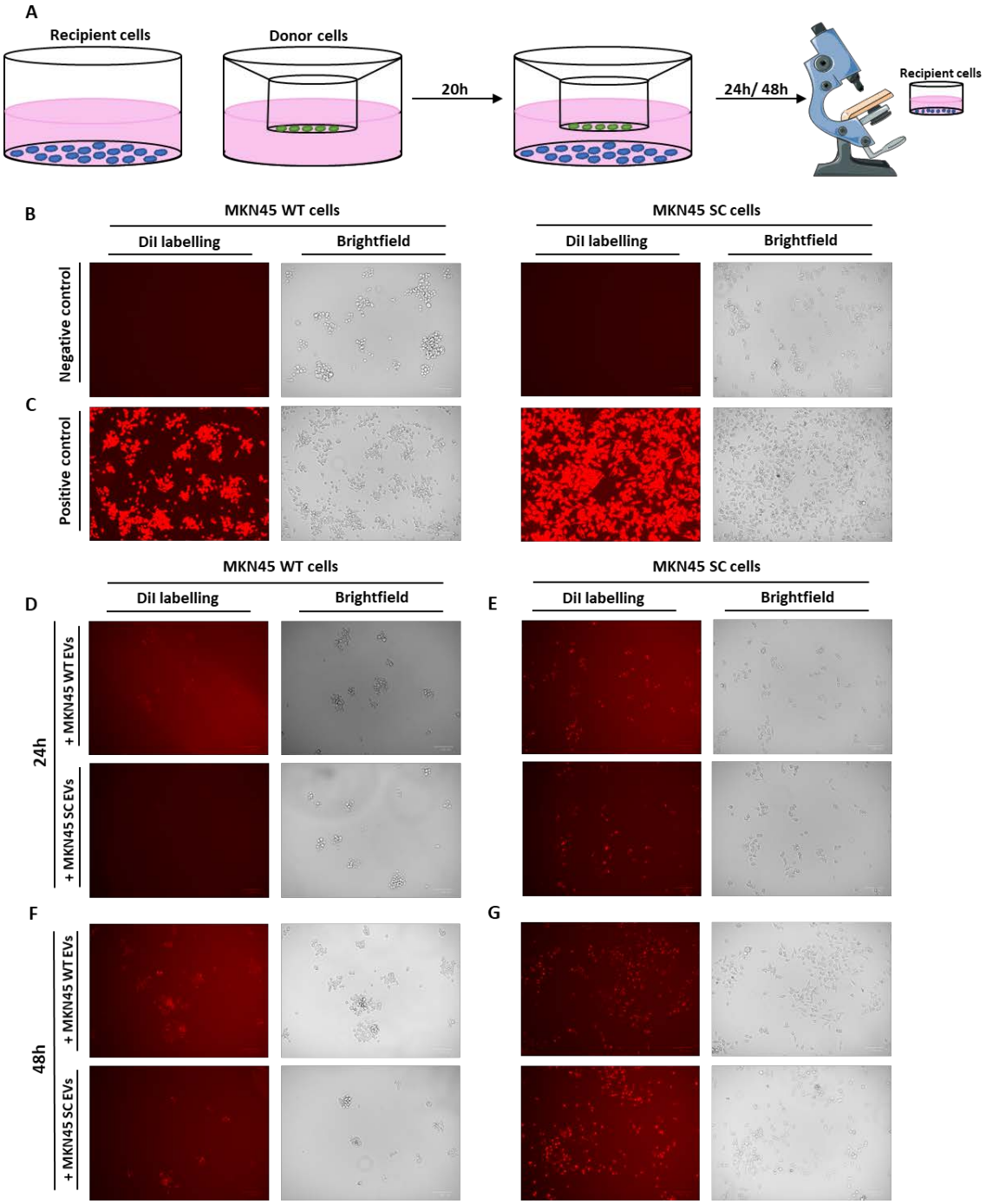

Figure 10. Fluorescence microscopy uptake analysis of MKN45 WT- and MKN45 SC-derived EVs by MKN45 WT and SC cells using an indirect co-culture system. A) MKN45 WT and MKN45 SC cells were seeded and grown in cell culture medium in the bottom

wells of a 24-well plates or plated in 0.4µm inserts designated as recipient and donor cells, respectively. Donor cells were directly labeled with DiI dye using a proportion of 15µL of DiI per 500,000 cells for labeled EV production. After 20 hours of growth, donor cells were indirectly co-cultured with recipient cells to release DiI-labeled EVs that were internalized by recipient cells. Lastly, recipient cells that undergone indirect co-culture for 24 hours or 48 hours were visualized in fluorescent cell imager microscope. B) Unlabeled MKN45 WT and MKN45 SC cells were seeded and grown in 24-well plates as negative controls. C) MKN45 WT and MKN45 SC cells were directly labelled with DiI dye for positive controls using a proportion of 1µL of DiI per 200,000 cells. D) MKN45 WT cells and E) MKN45 SC cells were co-cultured with MKN45 WT and MKN45 SC labeled cells for 24 hours. F) MKN45 WT cells and G) MKN45 SC cells were co-cultured with MKN45 WT and MKN45 SC labeled cells for 48 hours. Brightfield (right panel) and fluorescent images (left panel) of DiI (red) were taken at ZOE fluorescent cell imager microscope. Scale bar represents 100µm.

7. Discussion

The main objective of this work was to study the impact of two different EV isolation methodologies in STn detection in EVs derived from a poorly differentiated gastric cancer cell line. Gastric cancer is one of the deadliest oncologic diseases worldwide, due to the lack of an early diagnosis, leading to poor prognosis of cancer patients. Aberrant glycosylation is a common feature of cancer cells and leads to inadequate cell/cell and cell/matrix interactions, reflecting a dysregulation in tumor cell behavior, such as uncontrollable cell growth, invasiveness and metastatic potential[69]. Particularly, the simple *O*-glycan STn was found highly expressed in gastric cancer[115,119], but has limited expression in normal tissues[120]. Moreover, STn has proven to be related with increased cell aggressiveness, invasiveness, metastatic potential, and poor prognosis of gastric cancer patients[123,129]. Due to its role and overexpression in cancer cells, STn is considered as an important prognostic marker and a target molecule appropriate for specific immunotherapy with anticancer vaccines[251,252]. As EVs released by cancer cells represent a valuable source for biomarker discovery and detection, more efficient methods for EV purification are required. Our group accessed the presence of STn in EVs from gastric cancer cells, which constituted an important step disclosing EV glycosylation and suggested that EVs could be used as a less invasive tool for gastric cancer diagnosis[131].

In this study we used a MKN45 parental cell line derived from a poorly differentiated gastric adenocarcinoma cell line that showed a heterogeneous glycan profile with mature *O*-glycans (Figure 5A). MKN45 WT cells were genetically modified targeting the core 1 synthase C1GALTC1 private chaperone *COSMC* by zinc-finger nuclease to produce MKN45 SC cells, which display a homogeneous *O*-glycosylation profile, with expression of cancer-associated glycans like Tn and STn[66]. Also, the MKN45 WT cells were stably transfected with the full-length *ST6GalNAc1* gene (ST6) or with an empty vector pcDNA3.1 (Mock) as previously described[240,241]. MKN45 ST6 cells showed a heterogeneous panel of elongated and truncated *O*-glycans, with expression of STn at lower extent compared to MKN45 SC cells. This phenomenon was observed in our study by immunofluorescence, with the totality of MKN45 SC cells expressing STn and relatively less MKN45 ST6 cells positive for STn (Figure 5C), confirming their biosynthetic process[240]. While *COSMC* knockout results in the premature termination of *O*-glycan elongation and consequent accumulation of Tn and synthesis of STn, overexpression of ST6GalNAc1 enzyme induces the synthesis of STn without inhibiting the *O*-glycan

elongation pathway (Figure 5A). Also, STn expression is not affected when cell culture conditions are altered by the removal of FBS (Figure 5C), as proven by our group[131].

Considering that FBS contains high levels of glycoproteins that can be co-purified with EVs and may affect the glycosylation downstream analysis. FBS removal from the cell culture medium is highly recommended in this case before performing any EV isolation methodology[131]. Likewise, all EV isolations were performed with medium depleted of FBS. In our study, we showed that cell viability is not significantly altered when cells grow in absence of FBS for 72 hours (Figure 5E). At contrary, the proliferation rate of all four cell lines decreased significantly when cells were deprived of serum (Figure 5D), as FBS contains a complex mixture of biomolecules that include growth factors, proteins, vitamins, and hormones that supply cell growth and maintenance of *in vitro* cells[253]. Also, deprivation of FBS led to a more elongated shape, characteristic of a mesenchymal-like phenotype and particularly observed in the glycoengineered gastric cancer cell lines as demonstrated previously by our group[131]. Moreover, they showed that MKN45 cells expressing STn displayed an increased migratory and invasive capacities. A previous study examined the main behavior alterations affected by truncated *O*-glycans in prostate cancer cells and shows that ST6GalNAc1 expression leads to a switch to reduced cell adhesion and increased motility, characteristic from a mesenchymal-like cell phenotype[254]. Also, our group have proven that the synthesis of STn lead to a more aggressive phenotype, which is associated with a poor prognosis of gastric cancer patients[129]. Importantly, MKN45 ST6 and MKN45 SC cells, both expressing STn, secreted more and smaller EVs (Figure 6). As cancer-derived EVs are able to efficiently propagate oncogenic signals, and STn is known to lead to a more aggressive phenotype, it is probable that cells expressing STn were able to secrete a much higher number of EVs to meet the needs of cellular communication and tumor growth, increasing the potential of reprogramming cells into malignancy[187]. In cancer context, a higher number of secreted EVs will reach the bloodstream and other body fluids, facilitating the detection of STn positive EVs in a minimally invasive manner for prognostic and diagnostic evaluation of gastric cancer patients[216].

In our study, we used UC and UC+SEC protocols to isolate EVs and to compare the size, yield, purity and STn detection in the isolated EV samples. Unbiased isolation of EVs remains a challenge due to its heterogeneity and co-isolation of protein contaminants[255]. UC remains by far the most used technique to isolate and analyze EVs[256]. However, UC leads to the co-isolation of large amounts of protein complexes, compromising the purity of EV isolates[181]. On the other hand, SEC has proven to be more

efficient in separating the vast majority of soluble proteins, providing purer EV samples with higher functionality[257,258]. NTA is usually used to calculate particle concentration distributed according to their size, with diameter >50nm[259], which includes EVs, soluble proteins and/or protein aggregates that may co-isolate with EVs during the isolation protocols. Thereafter, the determination of the real EV concentration and size distribution will be affected if protein contaminants are present. Regarding protein/particle ratios, a complete reverse tendency was observed when comparing UC- and UC+SEC-isolates. Our group have already demonstrated that aberrant *O*-glycosylation may, therefore, influence the transcription of several genes implicated in cancer progression and motility processes of MKN45 and AGS cell lines, such as *SRPX2* and *RUNX1* genes[129]. STn positive EVs (MKN45 ST6- and SC-derived EVs) presented a higher ratio of protein/particle when adding SEC (Figure 6J and T). On the other hand, STn negative EVs (MKN45 Mock- and WT-derived EVs) showed a decrease on protein/particle ratio when the combination of protocols was used (Figure 6J and T). Thus, the specific cargo of EVs may impact the metastatic ability and the overall effects of cancer. The combination of protocols led to purer EV samples as confirmed by TEM imaging acquisition (Figure 7) and by the detection of specific EV markers by western blotting (Figure 8). Some recent reports indicate similar yields and purities[178], while others showed higher yields and purer EVs isolated by SEC compared to UC[258]. We therefore observed a significant decrease in EV yield when adding an extra step of purification, but more pure populations of EVs confirmed by protein/particle ratios and EV marker analysis, as proved before[131,181]. Others also suggest that the combination of EV isolation methods is inevitable to increase purity of EV samples[211,260]. There are even studies that considered a standard for EV purity with 10^{10} EVs containing ~1µg of protein or even higher ratios of particle/protein[239]. However, this may not be always necessary and careful attention must be given when choosing the isolation method, as it should also depend on the question under investigation, type and volume of the starting material.

TEM was used for size, morphology, integrity and EV purity analysis. EVs appeared as cup-shaped morphology (Figure 7, red arrows), while soluble proteins have a typical white ranged appearance (Figure 7, green arrows)[169]. These smaller sized protein structures appeared more evident in UC-isolates (Figure 7A-D) when compared to UC+SEC-isolates (Figure 7E-H). Therefore, our results have, as well, proven the efficiency of SEC, as an additional step for EV purification, in isolating highly pure EVs compared to UC. NTA and TEM analysis also provided EV size measurements of isolated EVs. STn positive EVs presented a smaller size when compared to STn negative EVs.

The size of EVs may impact several cancer processes such as its metastatic potential, since EVs from different sizes are internalized in different ways by the recipient cells. Whereas large EVs might induce phagocytosis, can be internalized by non-phagocytic pathways. Also, UC (Figure 6F and P) showed to isolate EVs with smaller sizes compared to UC+SEC-isolates (Figure 6K and U), as measured by NTA. However, as NTA does not only read EVs, this shift to the left in the x-axis of NTA histograms may correspond to the overlapping characteristics of proteins co-isolated with EVs[261]. When SEC was performed and the small size protein contaminants were separated from EV fractions, NTA measurements were more accurate as less proteins were considered to establish the size peak (Figure 6K and U). Considering all the evidence, UC+SEC seemed to be more adequate in isolating highly pure EV samples. In fact, our group[131] and others[186,258] have already reported that combination methods with SEC lead to improved EV preparations with less contaminating particles.

Our evaluation of the presence of specific known EV markers on EV samples isolated by UC or UC+SEC added another level of certainty that the two-step methodology UC+SEC provided purer EVs (Figure 8). EV markers such as cytoplasmic alix and Hsp70 proteins, cytosolic protein syntenin-1 and transmembrane protein CD9 were tested in all cell lysates and EV isolates, as well as the cytoskeleton protein actin and mitochondrial protein cytochrome c[135]. Overall, EV markers were enriched in EVs compared to the cells of origin, as demonstrated in previous findings[262,263]. Also, EV markers were more intense in UC+SEC-isolates (Figure 8C and D) compared with UC-isolates (Figure 8A and B), confirming that purer EV samples were obtained when performing a two-step EV isolation approach, according to what has been previously reported[258].

Relating to glycosylation analysis, aberrant expression of glycans displayed by cancer cells proved to influence the tumor progression[69,264]. Particularly STn, which correlates with poor patient prognosis in several types of cancer[115,265,266]. As expected, western blotting demonstrated that both cell types (MKN45 ST6 and MKN45 SC) were positive for STn in contrary of the two control cell lines (MKN45 Mock and MKN45 WT) (Figure 8). EV glycosylation analysis remains a very challenging area of research. Thus, it has been recent the pursuit for glycomic methods applied for EVs. In fact, only in 2009 investigators demonstrated that EVs possess a vast repertoire of glycans[267]. As proved by our group, EVs secreted by MKN45 SC cells are enriched on specific high molecular weight glycoproteins carrying the STn antigen when compared to the secreting cells[131]. Also, our results showed an increase of STn expression in MKN45 SC-derived EVs isolated by UC+SEC (Figure 8H), proving once again that UC+SEC leads to enhance EV content

detection and, therefore, purer EV samples when compared to UC-isolates (Figure 8F). The same pattern was observed in MKN45 ST6-derived EVs when isolated by the combination of the two methodologies, however this was less noticeable (Figure 8G). This may happen as the originating MKN45 ST6 cells display a heterogeneous glycan profile, with less glycoproteins carrying the cancer-associated *O*-glycan STn. However, more experiments would be necessary to clarify this result. Together, these results might provide a more sensitive STn detection *in vitro* and may be extrapolated to biological samples due to its feasible characteristics in circulation, opening new areas of research for biomarker discovery and detection and in current cancer-targeted therapies[268].

To the best of our knowledge, STn localization at EV membrane has never been reported. Our evaluation of an immunolabelling technique with mAb B72.3 followed by a secondary antibody coated with gold particles, revealed that STn localizes at EV membrane of MKN45 SC-derived EVs isolated by UC+SEC (Figure 9B). The detection of STn at the surface of EVs holds the potential to be targetable for the development of new EV detection and isolation approaches. Interestingly, a lectin recognition-mediated *in situ* rolling circle assembly was reported to improve the detection capacity of the other glycan patterns present in cancer EV samples[269]. Similarly, when using an evanescent-field fluorescence-assisted lectin array system, it was possible to analyze the glycan profile of EVs derived from mesenchymal stem cells[158]. Furthermore, these approaches contributed to the development of high-throughput profiling of EV glycosylation and to the detection of glycan-based biomarkers in cancer-derived EVs. As STn antigen showed to be present and enriched at EV membranes secreted by gastric cancer cells in our study, its sensitive detection would be a valuable source for better stratification and monitor of gastric cancer patients.

Aberrant EV glycosylation has been described to affect its biodistribution *in vivo* by increasing the migration and invasion potential of cancer cells[270]. The effect of EV surface glycans in EV uptake by recipient cells was extensively studied, particularly the effect of proteoglycans, as reviewed elsewhere[157]. In the other hand, the impact of sialic acids has only been reported once[164]. Interestingly, the investigators showed, for most cells tested, that desialylated EVs showed a greater EV uptake efficacy. Another investigation, using an ovarian carcinoma cell line observed a non-significant increase in EV uptake when desialylated[166]. In agreement with these findings, our results showed that the presence of STn on EVs led to a lower EV uptake by cells displaying a homogeneous mature *O*-glycan pattern (Figure 10). The increase in the negative charge of EVs caused by the presence of sialic acid residues could lead to structural or functional alterations in EV membrane or

exposition of different ligands at the surface of the recipient cells that would mediate the binding, making it difficult to internalize EVs[271]. Another explanation relies on the fact that sialylation may alter steric hindrance of other ligands at EV membranes[272], resulting in decreased internalization by recipient cells. Our pivotal experiment demonstrated different affinities in the extent of uptake by the different cell lines (Figure 10D-G). There seems to be a tendency for cells to uptake EVs derived from the same cells, as they naturally produce similar EV content. Studies showed that epithelial cells internalize more epithelial-derived EVs compared to other recipient cells[273], whereas mesenchymal stem-derived EVs were rather up-taken by mesenchymal stem cells compared to other cell lines *in vitro*[274]*.* This evidence suggests that the specific signature of EVs is preserved and used as recognition moiety for the recipient cell. Although others have found that EVs display a non-selective biodistribution[275], our results agree with previous works, suggesting that EVs are able to target specific cells. Despite this promising evidence, further investigations are required to provide a quantitative confirmation of the impact of STn in EV uptake by gastric cancer cells.

8. Conclusions and Future Perspectives

8.1. Main conclusions

In this work, we aimed to isolate EVs from two glycoengineered MKN45 gastric cancer cell lines expressing the cancer-associated antigen STn and two control cell lines to compare the efficacy of two different EV isolation protocols. UC+SEC allowed the separation of low yield, but purer EV samples when compared to UC. Considering the potential use of EVs as a valuable source for biomarkers detection and discovery, this study showed an enrichment of STn levels in EVs compared to the cells of origin. Also, STn positive cells secrete more EVs. In cancer context, this may facilitate the detection of STn positive EVs, as more EVs might reach the circulation and body fluids. Remarkably, STn was first detected at the membranes of EVs secreted by gastric cancer cells, highlighting the value of STn as gastric cancer biomarker and its further application in EV isolation methodologies to better diagnose and monitor gastric cancer patients, contributing to a precise stratification of patients and application of personalized therapies. Additionally, STn impacts EV uptake by recipient cells, suggesting an ability to reprogram cell function. These methodologies can be further expanded to explore new EV detection methods regarding STn expression and the impact of STn positive EVs in different biological processes.

8.2. Future perspectives

Despite the technological advances in the field, the study of EVs is still technically challenging. Particularly, innovative, less laborious detection and better isolation methods are an urgent need to facilitate an in-depth study of the different EV cargos as a reliable source of biomarkers. As specific glycans are exposed at EV surface, affinity interactions can be employed to capture EVs by binding to their surface receptor. Despite the increased knowledge concerning the role of glycans in physiologic and pathologic conditions, the study of glycans as candidates to incorporate EV isolation methods remains poor. In gastric cancer, the presence of specific glycans, particularly STn at EV surface, as we have proven in this study, constitute a valuable source to potentiate the development of more sensitive and specific EV detection and isolation methodologies, with the potential to be translated into the clinical practice. Thus, the potential of STn as binding-ligand in isolation methods could be considered. The application of this antigen to capture EVs from cell lines must be tested to validate the efficacy of this methodology,

with further application of an optimized protocol to stablish a fast and reproducible method for EV isolation from biological samples. The implementation of a novel methodology for EV capture based on glycans can open new avenues regarding the potential of such molecules as biomarkers for less invasive diagnosis and monitoring.

For that, we purpose the development and optimization of an immunoaffinity isolation methodology to isolate and separate EVs that carry STn at their membranes (Figure 11). This approach would highlight the value of STn as gastric cancer biomarker and open new areas for cancer diagnosis and prognosis improvement, allowing a better patient stratification for rapid and personalized therapeutics.

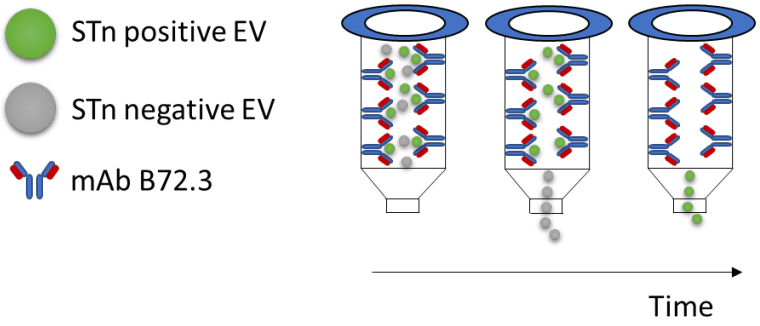

Figure 11. Proposed mechanism of an immunoaffinity methodology to isolate EVs carrying the tumor-associated carbohydrate STn. The coating of an affinity column with the monoclonal antibody B72.3 would allow the capture of EVs displaying STn at their membrane that are eluted after the EVs negative for STn.

Other questions that require investigation are related the impact of STn in EV uptake. EVs present a vast repertoire of exposed surface glycans that participate in cellular uptake, disrupting the native glycosylation pattern of the recipient cells. Herein, we aim to repeat EV uptake experiments to perform a quantitative analysis using flow cytometry. Thus, we could calculate the percentage of DiI-labeled EVs that are internalized by MKN45 cells and translate this methodology to other cell types, taking into consideration the biodistribution tropism of gastric cancer cells.

There are still many questions to be answered regarding the functional role of EV glycosylation in gastric cancer as well as challenges on how to address these questions. Future studies will allow us to solidify the value of STn in gastric cancer EVs for a better

diagnosis/prognosis/patient stratification and develop innovative therapeutic strategies that can be applied for cancer treatment.

9. Other projects

Simultaneously with my master thesis, I was included in some other projects that help me to consolidate the technics and knowledge that I acquired over time, as well as to understand the applicability of our investigation in the clinical context. This integration was possible due to the exceptional leadership of Dra. Daniela Freitas and Dr. Celso Reis, who recognize my potential capacities to work with other group workers and incite me to participate in several projects.

Our group was pioneer in detecting STn in EV samples derived from gastric cancer cells. To pursue this research, my supervisor's team is developing a project that involve the processing of biological samples from patients with gastric cancer with collaboration with Hospital Santo António, Porto. The aim of this project is to isolate EVs from human gastric cancer plasma samples to detect and access the presence of the truncated *O*-glycan STn in circulating EVs.

Additionally, I am currently participating in a project together with a PhD student in the group that is working on 3D cell culture optimization and EVs isolation to compare the behavior of MKN45 cell line in different culture conditions and address the protein and glycan profile of the secreted EVs isolated by UC and UC+SEC. We intend to do a comparative protein and glycan cargo analysis of the EVs isolated from 2D and 3D cell cultures that express different levels of STn.

In the future, I aim to pursue a PhD degree in cancer glycobiology and increase my knowledge and perspectives in the investigation field.

10. Bibliography

1. Sung, H.; Ferlay, J.; Siegel, R. L.; Laversanne, M.; Soerjomataram, I.; Jemal, A. & Bray, F. Global cancer statistics 2020: GLOBOCAN estimates of incidence and mortality worldwide for 36 cancers in 185 countries. *CA. Cancer J. Clin.* **0**, 1–41 (2021).

2. Laird, P. W. Cell-of-origin patterns dominate the molecular classification of 10,000 tumors from 33 types of cancer. *Cell* **173**, 291–304 (2018).

3. Harper, J. W. & Elledge, S. J. The DNA damage response: ten years after. *Mol. Cell* **28**, 739–745 (2007).

4. Feinberg, A. P. & Vogelstein, B. Hypomethylation distinguishes genes of some human cancers from thir normal conterparts. *Nature* **301**, 89–92 (1983).

5. Eden, A.; Gaudet, F.; Waghmare, A. & Jaenisch, R. Chromosomal instability and tumors promoted by DNA hypomethylation. *Science (80-.).* **300**, 455 (2003).

6. Hanahan, D. & Weinberg, R. A. The hallmarks of cancer. *Cell* **100**, 57–70 (2000).

7. Sherr, C. J. Cancer cell cycles. *Science (80-.).* **274**, 1672–1674 (1996).

8. Park, M.; Chae, H. D.; Yun, J.; Jung, M.; Kim, Y. S.; Kim, S. H.; Han, M. H. & Shin, D. Y. Constitutive activation of cyclin B1-associated cdc2 kinase overrides p53-mediated G2-M arrest. *Cancer Res.* **60**, 542–545 (2000).

9. Symonds, H.; Krall, L.; Remington, L.; Saenz-Robles, M.; Lowe, S.; Jacks, T. & Van Dyke, T. p53-Dependent apoptosis suppresses tumor growth and progression in vivo. *Cell* **78**, 703–711 (1994).

10. Innocente, S. A.; Abrahamson, J. L. A.; Cogswell, J. P. & Lee, J. M. p53 regulates a G2 checkpoint through cyclin B1. *Proc. Natl. Acad. Sci. U. S. A.* **96**, 2147–2152 (1999).

11. Dulić, V.; Kaufmann, W. K.; Wilson, S. J.; Tisty, T. D.; Lees, E.; Harper, J. W.; Elledge, S. J. & Reed, S. I. p53-dependent inhibition of cyclin-dependent kinase activities in human fibroblasts during radiation-induced G1 arrest. *Cell* **76**, 1013–1023 (1994).

12. Reed, J. C. Dysregulation of apoptosis in cancer. *J. Clin. Oncol.* **17**, 2941–2953 (1999).

13. Shankaran, V.; Ikeda, H.; Bruce, A. T.; White, J. M.; Swanson, P. E.; Old, L. J. & Schreiber, R. D. IFNγ, and lymphocytes prevent primary tumour development and shape tumour immunogenicity. *Nature* **410**, 1107–1111 (2001).

14. Smyth, M. J.; Thia, K. Y. T.; Street, S. E. A.; Cretney, E.; Trapani, J. A.; Taniguchi, M.; Kawano, T.; Pelikan, S. B.; Crowe, N. Y. & Godfrey, D. I. Differential tumor surveillance by natural killer (NK) and NKT cells. *J. Exp. Med.* **191**, 661–668 (2000).

15. Folkman, J. What is the evidence that tumors are angiogenesis dependent? *J. Natl. Cancer Inst.* **82**, 4–7 (1990).

16. Andrews, N. A.; Jones, A. S.; Helliwell, T. R. & Kinsella, A. R. Expression of the E-cadherin-catenin cell adhesion complex in primary squamous cell carcinomas of the head and neck and their nodal metastases. *Br. J. Cancer* **75**, 1474–1480 (1997).

17. Bailey, T.; Biddlestone, L.; Shepherd, N.; Barr, H.; Warner, P. & Jankowski, J. Altered cadherin and catenin complexes in the Barrett's esophagus- dysplasia-adenocarcinoma sequence. *Am. J. Pathol.* **152**, 135–144 (1998).

18. Paredes, J.; Albergaria, A.; Oliveira, J. T.; Jeronimo, C.; Milanezi, F. & Schmitt, F. C. P-cadherin overexpression is an indicator of clinical outcome in invasive breast carcinomas and is associated with CDH3 promoter hypomethylation. *Clin. Cancer Res.* **11**, 5869–5877 (2005).

19. Patel, I. S.; Madan, P.; Getsios, S.; Bertrand, M. A. & MacCalman, C. D. Cadherin switching in ovarian cancer progression. *Int. J. Cancer* **106**, 172–177 (2003).

20. Agrez, M.; Chen, A.; Cone, R. I.; Pytela, R. & Sheppard, D. The αvβ6 integrin promotes proliferation of colon carcinoma cells through a unique region of the β6 cytoplasmic domain. *J. Cell Biol.* **127**, 547–556 (1994).

21. Ren, B.; Yu, Y. P.; Tseng, G. C.; Wu, C.; Chen, K.; Rao, U. N.; Nelson, J.; Michalopoulos, G. K. & Luo, J. H. Analysis of integrin α7 mutations in prostate cancer, liver cancer, glioblastoma multiforme, and leiomyosarcoma. *J. Natl. Cancer Inst.* **99**, 868–880 (2007).

22. Weiss, L.; Nannmark, U.; Johansson, B. R. & Bagge, U. Lethal deformation of cancer cells in the microcirculation: A potential rate regulator of hematogenous metastasis. *Int. J. Cancer* **50**, 103–107 (1992).

23. Stephen Paget. The distribution of secondary growths in cancer of the breast. *Cancer Metastasis Rev.* **2**, 98–101 (1889).

24. Peinado, H.; Lavotshkin, S. & Lyden, D. The secreted factors responsible for pre-metastatic niche formation: Old sayings and new thoughts. *Semin. Cancer Biol.* **21**, 139–146 (2011).

25. Talmadge, J. E. & Fidler, I. J. . AACR Centennial Series: The biology of cancer metastasis: Historical perspective. *Cancer Res.* **70**, 5649–5669 (2010).

26. Lyden, D. C. Pancreatic cancer exosomes initiate pre-metastatic niche formation in the liver. *Nat. Cell Biol.* **17**, 816–826 (2015).

27. Ueno, M.; Oya, M.; Azekura, K.; Yamaguchi, T. & Muto, T. Incidence and prognostic significance of lateral lymph node metastasis in patients with advanced low rectal cancer. *Br. J. Surg.* **92**, 756–763 (2005).

28. Boxberg, M.; Leising, L.; Steiger, K.; Jesinghaus, M.; Alkhamas, A.; Mielke, M.; Pfarr, N.; Götz, C.; Wolff, K. D.; Weichert, W. & Kolk, A. Composition and clinical impact of the immunologic tumor microenvironment in oral squamous cell carcinoma. *J. Immunol.* **202**, 278–291 (2019).

29. Leek, R. D.; Lewis, C. E.; Whitehouse, R.; Greenall, M.; Clarke, J. & Harris, A. L. Association of macrophage infiltration with angiogenesis and prognosis in invasive breast carcinoma. *Cancer Res.* **56**, 4625–4629 (1996).

30. Alberts, B.; Johnson, A.; Lewis, J.; Raff, M.; Roberts, K. & Walter, P. *Molecular biology of the cell*. *Annals of Botany* **3**, (2003).

31. Levental, K. R.; Yu, H.; Kass, L.; Lakins, J. N.; Egeblad, M.; Erler, J. T.; Fong, S. F. T.; Csiszar, K.; Giaccia, A.; Weninger, W.; Yamauchi, M.; Gasser, D. L. & Weaver, V. M. Matrix crosslinking forces tumor progression by enhancing integrin signaling. *Cell* **139**, 891–906 (2009).

32. Toshima, M.; Ohtani, Y. & Ohtani, O. Three-dimensional architecture of elastin and collagen fiber networks in the human and rat lung. *Arch. Histol. Cytol.* **67**, 31–40 (2004).

33. Morla, A. & Ruoslahti, E. A fibronectin self-assembly site involved in fibronectin matrix assembly: Reconstruction in a synthetic peptide. *J. Cell Biol.* **118**, 421–429 (1992).

34. Terranova, V. P.; Williams, J. E.; Liotta, L. A. & Martin, G. R. Modulation of the metastatic activity of melanoma cells by laminin and fibronectin. *Science (80-.).* **226**, 982–985 (1983).

35. Paszek, M. J.; Zahir, N.; Johnson, K. R.; Lakins, J. N.; Rozenberg, G. I.; Gefen, A.; Reinhart-King, C. A.; Margulies, S. S.; Dembo, M.; Boettiger, D.; Hammer, D. A. & Weaver, V. M. Tensional homeostasis and the malignant phenotype. *Cancer Cell* **8**, 241–254 (2005).

36. Moon, J. J.; Matsumoto, M.; Patel, S.; Lee, L.; Guan, J. L. & Li, S. Role of cell surface heparan sulfate proteoglycans in endothelial cell migration and mechanotransduction. *J. Cell. Physiol.* **203**, 166–176 (2005).

37. Zhang, Y.; Cao, L.; Yang, B. L. & Yang, B. B. The G3 domain of versican enhances cell proliferation via epidermial growth factor-like motifs. *J. Biol. Chem.* **273**, 21342–21351 (1998).

38. Zhu, H.; Mitsuhashi, N.; Klein, A.; Barsky, L. W.; Weinberg, K.; Barr, M. L.; Demetriou, A. & Wu, G. D. The role of the hyaluronan receptor CD44 in mesenchymal stem cell migration in the extracellular matrix. *Stem Cells* **24**, 928–935 (2006).

39. Kannagi, R. Carbohydrate-mediated cell adhesion involved in hematogenous metastasis of cancer. *Glycoconj. J.* **14**, 577–584 (1997).

40. Moss, E. L.; Hollingworth, J. & Reynolds, T. M. The role of CA125 in clinical practice. *J. Clin. Pathol.* **58**, 308–312 (2005).

41. Bast, R. C.; Klug, T. L.; St. John, E. S.; Jenison, E.; Niloff, J. M.; Lazarus, H.; Berkowtiz, R. S.; Leavitt, T.; Griffiths, C. T.; Parker, L.; Zurawski, V. R. & Knapp, R. C. A radioimmunoassay using a monoclonal antibody to monitor the course of epithelial ovarian cancer. *N. Engl. J. Med.* **309**, 883–887 (1983).

42. Ferlay J, Ervik M, Lam F, et al. Global Cancer Observatory: Cancer Today. Lyon, France: International Agency for Research on Cancer; Available from: https://gco.iarc.fr/today. Accessed 27 September 2021.

43. Ward, M. H. & López-Carrillo, L. Dietary factors and the risk of gastric cancer in

Mexico City. *Am. J. Epidemiol.* **149**, 925–932 (1999).

44. Karimi, P.; Islami, F.; Anandasabapathy, S.; Freedman, N. D. & Kamangar, F. Gastric cancer: Descriptive epidemiology, risk factors, screening and prevention. *Cancer Epidemiol Biomarkers Prev.* **23**, 700–713 (2014).

45. Lauren, P. The two histological main types of gastric carcinoma: Diffuse and so-called intestinal-type carcinoma. *Acta Pathol.* **64**, 31–49 (1965).

46. Zanghieri, G.; Gregorio, D.; Sacchetti, C.; Fante, R.; Sassatelli, R.; Cannizzo, G.; Carriero, A. & Leon, M. P. De. Familial occurrence of gastric cancer in the 2- year experience of a population-based registry. *Cancer* **66**, 2047–2051 (1990).

47. Correa, P. Human gastric carcinogenesis: A multistep and multifactorial process-first american cancer society award lecture on cancer epidemiology and prevention. *Cancer Res.* **52**, 6735–6740 (1992).

48. Reis, C. A.; David, L.; Correa, P.; Carneiro, F.; De Bolós, C.; Garcia, E.; Mandel, U.; Clausen, H. & Sobrinho-Simões, M. Intestinal metaplasia of human stomach displays distinct patterns of mucin (MUC1, MUC2, MUC5AC, and MUC6) expression. *Cancer Res.* **59**, 1003–1007 (1999).

49. Riquelme, I.; Saavedra, K.; Espinoza, J. A.; Weber, H.; García, P.; Nervi, B.; Garrido, M.; Corvalán, A. H.; Roa, J. C. & Bizama, C. Molecular classification of gastric cancer: Towards a pathway driven targeted therapy. *Oncotarget* **6**, 24750–24779 (2015).

50. Chiaravalli, A. M.; Klersy, C.; Vanoli, A.; Ferretti, A.; Capella, C. & Solcia, E. Histotype-based prognostic classification of gastric cancer. *World J. Gastroenterol.* **18**, 896–904 (2012).

51. Lee, J. Y.; Gong, E. J.; Chung, E. J.; Park, H. W.; Bae, S. E.; Kim, E. H.; Kim, J.; Do, Y. S.; Kim, T. H.; Chang, H.; Song, H. J.; Choe, J. & Jung, H. The characteristics and prognosis of diffuse-type early gastric cancer diagnosed during health check-ups. *Gut Liver* **11**, 807–812 (2017).

52. The Cancer Genome Atlas Research Network. Comprehensive molecular characterization of gastric adenocarcinoma. *Nature* **513**, 202–209 (2014).

53. Watanabe, M.; Kato, J.; Inoue, I.; Yoshimura, N.; Yoshida, T. & Mukoubayashi, C. Development of gastric cancer in nonatrophic stomach with highly active inflammation identified by serum levels of pepsinogen and Helicobacter pylori antibody together with endoscopic rugal hyperplastic gastritis. *Int. J. Cancer* **2642**, 2632–2642 (2012).

54. Riboli, E. Fruit and vegetable intake and the risk of stomach and oesophagus adenocarcinoma in the European Prospective Investigation into Cancer and Nutrition (EPIC-EURGAST). *Int. J. Cancer* **118**, 2559–2566 (2006).

55. Riboli, E. Smoking and the risk of gastric cancer in the European Prospective Investigation into Cancer and Nutrition (EPIC). *Int. J. Cancer* **107**, 629–634 (2003).

56. Van Cutsem, E.; Sagaert, X.; Topal, B.; Haustermans, K. & Prenen, H. Gastric cancer. *Lancet* **388**, 2654–2664 (2016).

57. Mocellin, S. & Pasquali, S. Diagnostic accuracy of endoscopic ultrasonography (EUS) for the preoperative locoregional staging of primary gastric cancer. *Cochrane Database Syst. Rev.* **2015**, CD009944 (2015).

58. Apweiler, R.; Hermjakob, H. & Sharon, N. On the frequency of protein glycosylation, as deduced from analysis of the SWISS-PROT database. *Biochim. Biophys. Acta* **1473**, 4–8 (1999).

59. Jun, C. P.; Yong, C. L.; Kim, J. H.; Yu, J. K.; Sang, K. L.; Woo, J. H.; Sung, H. N. & Choong, B. K. Clinicopathological aspects and prognostic value with respect to age: An analysis of 3,362 consecutive gastric cancer patients. *J. Surg. Oncol.* **99**, 395–401 (2009).

60. Ychou, M.; Duffour, J. & Kramar, A. Clinical significance and prognostic value of CA72-4 compared with CEA and CA19-9 in patients with gastric cancer. *Dis. Markers* **16**, 105–110 (2000).

61. Byrne, D. J.; Browning, M. C. K. & Cuschieri, A. CA72-4: a new tumour marker for gastric cancer. *Br. J. Surg.* **77**, 1010–1013 (1990).

62. Louhimo, J.; Kokkola, A.; Alfthan, H.; Stenman, U.-H. & Haglund, C. Preoperative hCG and CA 72-4 are prognostic factors in gastric cancer. *Int. J. Cancer* **933**, 929–933 (2004).

63. Yin, B. W. T.; Dnistrian, A. & Lloyd, K. O. Ovarian cancer antigen CA125 is encoded by the MUC16 mucin gene. *Int. J. Cancer* **740**, 737–740 (2002).

64. Nakata, B.; Chung, K. H. Y.; Kato, Y.; Yamashita, Y.; Maeda, K.; Onoda, N.; Sawada, T. & Sowa, M. Serum CA 125 level as a predictor of peritoneal dissemination in patients with gastric carcinoma. *Cancer* **83**, 2488–2492 (1998).

65. Haga, Y.; Sakamoto, K.; Egami, H.; Yoshimura, R.; Mori, K. & Akagi, M. Clinical significance of serum CA125 values in patients with cancers of the digestive system. *Am. J. Med. Sci.* **292**, 30–34 (1986).

66. Campos, D.; Freitas, D.; Gomes, J.; Magalhães, A.; Steentoft, C.; Gomes, C.; Vester-Christensen, M. B.; Ferreira, J. A.; Afonso, L. P.; Santos, L. L.; De Sousa, J. P.; Mandel, U.; Clausen, H.; Vakhrushev, S. Y. & Reis, C. A. Probing the O-glycoproteome of gastric cancer cell lines for biomarker discovery. *Mol. Cell. Proteomics* **14**, 1616–1629 (2015).

67. Deribe, Y. L.; Pawson, T. & Dikic, I. Post-translational modifications in signal integration. *Nat. Struct. Mol. Biol.* **17**, 666–672 (2010).

68. Ohtsubo, K. & Marth, J. D. Glycosylation in cellular mechanisms of health and disease. *Cell* **126**, 855–867 (2006).

69. Pinho, S. S. & Reis, C. A. Glycosylation in cancer: Mechanisms and clinical implications. *Nat. Rev. Cancer* **15**, 540–555 (2015).

70. Varki, A. Biological roles of oligosaccharides: all of the theories are correct. *Glycobiology* **3**, 97–130 (1993).

71. Aebi, M.; Bernasconi, R.; Clerc, S. & Molinari, M. N-glycan structures: recognition and processing in the ER. *Trends Biochem. Sci.* **35**, 74–82 (2010).

72. Banerjee, S.; Vishwanath, P.; Cui, J.; Kelleher, D. J.; Gilmore, R.; Robbins, P. W. & Samuelson, J. The evolution of N-glycan-dependent endoplasmic reticulum quality control factors for glycoprotein folding and degradation. *Proc. Natl. Acad. Sci. U. S. A.* **104**, 11676–11681 (2007).

73. Reily, C.; Stewart, T. J.; Renfrow, M. B. & Novak, J. Glycosylation in health and disease. *Nat. Rev. Nephrol.* **15**, 346–366 (2019).

74. Holts, G. D. & Hart, G. W. The subcellular distribution of terminal N-acetylglucosamine moieties. *J. Biol. Chem.* **261**, 8049–8057 (1986).

75. Brockhausen, I.; Schachter, H. & Stanley, P. *Essentials of Glycobiology*. (Cold Spring Harbor Laboratory Press, 2009).

76. Silva, E.; Teixeira, A.; David, L.; Carneiro, F.; Reis, C. A.; Sobrinho-Simões, J.; Serpa, J.; Veerman, E.; Bolscher, J. & Sobrinho-Simões, M. Mucins as key molecules for the classification of intestinal metaplasia of the stomach. *Virchows Arch.* **440**, 311–317 (2002).

77. Christlet, T. H. T. & Veluraja, K. Database analysis of O-glycosylation sites in proteins. *Biophys. J.* **80**, 952–960 (2001).

78. Harris, R. J. & Spellman, M. W. O-linked fucose and other post-translational modifications unique to EGF modules. *Glycobiology* **3**, 219–224 (1993).

79. Ho, S. B.; Niehans, G. A.; Lyftogt, C.; Yan, P. S.; Cherwitz, D. L.; Gum, E. T.; Dahiya, R. & Kim, Y. S. Heterogeneity of mucin gene expression in normal and neoplastic tissues. *Cancer Res.* **53**, 641–651 (1993).

80. Lindahl, U.; Couchman, J.; Kimata, K. & Esko, J. *Essentials of Glycobiology*. (Cold Spring Harbor Laboratory Press, 2017).

81. Silbert, J. E. Structure and metabolism of proteoglycans and glycosaminoglycans. *J. Invest. Dermatol.* **79**, 31–37 (1982).

82. Rapraeger, A.; Jalkanens, M.; Koda, J. & Bernfield, M. The cell surface proteoglycan from mouse mammary epithelial cells bears chondroitin sulfate and heparan sulfate glycosaminoglycans. *J. Biol. Chem.* **260**, 11046–11052 (1985).

83. Couchman, J. R. & Pataki, C. A. An introduction to proteoglycans and their localization. *J. Histochem. Cytochem.* **60**, 885–897 (2012).

84. Adany, R.; Heimer, R.; Caterson, B.; Sorrell, J. M. & Iozzo, R. V. Altered expression of chondroitin sulfate proteoglycan in the stroma of human colon carcinoma. *J. Biol. Chem.* **265**, 11389–11396 (1990).

85. Park, H.; Zhou, Y. & Costello, C. E. Direct analysis of sialylated or sulfated glycosphingolipids and other polar and neutral lipids using TLC-MS interfaces. *J. Lipid Res.* **55**, 773–781 (2014).

86. Paladino, S.; Lebreton, S. & Zurzolo, C. *Trafficking and membrane organization of GPI-anchored proteins in health and diseases*. *Current Topics in Membranes* **75**, (Elsevier Ltd, 2015).

87. Hakomori, S. Glycosylation defining cancer malignancy: New wine in an old bottle.

Proc. Natl. Acad. Sci. U. S. A. **99**, 10231–10233 (2002).

88. Mereiter, S.; Balmaña, M.; Gomes, J.; Magalhães, A. & Reis, C. A. Glycomic approaches for the discovery of targets in gastrointestinal cancer. *Front. Oncol.* **6**, 55 (2016).

89. Pinho, S. S.; Oliveira, P.; Cabral, J.; Carvalho, S.; Huntsman, D.; Gärtner, F.; Seruca, R.; Reis, C. A. & Oliveira, C. Loss and recovery of Mgat3 and GnT-III mediated E-cadherin N-glycosylation is a mechanism involved in epithelial-Mesenchymal-Epithelial transitions. *PLoS One* **7**, e33191 (2012).

90. Kakugawa, Y.; Wada, T.; Yamaguchi, K.; Yamanami, H.; Ouchi, K.; Sato, I. & Miyagi, T. Up-regulation of plasma membrane-associated ganglioside sialidase (Neu3) in human colon cancer and its involvement in apoptosis suppression. *Proc. Natl. Acad. Sci. U. S. A.* **99**, 10718–10723 (2002).

91. Aryal, R. P.; Ju, T. & Cummings, R. D. The endoplasmic reticulum chaperone cosmc directly promotes in vitro folding of T-synthase. *J. Biol. Chem.* **285**, 2456–2462 (2010).

92. Kumamoto, K.; Goto, Y.; Sekikawa, K.; Takenoshita, S.; Ishida, N.; Kawakita, M. & Kannagi, R. Increased expression of UDP-galactose transporter messenger RNA in human colon cancer tissues and its implication in synthesis of Thomsen-Friedenreich antigen and sialyl Lewis A/X determinants. *Cancer Res.* **61**, 4620–4627 (2001).

93. Kellokumpu, S.; Sormunen, R. & Kellokumpu, I. Abnormal glycosylation and altered Golgi structure in colorectal cancer: Dependence on intra-Golgi pH. *FEBS Lett.* **516**, 217–224 (2002).

94. Dennis, J. W.; Laferté, S.; Waghorne, C.; Breitman, M. L. & Kerbel, R. S. β1-6 branching of Asn-linked oligosaccharides is directly associated with metastasis. *Science (80-.).* **236**, 582–585 (1987).

95. Pinho, S. S.; Figueiredo, J.; Cabral, J.; Carvalho, S.; Dourado, J.; Magalhães, A.; Gärtner, F.; Mendonça, A. M.; Isaji, T.; Gu, J.; Carneiro, F.; Seruca, R.; Taniguchi, N. & Reis, C. A. E-cadherin and adherens-junctions stability in gastric carcinoma: Functional implications of glycosyltransferases involving N-glycan branching biosynthesis, N-acetylglucosaminyltransferases III and v. *Biochim. Biophys. Acta - Gen. Subj.* **1830**, 2690–2700 (2013).

96. Pinho, S. S. Preventing E-cadherin aberrant N-glycosylation at Asn-554 improves its critical function in gastric cancer. *Oncogene* **35**, 1619–1631 (2016).

97. Zhao, Y.; Nakagawa, T.; Itoh, S.; Inamori, K. I.; Isaji, T.; Kariya, Y.; Kondo, A.; Miyoshi, E.; Miyazaki, K.; Kawasaki, N.; Taniguchi, N. & Gu, J. N-Acetylglucosaminyltransferase III antagonizes the effect of N-acetylglucosaminyltransferase V on α3β1 integrin-mediated cell migration. *J. Biol. Chem.* **281**, 32122–32130 (2006).

98. Ishikawa, M.; Kitayama, J.; Nariko, H.; Kohno, K. & Nagawa, H. The expression pattern of UDP- N -Acetyl- a - D -Galactosamine : Polypeptide N - Acetylgalactosaminyl transferase-3 in early gastric carcinoma. *J. Surg. Oncol.* **86**,

28–33 (2004).

99. Brockhausen, I.; Yang, J.; Lehotay, M.; Ogata, S. & Itzkowitz, S. Pathways of mucin O -glycosylation in normal and malignant rat colonic epithelial cells reveal a mechanism for cancer-associated sialyl-Tn antigen expression. *J. Biol. Chem.* **382**, 219–232 (2001).

100. Hakomori, S. & Kannagi, R. Glycosphingolipids as tumor-associated and differentiation markers. *J. Clin. Immunol.* **71**, 231–251 (1983).

101. Marcos, N. T.; Bennett, E. P.; Gomes, J.; Magalhaes, A.; Gomes, C.; David, L.; Dar, I.; Jeanneau, C.; DeFrees, S.; Krustrup, D.; Vogel, L. K.; Kure, E. H.; Burchell, J.; Taylor-Papadimitriou, J.; Clausen, H.; Mandel, U. & Reis, C. A. ST6GalNAc-I controls expression of sialyl-Tn antigen in gastrointestinal tissues. *Front. Biosci.* **3**, 1443–1455 (2011).

102. Sakamoto, J.; Watanabe, T.; Tokumaru, T.; Takagi, H.; Nakazato, H. & Lloyd, K. O. Expression of Lewisa, Lewisb, Lewisx, Lewisy, Sialyl-Lewisa, and Sialyl-Lewisx blood group antigens in human gastric carcinoma and in normal gastric tissue. *Cancer Res.* **49**, 745–752 (1989).

103. Costa, N. R.; Mendes, N.; Marcos, N. T.; Reis, C. A.; Caffrey, T.; Hollingsworth, M. A. & Santos-Silva, F. Relevance of MUC1 mucin variable number of tandem repeats polymorphism in H pylori adhesion to gastric epithelial cells. *World J. Gastroenterol.* **14**, 1411–1414 (2008).

104. Borén, T. Helicobacter pylori sabA adhesin in persistent infection and chronic inflammation. *Science (80-.).* **297**, 573–578 (2002).

105. Gerhard, M.; Lehn, N.; Neumayer, N.; Bore, T.; Rad, R.; Schepp, W.; Miehlke, S.; Classen, M. & Prinz, C. Clinical relevance of the Helicobacter pylori gene for blood-group antigen-binding adhesin. *Proc. Natl. Acad. Sci.* **96**, 12778–12783 (1999).

106. Marcos, N. T.; Magalhães, A.; Ferreira, B.; Oliveira, M. J.; Carvalho, A. S.; Mendes, N.; Gilmartin, T.; Head, S. R.; Figueiredo, C.; David, L.; Santos-Silva, F. & Reis, C. A. Helicobacter pylori induces β3GnT5 in human gastric cell lines, modulating expression of the SabA ligand sialyl-Lewis x. *J. Clin. Invest.* **118**, 2325–2336 (2008).

107. Shoji Nakamori; Kameyama, M.; Imaoka, S.; Furukawa, H.; Ishikawa, O.; Sasaki, Y.; Kabuto, T.; Iwanaga, T.; Matsushita, Y. & Irimura, T. Increased expression of sialyl Lewis x antigen correlates with poor survival in patients with colorectal carcinoma: clinicopathological and immunohistochemical study. *Cancer Res.* **53**, 3632–3637 (1993).

108. Peixoto, A.; Relvas-Santos, M.; Azevedo, R.; Lara Santos, L. & Ferreira, J. A. Protein glycosylation and tumor microenvironment alterations driving cancer hallmarks. *Front. Oncol.* **9**, 380 (2019).

109. Navabi, N.; Johansson, M. E. V.; Raghavan, S. & Lindéna, S. K. Helicobacter pylori infection impairs the mucin production rate and turnover in the murine gastric mucosa. *Infect. Immun.* **81**, 829–837 (2013).

110. Teixeira, A.; David, L.; Reis, C. A.; Costa, J. & Sobrinho-Simões, M. Expression of

mucins (MUCI, MUC2, MUC5AC, and MUC6) and type I Lewis antigens in cases with and without Helicobacter pylori colonization in metaplastic glands of the human stomach. *J. Pathol.* **197**, 37–43 (2002).

111. Ho, S. B.; Shekels, L. L.; Toribara, N. W.; Kim, Y. S.; Lyftogt, C.; Cherwitz, D. L. & Niehans, G. A. Mucin gene expression in normal, preneoplastic, and neoplastic human gastric epithelium. *Cancer Res.* **55**, 2681–2690 (1995).

112. Sakamoto, H.; Yonezawa, S.; Utsunomiya, T.; Tanaka, S.; Kim, Y. S. & Sato, E. Mucin antigen expression in gastric carcinomas of young and old adults. *Hum. Pathol.* **28**, 1056–1065 (1997).

113. Hilkens, J.; Vos, H. L.; Wesseling, J.; Boer, M.; Storm, J.; van der Valk, S.; Calafat, J. & Patriarca, C. Is episialin/MUC1 involved in breast cancer progression? *Cancer Lett.* **90**, 27–33 (1995).

114. Reis, C. A.; David, L.; Carvalho, F.; Mandel, U.; Bolós, C. De; Mirgorodskaya, E.; Clausen, H. & Simões, M. S. Immunohistochemical study of the expression of MUC6 mucin and co-expression of other secreted mucins (MUC5AC and MUC2) in human gastric carcinomas. *J. Histochem. Cytochem.* **48**, 377–388 (2000).

115. Victorzon, M.; Nordling, S.; Nilsson, O.; Roberts, P. J. & Haglund, C. Sialyl Tn antigen is an independent predictor of outcome in patients with gastric cancer. *Int. J. Cancer* **65**, 295–300 (1996).

116. Joncquel Chevalier Curt, M.; Lecointe, K.; Mihalache, A.; Rossez, Y.; Gosset, P.; Léonard, R. & Robbe-Masselot, C. Alteration or adaptation, the two roads for human gastric mucin glycosylation infected by Helicobacter pylori. *Glycobiology* **25**, 617–631 (2014).

117. Nakasaki, H.; Mitomi, T.; Noto, T.; Ogoshi, K.; Hanaue, H.; Tanaka, Y.; Makuuchi, H.; Clausen, H. & Hakomori, S. itiroh. Mosaicism in the expression of tumor-associated carbohydrate antigens in human colonic and gastric cancers. *Cancer Res.* **49**, 3662–3669 (1989).

118. Kudelka, M. R.; Ju, T.; Heimburg-Molinaro, J. & Cummings, R. D. Simple sugars to complex disease - Mucin-type O-glycans in cancer. *Adv. Cancer Res.* **126**, 53–135 (2015).

119. David, L.; Nesland, J. M.; Clausen, H.; Carneiro, F. & Simões, M. S. Simple mucin-type carbohydrate antigens (Tn, sialosyl-Tn and T) in gastric mucosa, carcinomas and metastases. *APMIS* **27**, 162–172 (1992).

120. Cao, Y.; Stosiek, P.; Springer, G. F. & Karsten, U. Thomsen-Friedenreich-related carbohydrate antigens in normal adult human tissues: A systematic and comparative study. *Histochem. Cell Biol.* **106**, 197–207 (1996).

121. Carneiro, F.; Santos, L.; David, L.; Dabelsteen, E.; Clausen, H. & Simões, M. S. T (Thomsen–Friedenreich) antigen and other simple mucin-type carbohydrate antigens in precursor lesions of gastric carcinoma. *Histopathology* **24**, 105–113 (1994).

122. Kato, J. RNAi-mediated gene silencing of ST6GalNAc I suppresses the metastatic potential in gastric cancer cells. *Gastric Cancer* **19**, 85–97 (2016).

123. Werther, J. L.; Rivera-MacMurray, S.; Bruckner, H.; Tatematsu, M. & Itzkowitz, S. H. Mucin-associated sialosyl-Tn antigen expression in gastric cancer correlates with an adverse outcome. *Br. J. Cancer* **69**, 613–616 (1994).

124. Ju, T.; Lanneau, G. S.; Gautam, T.; Wang, Y.; Xia, B.; Stowell, S. R.; Willard, M. T.; Wang, W.; Xia, J. Y.; Zuna, R. E.; Laszik, Z.; Benbrook, D. M.; Hanigan, M. H. & Cummings, R. D. Human tumor antigens Tn and sialyl Tn arise from mutations in Cosmc. *Cancer Res.* **68**, 1636–1646 (2008).

125. Sewell, R.; Bäckström, M.; Dalziel, M.; Gschmeissner, S.; Karlsson, H.; Noll, T.; Gätgens, J.; Clausen, H.; Hansson, G. C.; Burchell, J. & Taylor-Papadimitriou, J. The ST6GalNAc-I sialyltransferase localizes throughout the golgi and is responsible for the synthesis of the tumor-associated sialyl-Tn O-glycan in human breast cancer. *J. Biol. Chem.* **281**, 3586–3594 (2006).

126. Takahashi, I.; Maehara, Y.; Kusumoto, T.; Yoshida, M.; Kakeji, Y.; Kusumoto, H.; Furusawa, M. & Sugimachi, K. Predictive Value of Preoperative Serum Sialyl Tn Antigen Levels in Prognosis of Patients with Gastric Cancer. *Cancer* **72**, 1836–1840 (1986).

127. Ohuchi, N.; Thor, A.; Nose, M.; Fujita, J.; Kyogoku, M. & Schlom, J. Tumor-associated glycoprotein (TAG-72) detected in adenocarcinomas and benign lesions of the stomach. *Int. J. Cancer* **38**, 643–650 (1986).

128. Werther, J. L.; Tatematsu, M.; Klein, R.; Kurihara, M.; Kumaga, K.; Llorens, P.; Neto, J. G.; Bodian, C.; Pertsemlidis, D.; Yamachika, T.; Kitou, T. & Itzkowitz, S. Sialosyl-Tn antigen as a marker of gastric cancer progression: An international study. *Int. J. Cancer* **69**, 193–199 (1996).

129. Freitas, D.; Campos, D.; Gomes, J.; Pinto, F.; Macedo, J. A.; Matos, R.; Mereiter, S.; Pinto, M. T.; Polónia, A.; Gartner, F.; Magalhães, A. & Reis, C. A. O-glycans truncation modulates gastric cancer cell signaling and transcription leading to a more aggressive phenotype. *EBioMedicine* **40**, 349–362 (2019).

130. Ma, X. C.; Terata, N.; Kodama, M.; Jancic, S.; Hosokawa, Y. & Hattori, T. Expression of sialyl-Tn antigen is correlated with survival time of patients with gastric carcinomas. *Eur. J. Cancer* **29**, 1820–1823 (1993).

131. Freitas, D.; Balmaña, M.; Poças, J.; Campos, D.; Osório, H.; Konstantinidi, A.; Vakhrushev, S. Y.; Magalhães, A. & Reis, C. A. Different isolation approaches lead to diverse glycosylated extracellular vesicle populations. *J. Extracell. Vesicles* **8**, 1621131 (2019).

132. Chargaff, E. & West, R. The biological significance of the thromboplastic protein of blood. *J. Biol. Chem.* **166**, 189–197 (1946).

133. Wolf, P. The nature and significance of platelet products in human plasma. *Br. J. Haematol.* **13**, 269–288 (1967).

134. Witwer, K. W. & Théry, C. Extracellular vesicles or exosomes? On primacy, precision, and popularity influencing a choice of nomenclature. *J. Extracell. Vesicles* **8**, 1648167 (2019).

135. Lötvall, J.; Hill, A. F.; Hochberg, F.; Buzás, E. I.; Vizio, D. Di; Gardiner, C.; Gho, Y.

S.; Kurochkin, I. V.; Mathivanan, S.; Quesenberry, P.; Sahoo, S.; Tahara, H.; Wauben, M. H.; Witwer, K. W. & Théry, C. Minimal experimental requirements for definition of extracellular vesicles and their functions: A position statement from the International Society for Extracellular Vesicles. *J. Extracell. Vesicles* **3**, 26913 (2014).

136. Johnstone, R. M.; Adam, M.; Hammond, J. R.; Orr, L. & Turbide, C. Vesicle formation during reticulocyte maturation. *J. Biol. Chem.* **262**, 9412–9420 (1987).

137. Pan, B. T.; Teng, K.; Wu, C.; Adam, M. & Johnstone, R. M. Electron microscopic evidence for externalization of the transferrin receptor in vesicular form in sheep reticulocytes. *J. Cell Biol.* **101**, 942–948 (1985).

138. Baietti, M. F.; Zhang, Z.; Mortier, E.; Melchior, A.; Degeest, G.; Geeraerts, A.; Ivarsson, Y.; Depoortere, F.; Coomans, C.; Vermeiren, E.; Zimmermann, P. & David, G. Syndecan – syntenin – ALIX regulates the biogenesis of exosomes. *Nat. Cell Biol.* **14**, 677–685 (2012).

139. Stuffers, S.; Wegner, C. S.; Stenmark, H. & Brech, A. Multivesicular Endosome Biogenesis in the Absence of ESCRTs. *Traffic* **10**, 925–937 (2009).

140. Hsu, C.; Morohashi, Y.; Yoshimura, S. I.; Manrique-Hoyos, N.; Jung, S. Y.; Lauterbach, M. A.; Bakhti, M.; Grønborg, M.; Möbius, W.; Rhee, J. S.; Barr, F. A. & Simons, M. Regulation of exosome secretion by Rab35 and its GTPase-activating proteins TBC1D10A-C. *J. Cell Biol.* **189**, 223–232 (2010).

141. Savina, A.; Fader, C. M.; Damiani, M. T. & Colombo, M. I. Rab11 promotes docking and fusion of multivesicular bodies in a calcium-dependent manner. *Traffic* **6**, 131–143 (2005).

142. Thery, C. Rab27a and Rab27b control different steps of the exosome secretion pathway. *Nat. Cell Biol.* **12**, 19–30 (2010).

143. Sims, P. J.; Faioni, E. M.; Wiedmer, T. & Shattil, S. J. Complement proteins C5b-9 cause release of membrane vesicles from the platelet surface that are enriched in the membrane receptor for coagulation factor Va and express prothrombinase activity. *J. Biol. Chem.* **263**, 18205–18212 (1988).

144. Heijnen, H. F. G.; Schiel, A. E.; Fijnheer, R.; Geuze, H. J. & Sixma, J. J. Activated platelets release two types of membrane vesicles: Microvesicles by surface shedding and exosomes derived from exocytosis of multivesicular bodies and α-granules. *Blood* **94**, 3791–3799 (1999).

145. Nabhan, J. F.; Hu, R.; Oh, R. S.; Cohen, S. N. & Lu, Q. Formation and release of arrestin domain-containing protein 1-mediated microvesicles (ARMMs) at plasma membrane by recruitment of TSG101 protein. *Proc. Natl. Acad. Sci. U. S. A.* **109**, 4146–4151 (2012).

146. Hristov, M.; Erl, W.; Linder, S. & Weber, P. C. Apoptotic bodies from endothelial cells enhance the number and initiate the differentiation of human endothelial progenitor cells in vitro. *Blood* **104**, 2761–2766 (2004).

147. Gustafson, D.; Veitch, S. & Fish, J. E. Extracellular vesicles as protagonists of diabetic cardiovascular pathology. *Front. Cardiovasc. Med.* **4**, 1–12 (2017).

148. Bergsmedh, A.; Szeles, A.; Henriksson, M.; Bratt, A.; Folkman, M. J.; Spetz, A. L. & Holmgren, L. Horizontal transfer of oncogenes by uptake of apoptotic bodies. *Proc. Natl. Acad. Sci. U. S. A.* **98**, 6407–6411 (2001).

149. Quesenberry, P. J.; Aliotta, J.; Deregibus, M. C. & Camussi, G. Role of extracellular RNA-carrying vesicles in cell differentiation and reprogramming. *Stem Cell Res. Ther.* **6**, 153 (2015).

150. Mathivanan, S. & Simpson, R. J. ExoCarta: A compendium of exosomal proteins and RNA. *Proteomics* **9**, 4997–5000 (2009).

151. Guescini, M.; Genedani, Æ. S.; Stocchi, V. & Agnati, L. F. Astrocytes and Glioblastoma cells release exosomes carrying mtDNA. *J. Neural Transm.* **117**, 1–4 (2010).

152. Vidal, M.; Sainte-marie, J.; Philippot, J. R. & Bienvenue, A. Asymmetric distribution of phospholipids in the membrane of vesicles released during in vitro maturation of guinea pig reticulocytes : evidence precluding a role for ' aminophospholipid translocase'. *J. Cell. Physiol.* **140**, 455–462 (1989).

153. Østergaard, O.; Nielsen, C. T.; Iversen, L. V; Jacobsen, S.; Tanassi, J. T. & Heegaard, N. H. H. Quantitative proteome profiling of normal human circulating microparticles. *J. Proteome Res.* **11**, 2154–2163 (2012).

154. Crescitelli, R.; Lässer, C.; Szabó, T. G.; Kittel, A.; Eldh, M.; Dianzani, I.; Buzás, E. I. & Lötvall, J. Distinct RNA profiles in subpopulations of extracellular vesicles: apoptotic bodies, microvesicles and exosomes. *J. Extracell. Vesicles* **2**, 20677–20686 (2013).

155. Gassart, A. De; Géminard, C.; Février, B.; Raposo, G. & Vidal, M. Lipid raft – associated protein sorting in exosomes. *Hematopoesis* **102**, 4336–4345 (2003).

156. Valadi, H.; Ekström, K.; Bossios, A.; Sjöstrand, M.; Lee, J. J. & Lötvall, J. O. Exosome-mediated transfer of mRNAs and microRNAs is a novel mechanism of genetic exchange between cells. *Nat. Cell Biol.* **9**, 654–659 (2007).

157. Mulcahy, L. A.; Pink, R. C. & Carter, D. R. F. Routes and mechanisms of extracellular vesicle uptake. *J. Extracell. Vesicles* **3**, 24641 (2014).

158. Shimoda, A.; Tahara, Y.; Sawada, S. ichi; Sasaki, Y. & Akiyoshi, K. Glycan profiling analysis using evanescent-field fluorescence-assisted lectin array: Importance of sugar recognition for cellular uptake of exosomes from mesenchymal stem cells. *Biochem. Biophys. Res. Commun.* **491**, 701–707 (2017).

159. Batista, B. S.; Eng, W. S.; Pilobello, K. T.; Hendricks-Muñoz, K. D. & Mahal, L. K. Identification of a conserved glycan signature for microvesicles. *J. Proteome Res.* **10**, 4624–4633 (2012).

160. Christianson, H. C.; Svensson, K. J.; Kuppevelt, T. H. Van; Li, J. & Belting, M. Cancer cell exosomes depend on cell-surface heparan sulfate proteoglycans for their internalization and functional activity. *Proc. Natl. Acad. Sci.* **110**, 17380–17385 (2013).

161. Xiao, H.; Lässer, C.; Shelke, G. V.; Wang, J.; Rådinger, M.; Lunavat, T. R.;

Malmhä, C.; Lin, L. H.; Li, J.; Li, L. & Lötva, J. Mast cell exosomes promote lung adenocarcinoma cell proliferation-role of KIT-stem cell factor signaling. *Cell Commun. Signal.* **12**, 1–10 (2014).

162. Ekström, K.; Omar, O.; Granéli, C.; Wang, X.; Vazirisani, F. & Thomsen, P. Monocyte exosomes stimulate the osteogenic gene expression of mesenchymal stem cells. *PLoS One* **8**, 75227 (2013).

163. Tian, T.; Wang, Y.; Wang, H.; Zhu, Z. & Xiao, Z. Visualizing of the cellular uptake and intracellular trafficking of exosomes by live-cell microscopy. *J. Cell. Biochem.* **111**, 488–496 (2010).

164. Williams, C.; Pazos, R.; Royo, F.; González, E.; Roura-ferrer, M.; Marti, A.; Gamiz, J.; Reichardt, N. & Falcón-pérez, J. M. Assessing the role of surface glycans of extracellular vesicles on cellular uptake. *Nature* **9**, 11920 (2019).

165. El-Andaloussi, S.; Lee, Y.; Lakhal-Littleton, S.; Li, J.; Seow, Y.; Gardiner, C.; Alvarez-Erviti, L.; Sargent, I. L. & Wood, M. J. A. Exosome-mediated delivery of siRNA in vitro and in vivo. *Nat. Protoc.* **7**, 2112–2126 (2012).

166. Escrevente, C.; Keller, S.; Altevogt, P. & Costa, J. Interaction and uptake of exosomes by ovarian cancer cells. *BMC Cancer* **11**, 108 (2011).

167. Saunderson, S. C.; Dunn, A. C.; Crocker, P. R. & McLellan, A. D. CD169 mediates the capture of exosomes in spleen and lymph node. *Blood* **123**, 208–216 (2014).

168. Tauro, B. J.; Greening, D. W.; Mathias, R. A.; Ji, H.; Mathivanan, S.; Scott, A. M. & Simpson, R. J. Comparison of ultracentrifugation , density gradient separation , and immunoaffinity capture methods for isolating human colon cancer cell line LIM1863-derived exosomes. *Methods* **56**, 293–304 (2012).

169. Théry, C.; Amigorena, S.; Raposo, G. & Clayton, A. Isolation and characterization of exosomes from cell culture supernatants and biological fluids. *Curr. Protoc. Cell Biol.* **30**, 1–29 (2006).

170. Taylor, D. D.; Zacharias, W. & Gercel-Taylor, C. Exosome isolation for proteomic analyses and RNA profiling. *Methods Mol. Biol.* **728**, 235–246 (2011).

171. Merchant, M. L.; Powell, D. W.; Wilkey, D. W.; Cummins, T. D.; Deegens, J. K.; Rood, I. M.; McAfee, K. J.; Fleischer, C.; Klein, E. & Klein, J. B. Microfiltration isolation of human urinary exosomes for characterization by MS. *Proteomics - Clin. Appl.* **4**, 84–96 (2010).

172. Chen, C.; Skog, J.; Hsu, C. H.; Lessard, R. T.; Balaj, L.; Wurdinger, T.; Carter, B. S.; Breakefield, X. O.; Toner, M. & Irimia, D. Microfluidic isolation and transcriptome analysis of serum microvesicles. *Lab Chip* **10**, 505–511 (2010).

173. Karttunen, J.; Heiskanen, M.; Navarro-Ferrandis, V.; Das Gupta, S.; Lipponen, A.; Puhakka, N.; Rilla, K.; Koistinen, A. & Pitkänen, A. Precipitation-based extracellular vesicle isolation from rat plasma co-precipitate vesicle-free microRNAs. *J. Extracell. Vesicles* **8**, 1555410 (2019).

174. Livshits, M. A.; Khomyakova, E.; Evtushenko, E. G.; Lazarev, V. N.; Kulemin, N. A.; Semina, S. E.; Generozov, E. V. & Govorun, V. M. Isolation of exosomes by

differential centrifugation : Theoretical analysis of a commonly used protocol. *Nature* **5**, 17319 (2015).

175. Sódar, B. W.; Kittel, Á.; Pálóczi, K.; Vukman, K. V; Osteikoetxea, X.; Szabó-taylor, K.; Németh, A.; Sperlágh, B.; Baranyai, T.; Giricz, Z.; Wiener, Z.; Turiák, L.; Drahos, L.; Pállinger, É.; Vékey, K.; Ferdinandy, P.; Falus, A. & Buzás, E. I. Low-density lipoprotein mimics blood plasma-derived exosomes and microvesicles during isolation and detection. *Nature* **6**, 24316 (2016).

176. Böing, A. N.; Pol, E. van der; Grootemaat, A. E.; Frank, A. W.; Sturk, A. & Nieuwland, R. Single-step isolation of extracellular vesicles by size-exclusion chromatography. *J. Extracell. Vesicles* **3**, 23430 (2014).

177. Konoshenko, M. Y.; Lekchnov, E. A.; Vlassov, A. V. & Laktionov, P. P. Isolation of extracellular vesicles: General methodologies and latest trends. *Biomed Res. Int.* **2018**, 8545347 (2018).

178. Mol, E. A.; Goumans, M. J.; Doevendans, P. A.; Sluijter, J. P. G. & Vader, P. Higher functionality of extracellular vesicles isolated using size-exclusion chromatography compared to ultracentrifugation. *Nanomedicine Nanotechnology, Biol. Med.* **13**, 2061–2065 (2017).

179. Gámez-Valero, A.; Monguió-Tortajada, M.; Carreras-Planella, L.; Franquesa, M.; Beyer, K. & Borràs, F. E. Size-exclusion chromatography-based isolation minimally alters extracellular vesicles' characteristics compared to precipitating agents. *Sci. Rep.* **6**, 33641 (2016).

180. Abramowicz, A.; Marczak, L.; Wojakowska, A.; Zapotoczny, S.; Whiteside, T. L.; Widlak, P. & Pietrowska, M. Harmonization of exosome isolation from culture supernatants for optimized proteomics analysis. *PLoS One* **13**, 0205496 (2018).

181. Deun, J. Van; Mestdagh, P.; Sormunen, R.; Cocquyt, V.; Vermaelen, K.; Vandesompele, J.; Bracke, M.; Wever, O. De & Hendrix, A. The impact of disparate isolation methods for extracellular vesicles on downstream RNA profiling. *J. Extracell. Vesicles* **3**, 24858 (2014).

182. Zhang, H.; Freitas, D.; Kim, H. S.; Fabijanic, K.; Li, Z.; Chen, H.; Mark, M. T.; Molina, H.; Martin, A. B.; Bojmar, L.; Fang, J.; Rampersaud, S.; Hoshino, A.; Matei, I.; Kenific, C. M.; Nakajima, M.; Mutvei, A. P. & Sansone, P. et al. Identification of distinct nanoparticles and subsets of extracellular vesicles by asymmetric flow field-flow fractionation. *Nat. Cell Biol.* **20**, 332–343 (2018).

183. Koliha, N.; Wiencek, Y.; Heider, U.; Jüngst, C.; Kladt, N.; Krauthäuser, S.; Johnston, I. C. D.; Bosio, A.; Schauss, A.; Koliha, N.; Wiencek, Y.; Heider, U.; Jüngst, C. & Kladt, N. A novel multiplex bead-based platform highlights the diversity of extracellular vesicles. *J. Extracell. Vesicles* **5**, 29975 (2016).

184. Royo, F.; Zun, P.; Egia, A.; Perez, A.; Loizaga, A.; Arceo, R.; Lacasa, I.; Rabade, A.; Arrieta, E.; Bilbao, R.; Unda, M.; Carracedo, A. & Falcon-perez, J. M. Different EV enrichment methods suitable for clinical settings yield different subpopulations of urinary extracellular vesicles from human samples. *J. Extracell. Vesicles* **5**, 29497 (2016).

185. Liangsupree, T.; Multia, E. & Riekkola, M. L. Modern isolation and separation techniques for extracellular vesicles. *J. Chromatogr. A* **1636**, 461773 (2021).

186. Zhang, X.; Borg, E. G. F.; Liaci, A. M.; Vos, H. R. & Stoorvogel, W. A novel three step protocol to isolate extracellular vesicles from plasma or cell culture medium with both high yield and purity. *J. Extracell. Vesicles* **20**, 1791450 (2019).

187. Kharmate, G.; Hosseini-Beheshti, E.; Caradec, J.; Chin, M. Y. & Tomlinson Guns, E. S. Epidermal growth factor receptor in prostate cancer derived exosomes. *PLoS One* **11**, 0154967 (2016).

188. Zorrilla, S. R.; Pérez-Sayans, M.; Fais, S.; Logozzi, M.; Torreira, M. G. & García, A. G. A pilot clinical study on the prognostic relevance of plasmatic exosomes levels in oral squamous cell carcinoma patients. *Cancers (Basel).* **11**, 429–440 (2019).

189. Peinado, H.; Ale, M.; Lavotshkin, S.; Matei, I.; Costa-Silva, B.; Moreno-Bueno, G.; Hergueta-Redondo, M.; Williams, C.; García-Santos, G.; Nitadori-Hoshino, A.; Hoffman, C.; Badal, K.; Garcia, B. A.; Callahan, M. K.; Yuan, J.; Martins, V. R. & Skog, J. et al. Melanoma exosomes educate bone marrow progenitor cells toward a pro-metastatic phenotype through MET. *Nat. Med.* **18**, 883–891 (2012).

190. Grange, C.; Tapparo, M.; Collino, F.; Vitillo, L.; Damasco, C.; Deregibus, M. C.; Tetta, C.; Bussolati, B. & Camussi, G. Microvesicles released from human renal cancer stem cells stimulate angiogenesis and formation of lung premetastatic niche. *Cancer Res.* **71**, 5346–5356 (2011).

191. Taraboletti, G.; Ascenzo, S. D.; Borsotti, P.; Giavazzi, R.; Pavan, A. & Dolo, V. Shedding of the matrix metalloproteinases MMP-2 , MMP-9 , and MT1-MMP as membrane vesicle-associated components by endothelial cells. *Am. J. Pathol.* **160**, 673–680 (2002).

192. Uno, K.; Homma, S.; Satoh, T.; Nakanishi, K.; Abe, D.; Matsumoto, K.; Oki, A.; Tsunoda, H.; Yamaguchi, I.; Nagasawa, T.; Yoshikawa, H. & Aonuma, K. Tissue factor expression as a possible determinant of thromboembolism in ovarian cancer. *Br. J. Cancer* **96**, 290–295 (2007).

193. Cheng, N.; Chytil, A.; Shyr, Y.; Joly, A. & Moses, H. L. Transforming growth factor-β signaling-deficient fibroblasts enhance hepatocyte growth factor signaling in mammary carcinoma cells to promote scattering and invasion. *Mol. Cancer Res.* **6**, 1521–1533 (2008).

194. Donnarumma, E.; Fiore, D.; Nappa, M.; Roscigno, G.; Adamo, A.; Iaboni, M.; Russo, V.; Affinito, A.; Puoti, I.; Quintavalle, C.; Rienzo, A.; Piscuoglio, S.; Thomas, R. & Condorelli, G. Cancer-associated fibroblasts release exosomal microRNAs that dictate an aggressive phenotype in breast cancer. *Oncotarget* **8**, 19592–19608 (2017).

195. Al-Nedawi, K.; Meehan, B.; Micallef, J.; Lhotak, V.; May, L.; Guha, A. & Rak, J. Intercellular transfer of the oncogenic receptor EGFRvIII by microvesicles derived from tumour cells. *Nat. Cell Biol.* **10**, 619–624 (2008).

196. Qu, J. L.; Qu, X. J.; Zhao, M. F.; Teng, Y. E.; Zhang, Y.; Hou, K. Z.; Jiang, Y. H.; Yang, X. H. & Liu, Y. P. Gastric cancer exosomes promote tumour cell proliferation

through PI3K/Akt and MAPK/ERK activation. *Dig. Liver Dis.* **41**, 875–880 (2009).

197. Atay, S.; Banskota, S.; Crow, J.; Sethi, G.; Rink, L. & Godwin, A. K. Oncogenic KIT-containing exosomes increase gastrointestinal stromal tumor cell invasion. *Proc. Natl. Acad. Sci.* **111**, 711–716 (2014).

198. Park, J. E.; Tan, H. Sen; Datta, A.; Lai, R. C.; Zhang, H.; Meng, W.; Lim, S. K. & Sze, S. K. Microenvironment to enhance angiogenic and metastatic potential by secretion of proteins and exosomes. *Mol. Cell. Proteomics* **9**, 1085–1099 (2010).

199. Gomes, F. G.; Sandim, V.; Almeida, V. H.; Rondon, A. M. R.; Succar, B. B.; Hottz, E. D.; Leal, A. C.; Verçoza, B. R. F.; Rodrigues, J. C. F.; Bozza, P. T.; Zingali, R. B. & Monteiro, R. Q. Breast-cancer extracellular vesicles induce platelet activation and aggregation by tissue factor-independent and -dependent mechanisms. *Thromb. Res.* **159**, 24–32 (2017).

200. Mueller, B. M.; Reisfeld, R. A.; Edgington, T. S. & Ruf, W. Expression of tissue factor by melanoma cells promotes efficient hematogenous metastasis. *Proc. Natl. Acad. Sci.* **89**, 11832–11836 (1992).

201. Liu, Z. M.; Wang, Y. Bin & Yuan, X. H. Exosomes from murine-derived Gl26 cells promote glioblastoma tumor growth by reducing number and function of CD8+T cells. *Asian Pacific J. Cancer Prev.* **14**, 309–314 (2013).

202. Shao, Y.; Chen, T.; Zheng, X.; Yang, S.; Xu, K.; Chen, X.; Xu, F.; Wang, L.; Shen, Y.; Wang, T.; Zhang, M.; Hu, W.; Ye, C.; Yu, X.; Shao, J. & Zheng, S. Colorectal cancer-derived small extracellular vesicles establish an inflammatory premetastatic niche in liver metastasis. *Carcinogenesis* **39**, 1368–1379 (2018).

203. Renzo, M. F. Di; Poulsom, R.; Olivero, M.; Comoglio, P. M. & Lemoine, N. R. Expression of the Met/hepatocyte growth factor ceceptor in human pancreatic. *Cancer Res.* **55**, 1129–1138 (1995).

204. Tuck, A. B.; Park, M.; Sterns, E. E.; Boag, A. & Elliott, B. E. Coexpression of hepatocyte growth factor and receptor (Met) in human breast carcinoma. *Am. J. Pathol.* **148**, 225–232 (1996).

205. Rong, S.; Segal, S.; Anver, M.; Resau, J. H. & Vande Woude, G. F. Invasiveness and metastasis of NIH 3T3 cells induced by Met-hepatocyte growth factor/scatter factor autocrine stimulation. *Proc. Natl. Acad. Sci. U. S. A.* **91**, 4731–4735 (1994).

206. Guo, W. Exosomal PD-L1 contributes to immunosuppression and is associated with anti-PD-1 response. *Nature* **560**, 382–386 (2018).

207. Zhang, Q.; Higginbotham, J. N.; Jeppesen, D. K.; Yang, Y.; Li, W.; Mckinley, T. E.; Graves-deal, R.; Ping, J.; Britain, C. M.; Dorsett, K. A.; Hartman, C. L.; Ford, D. A.; Allen, R. M.; Vickers, K. C.; Liu, Q.; Jeffrey, L. F.; Bellis, S. L. & Coffey, R. J. Transfer of functional cargo in exomeres. *Cell* **27**, 940–954 (2019).

208. Théry, C.; Zitvogel, L.; Amigorena, S. & Roussy, I. G. Exosomes: Composition, biogenesis and function. *Nat. Rev. Immunol.* **2**, 569–579 (2002).

209. Momen-Heravi, F. & Bala, S. Extracellular vesicles in oral squamous carcinoma carry oncogenic miRNA profile and reprogramme monocytes via NF-κB pathway.

Oncotarget **9**, 34838–34854 (2018).

210. Rabinowits, G.; Gerçel-taylor, C.; Day, J. M.; Taylor, D. D. & Kloecker, G. H. Exosomal microRNA : A diagnostic marker for lung cancer. *Clin. Lung Cancer* **10**, 42–46 (2009).

211. Wever, O. De & Hendrix, A. A supporting ecosystem to mature extracellular vesicles into clinical application. *EMBO J.* **38**, e101412 (2019).

212. Dhondt, B.; Geeurickx, E.; Tulkens, J.; Deun, J. Van & Vergauwen, G. Unravelling the proteomic landscape of extracellular vesicles in prostate cancer by density-based fractionation of urine. *J. Extracell. Vesicles* **9**, 1736935 (2020).

213. Logozzi, M.; Milito, A. De; Lugini, L.; Borghi, M.; Calabro, L.; Spada, M.; Perdicchio, M.; Marino, M. L.; Federici, C.; Iessi, E.; Brambilla, D.; Venturi, G.; Lozupone, F.; Santinami, M.; Huber, V.; Maio, M.; Rivoltini, L. & Fais, S. High levels of exosomes expressing CD63 and caveolin-1 in plasma of melanoma patients. *PLoS One* **4**, 5219 (2009).

214. Liu, D.; Trojanowicz, B.; Ye, L.; Li, C.; Zhang, L.; Li, X.; Li, G.; Zheng, Y. & Chen, L. The invasion and metastasis promotion role of CD97 small isoform in gastric carcinoma. *PLoS One* **7**, 39989 (2012).

215. Ciravolo, V.; Huber, V.; Ghedini, G. C.; Venturelli, E.; Bianchi, F.; Campiglio, M.; Morelli, D.; Villa, A.; Mina, P. Della; Menard, S.; Filipazzi, P.; Rivoltini, L.; Tagliabue, E. & Pupa, S. M. Potential role of HER2-overexpressing exosomes in countering trastuzumab-based therapy. *J. Cell. Physiol.* **277**, 658–667 (2011).

216. Baran, J.; Baj-Krzyworzeka, M.; Weglarczyk, K.; Szatanek, R.; Zembala, M.; Barbasz, J.; Czupryna, A.; Szczepanik, A. & Zembala, M. Circulating tumour-derived microvesicles in plasma of gastric cancer patients. *Cancer Immunol. Immunother.* **59**, 841–850 (2010).

217. Taylor, D. D. & Gercel-Taylor, C. MicroRNA signatures of tumor-derived exosomes as diagnostic biomarkers of ovarian cancer. *Gynecol. Oncol.* **110**, 13–21 (2008).

218. Bryant, R. J.; Pawlowski, T.; Catto, J. W. F.; Marsden, G.; Vessella, R. L.; Rhees, B.; Kuslich, C.; Visakorpi, T. & Hamdy, F. C. Changes in circulating microRNA levels associated with prostate cancer. *Br. J. Cancer* **106**, 768–774 (2012).

219. Heneghan, H. M.; Miller, N.; Kelly, R.; Newell, J. & Kerin, M. J. Systemic miRNA-195 differentiates breast cancer from other malignancies and is a potential biomarker for detecting noninvasive and early stage disease. *Oncologist* **15**, 673–682 (2010).

220. Akers, J. C.; Ramakrishnan, V.; Kim, R.; Skog, J.; Nakano, I.; Pingle, S.; Kalinina, J.; Hua, W.; Kesari, S.; Mao, Y.; Breakefield, X. O.; Hochberg, F. H.; Meir, E. G. Van; Carter, B. S. & Chen, C. C. miR-21 in the extracellular vesicles (EVs) of cerebrospinal fluid (CSF): A platform for glioblastoma biomarker development. *PLoS One* **8**, 78115 (2013).

221. Imamura, T.; Komatsu, S.; Ichikawa, D.; Miyamae, M.; Okajima, W.; Ohashi, T.; Kiuchi, J.; Nishibeppu, K.; Kosuga, T.; Konishi, H.; Shiozaki, A.; Okamoto, K.; Fujiwara, H. & Otsuji, E. Low plasma levels of miR-101 are associated with tumor

progression in gastric cancer. *Oncotarget* **8**, 106538–106550 (2017).

222. Xiao, D.; Dong, Z.; Zhen, L.; Xia, G.; Huang, X.; Wang, T.; Guo, H.; Yang, B.; Xu, C.; Wu, W.; Zhao, X. & Xu, H. Combined exosomal GPC1, CD82, and serum CA19-9 as multiplex targets: A specific, sensitive, and reproducible detection panel for the diagnosis of pancreatic cancer. *Mol. Cancer Res.* **18**, 1300–1310 (2020).

223. Chen, K.; Gentry-Maharaj, A.; Burnell, M.; Steentoft, C.; Marcos-Silva, L.; Mandel, U.; Jacobs, I.; Dawnay, A.; Menon, U. & Blixt, O. Microarray glycoprofiling of CA125 improves differential diagnosis of ovarian cancer. *J. Proteome Res.* **12**, 1408–1418 (2013).

224. Chen, Z.; Liang, Q.; Zeng, H.; Zhao, Q.; Guo, Z.; Zhong, R.; Xie, M.; Cai, X.; Su, J.; He, Z.; Zheng, L. & Zhao, K. Exosomal CA125 as a promising biomarker for ovarian cancer diagnosis. *J. Cancer* **11**, 6445–6453 (2020).

225. Runz, S.; Keller, S.; Rupp, C.; Stoeck, A.; Issa, Y.; Koensgen, D.; Mustea, A.; Sehouli, J.; Kristiansen, G. & Altevogt, P. Malignant ascites-derived exosomes of ovarian carcinoma patients contain CD24 and EpCAM. *Gynecol. Oncol.* **107**, 563–571 (2007).

226. Hermann, P. C.; Huber, S. L.; Herrler, T.; Aicher, A.; Ellwart, J. W.; Guba, M.; Bruns, C. J. & Heeschen, C. Distinct populations of cancer stem cells determine tumor growth and metastatic activity in human pancreatic cancer. *Cell Stem Cell* **1**, 313–323 (2007).

227. Sakaue, T.; Koga, H.; Iwamoto, H.; Nakamura, T.; Ikezono, Y.; Abe, M.; Wada, F.; Masuda, A.; Tanaka, T.; Fukahori, M.; Ushijima, T.; Mihara, Y.; Naitou, Y.; Okabe, Y.; Kakuma, T.; Ohta, K.; Nakamura, K. & Torimura, T. Glycosylation of ascites-derived exosomal CD133 : a potential prognostic biomarker in patients with advanced pancreatic cancer. *Med. Mol. Morphol.* **4**, 198–208 (2019).

228. Britain, C. M.; Bhalerao, N.; Silva, A. D.; Chakraborty, A.; Buchsbaum, D. J.; Crowley, M. R.; Crossman, D. K.; Edwards, Y. J. K. & Bellis, S. L. Glycosyltransferase ST6Gal-I promotes the epithelial to mesenchymal transition in pancreatic cancer cells. *J. Biol. Chem.* **296**, 100034 (2021).

229. Hedlund, M.; Ng, E.; Varki, A. & Varki, N. M. α2-6-linked sialic acids on N-glycans modulate carcinoma differentiation in vivo. *Cancer Res.* **68**, 388–394 (2008).

230. Escrevente, C.; Grammel, N.; Kandzia, S.; Zeiser, J.; Tranfield, E. M.; Conradt, H. S. & Costa, J. Sialoglycoproteins and N-Glycans from secreted exosomes of ovarian carcinoma cells. *PLoS One* **8**, 78631 (2013).

231. Gomes, J.; Gomes-alves, P.; Carvalho, S. B.; Peixoto, C.; Alves, P. M.; Altevogt, P. & Costa, J. Extracellular vesicles from ovarian carcinoma cells display specific glycosignatures. *Biomolecules* **5**, 1741–1761 (2015).

232. North, S. J.; Hitchen, P. G.; Haslam, S. M. & Dell, A. Mass spectrometry in the analysis of N-linked and O-linked glycans. *Curr. Opin. Struct. Biol.* **19**, 498–506 (2009).

233. Miles, D. W.; Happerfield, L. C.; Smith, P.; Gillibrand, R.; Bobrow, L. G.; Gregory, W. M. & Rubens, R. D. Expression of sialyl-Tn predicts the effect of adjuvant

chemotherapy in node-positive breast cancer. *Br. J. Cancer* **70**, 1272–1275 (1994).

234. Miles, D. & Papazisis, K. Rationale for the clinical development of STn-KLH (Theratope) and anti-MUC-1 vaccines in breast cancer. *Clin. Breast Cancer* **3 Suppl 4**, S134–S138 (2003).

235. Miles, D. W.; Towlson, K. E.; Graham, R.; Reddish, M.; Longenecker, B. M.; Taylor-Papadimitriou, J. & Rubens, R. D. A randomised phase II study of sialyl-Tn and DETOX-B adjuvant with or without cyclophosphamide pretreatment for the active specific immunotherapy of breast cancer. *Br. J. Cancer* **74**, 1292–1296 (1996).

236. Miles, D.; Roché, H.; Martin, M.; Perren, T. J.; Cameron, D. A.; Glaspy, J.; Dodwell, D.; Parker, J.; Mayordomo, J.; Tres, A.; Murray, J. L. & Ibrahim, N. K. Phase III Multicenter Clinical Trial of the Sialyl-TN (STn)-Keyhole Limpet Hemocyanin (KLH) Vaccine for Metastatic Breast Cancer. *Oncologist* **16**, 1092–1100 (2011).

237. Nakagoe, T.; Sawai, T.; Tsuji, T.; Jibiki, M.; Nanashima, A.; Yamaguchi, H.; Yasutake, T.; Ayabe, H.; Arisawa, K. & Ishikawa, H. Pre-operative serum levels of sialyl Tn antigen predict liver metastasis and poor prognosis in patients with gastric cancer. *Eur. J. Surg. Oncol.* **27**, 731–739 (2001).

238. Rosa-Fernandes, L.; Rocha, V. B.; Carregari, V. C.; Urbani, A. & Palmisano, G. A perspective on extracellular vesicles proteomics. *Front. Chem.* **5**, 102 (2017).

239. Zuba-Surma, E. K. Minimal information for studies of extracellular vesicles 2018 (MISEV2018): a position statement of the International Society for Extracellular Vesicles and update of the MISEV2014 guidelines. *J. Extracell. Vesicles* **7**, 1535750 (2018).

240. Marcos, N. T.; Pinho, S.; Grandela, C.; Cruz, A.; Samyn-Petit, B.; Harduin-Lepers, A.; Almeida, R.; Silva, F.; Morais, V.; Costa, J.; Kihlberg, J.; Clausen, H. & Reis, C. A. Role of the human ST6GalNAc-I and ST6GalNAc-II in the synthesis of the cancer-associated Sialyl-Tn antigen. *Cancer Res.* **64**, 7050–7057 (2004).

241. Carvalho, A. S.; Harduin-Lepers, A.; Magalhães, A.; Machado, E.; Mendes, N.; Costa, L. T.; Matthiesen, R.; Almeida, R.; Costa, J. & Reis, C. A. Differential expression of α-2,3-sialyltransferases and α-1,3/4-fucosyltransferases regulates the levels of sialyl Lewis a and sialyl Lewis x in gastrointestinal carcinoma cells. *Int. J. Biochem. Cell Biol.* **42**, 80–89 (2010).

242. Colcher, D.; Hand, P. H.; Nuti, M. & Schlom, J. A spectrum of monoclonal antibodies reactive with human mammary tumor cells. *Proc. Natl. Acad. Sci. U. S. A.* **78**, 3199–3203 (1981).

243. Steentoft, C.; Vakhrushev, S. Y.; Vester-Christensen, M. B.; Schjoldager, K. T. B. G.; Kong, Y.; Bennett, E. P.; Mandel, U.; Wandall, H.; Levery, S. B. & Clausen, H. Mining the O-glycoproteome using zinc-finger nuclease-glycoengineered SimpleCell lines. *Nat. Methods* **8**, 977–982 (2011).

244. Magnani, J. L.; Schlom, J.; Paterson, A. J.; Bennett, J. & Colcher, D. Analysis of a human tumor associated glycoprotein (TAG-72) identified by monoclonal antibody B72.3. *Cancer Res.* **46**, 850–857 (1986).

245. Gold, D. V. & Mattes, M. J. Monoclonal antibody B72.3 reacts with a core region

structure of O-linked carbohydrates. *Tumor Biol.* **9**, 137–144 (1988).

246. Kjeldsen, J.; Clausen, H.; Hirohashi, S.; Owaga, T.; Iijma, H. & Hakomori, E. S. Preparation and characterization of monoclonal antibodies directed to the tumor-associated O-linked sialosyl-2-6a-N-acetylgalactosaminyl (sialosyl-Tn) epitope. *Cancer Res.* **48**, 2214–2220 (1988).

247. Zheng, X.; Baker, H.; Hancock, W. S.; Fawaz, F.; Mccaman, M. & Pungor, E. Proteomic analysis for the assessment of different lots of fetal bovine serum as a raw material for cell culture. *Biotechnol. Progr.* **22**, 1294–1300 (2006).

248. Soo, C. Y.; Song, Y.; Zheng, Y.; Campbell, E. C.; Riches, A. C.; Gunn-Moore, F. & Powis, S. J. Nanoparticle tracking analysis monitors microvesicle and exosome secretion from immune cells. *Immunology* **136**, 192–197 (2012).

249. Dragovic, R. A.; Gardiner, C.; Brooks, A. S.; Tannetta, D. S.; Ferguson, D. J. P.; Hole, P.; Carr, B.; Redman, C. W. G.; Harris, A. L.; Dobson, P. J.; Harrison, P. & Sargent, I. L. Sizing and phenotyping of cellular vesicles using Nanoparticle Tracking Analysis. *Nanomedicine Nanotechnology, Biol. Med.* **7**, 780–788 (2011).

250. Honig, M. G. & Hume, R. I. DiI and DiO: versatile fluorescent dyes for neuronal labelling and pathway tracing. *Trends Neurosci.* **12**, 333–341 (1989).

251. Sandmaier, B. M.; Oparin, D. V.; Holmberg, L. A.; Reddish, M. A.; MacLean, G. D. & Longenecker, B. M. Evidence of a cellular immune response against sialyl-Tn in breast and ovarian cancer patients after high-dose chemotherapy, stem cell rescue, and immunization with theratope STn-KLH cancer vaccine. *J. Immunother.* **22**, 54–66 (1999).

252. Julien, S.; Picco, G.; Sewell, R.; Vercoutter-Edouart, A. S.; Tarp, M.; Miles, D.; Clausen, H.; Taylor-Papadimitriou, J. & Burchell, J. M. Sialyl-Tn vaccine induces antibody-mediated tumour protection in a relevant murine model. *Br. J. Cancer* **100**, 1746–1754 (2009).

253. Eitan, E.; Zhang, S.; Witwer, K. W. & Mattson, M. P. Extracellular vesicle-depleted fetal bovine and human sera have reduced capacity to support cell growth. *J. Extracell. Vesicles* **4**, 1–10 (2015).

254. Elliott, D. J. The androgen receptor controls expression of the cancer associated STn antigen and cell adhesion through induction of ST6GalNAc1 in prostate cancer. *Oncotarget* **6**, 34358–34374 (2015).

255. Ludwig, N.; Whiteside, T. L. & Reichert, T. E. Challenges in exosome isolation and analysis in health and disease. *Int. J. Mol. Sci.* **20**, 4684 (2019).

256. Royo, F.; Théry, C.; Falcón-Pérez, J. M.; Nieuwland, R. & Witwer, K. W. Methods for separation and characterization of extracellular vesicles: Results of a worldwide survey performed by the ISEV rigor and standardization subcommittee. *Cells* **9**, 1955 (2020).

257. Yellon, D. M. & Davidson, S. M. Comparison of small extracellular vesicles isolated from plasma by ultracentrifugation or size-exclusion chromatography : yield , purity and functional potential. *J. Extracell. Vesicles* **8**, 1560809 (2019).

258. Lobb, R. J.; Becker, M.; Wen, S. W.; Wong, C. S. F.; Wiegmans, A. P.; Leimgruber, A. & Mo, A. Optimized exosome isolation protocol for cell culture supernatant and human plasma. *J. Extracell. Vesicles* **4**, 27031 (2015).

259. Gardiner, C.; Ferreira, Y. J.; Dragovic, R. A.; Redman, C. W. G. & Sargent, I. L. Extracellular vesicle sizing and enumeration by nanoparticle tracking analysis. *J. Extracell. Vesicles* **2**, 19671 (2013).

260. Simonsen, J. B. What are we looking at? Extracellular vesicles, lipoproteins, or both? *Circ. Res.* **121**, 920–922 (2017).

261. Karimi, N.; Cvjetkovic, A.; Jang, S. C.; Crescitelli, R.; Hosseinpour Feizi, M. A.; Nieuwland, R.; Lötvall, J. & Lässer, C. Detailed analysis of the plasma extracellular vesicle proteome after separation from lipoproteins. *Cell. Mol. Life Sci.* **75**, 2873–2886 (2018).

262. Bemis, L. T.; Witwer, K. W.; Buza, E. I.; Lo, J.; Nolte-, E. N.; Bora, A.; La, C.; Piper, M. G.; Sivaraman, S.; The, C. & Hochberg, F. Standardization of sample collection, isolation and analysis methods in extracellular vesicle research. *J. Extracell. Vesicles* **2**, 20360 (2013).

263. Sinha, A.; Ignatchenko, V.; Ignatchenko, A.; Mejia-guerrero, S. & Kislinger, T. In-depth proteomic analyses of ovarian cancer cell line exosomes reveals differential enrichment of functional categories compared to the NCI 60 proteome. *Biochem. Biophys. Res. Commun.* **445**, 694–701 (2014).

264. De Freitas-Junior, J. C. M. & Morgado-Díaz, J. A. The role of N-glycans in colorectal cancer progression: Potential biomarkers and therapeutic applications. *Oncotarget* **7**, 19395–19413 (2016).

265. Itzkowitz, S. H.; Bloom, E. J.; Kokal, W. A.; Modin, G.; Hakomori, S. & Kim, Y. S. Sialosyl- Tn: A novel mucin antigen associated with prognosis in colorectal cancer patients. *Cancer* **66**, 1960–1966 (1990).

266. Kobayashi, H.; Terao, T. & Kawashima, Y. Serum sialyl Tn antigen as a prognostic marker in patients with epithelial ovarian cancer. *Acta Obstet. Gynaecol. Jpn.* **44**, 14–20 (1992).

267. Krishnamoorthy, L.; Jr., J. W. B.; Preston, A. B.; Nagashima, K. & Mahal, L. K. HIV-1 and microvesicles from T-cells share a common glycome, arguing for a common origin. *Nat. Chem. Biol.* **5**, 244–250 (2009).

268. Mereiter, S.; Balmaña, M.; Campos, D.; Gomes, J. & Reis, C. A. Glycosylation in the era of cancer-targeted therapy: Where are we heading? *Cancer Cell* **36**, 6–16 (2019).

269. Feng, Y.; Guo, Y.; Li, Y.; Tao, J.; Ding, L.; Wu, J. & Ju, H. Lectin-mediated in situ rolling circle amplification on exosomes for probing cancer-related glycan pattern. *Anal. Chim. Acta* **1039**, 108–115 (2018).

270. Royo, F.; Cossío, U.; Angulo, A. R. De; Llop, J. & Falcon-perez, J. M. Modification of the glycosylation of extracellular vesicles alters their biodistribution in mice. *Nanoscale* **11**, 1531–1537 (2019).

271. Akagi, T.; Kato, K.; Hanamura, N.; Kobayashi, M. & Ichiki, T. Evaluation of desialylation effect on zeta potential of extracellular vesicles secreted from human prostate cancer cells by on-chip microcapillary electrophoresis. *Jpn. J. Appl. Phys.* **53**, 06JL01 (2014).

272. Chen, Y.-Q.; Lan, L. Y.-L.; Huang, M.; Henry, C. & Wilson, P. C. Hemagglutinin stalk-reactive antibodies interfere with influenza virus neuraminidase activity by steric hindrance. *J. Virol.* **93**, e01526-18 (2019).

273. Rana, S.; Yue, S.; Stadel, D. & Zöller, M. Toward tailored exosomes: The exosomal tetraspanin web contributes to target cell selection. *Int. J. Biochem. Cell Biol.* **44**, 1574–1584 (2012).

274. Sancho-Albero, M.; Navascués, N.; Mendoza, G.; Sebastián, V.; Arruebo, M.; Martín-Duque, P. & Santamaría, J. Exosome origin determines cell targeting and the transfer of therapeutic nanoparticles towards target cells. *J. Nanobiotechnology* **17**, 1–13 (2019).

275. Zech, D.; Rana, S.; Büchler, M. W. & Zöller, M. Tumor-exosomes and leukocyte activation: An ambivalent crosstalk. *Cell Commun. Signal.* **10**, 1–17 (2012).